AD-A168 263 EQUIPMENT FOR SUBPICOSECOND EXTREME ULTRAVIOLET FACILITY(U) ILLINOIS UNIV AT CHICAGO CIRCLE DEPT OF PHYSICS C K RHODES ET AL. 05 FEB 86 AFOSR-TR-86-0281 1/2

UNCLASSIFIED AFOSR-84-2289 F/G 20/5 NL

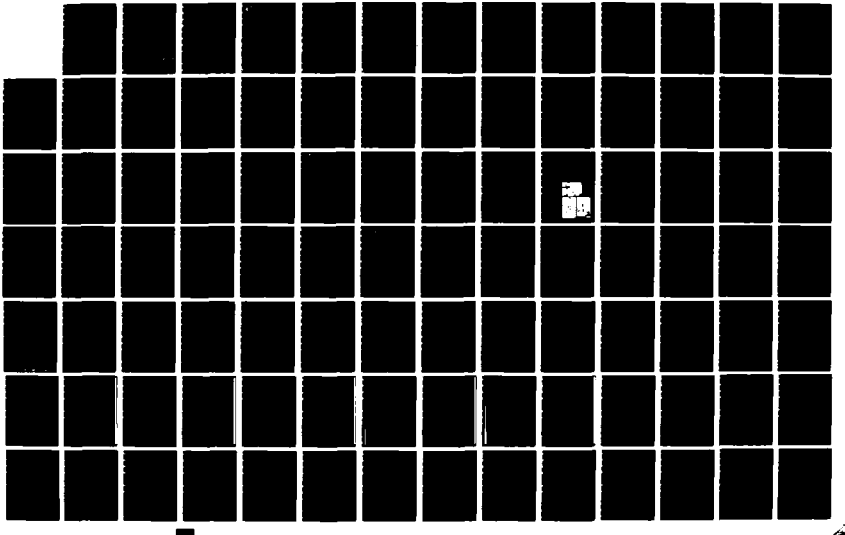

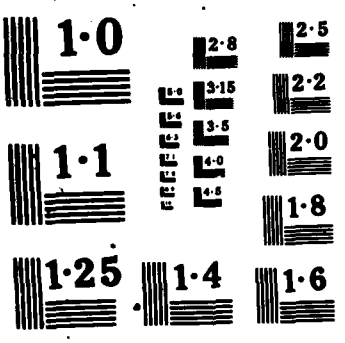

UNCLASSIFIED

SECURITY CLASSIFICATION OF THIS PAGE

REPORT DOCUMENTATION PAGE

AD-A168 263	1b. RESTRICTIVE MARKINGS: ---
2b. DECLASSIFICATION/DOWNGRADING SCHEDULE: ---	3. DISTRIBUTION/AVAILABILITY OF REPORT: Approved for public release; distribution unlimited. Reproduction in whole or in part is permitted for any purpose of the U.S. Gov.
4. PERFORMING ORGANIZATION REPORT NUMBER(S): ---	5. MONITORING ORGANIZATION REPORT NUMBER(S): --- AFOSR-TR- 86-0281
6a. NAME OF PERFORMING ORGANIZATION: University of Illinois at Chicago	6b. OFFICE SYMBOL (If applicable): ---
6c. ADDRESS (City, State and ZIP Code): Department of Physics, P. O. Box 4348, Chicago, Illinois 60680	7a. NAME OF MONITORING ORGANIZATION: USAF, AFSC
8a. NAME OF FUNDING/SPONSORING ORGANIZATION: ---	8b. OFFICE SYMBOL (If applicable): ---
8c. ADDRESS (City, State and ZIP Code): Air Force Office of Scientific Research, Building 410, Bolling Air Force Base, Washington, D.C. 20332	7b. ADDRESS (City, State and ZIP Code): Air Force Office of Scientific Research, Building 410, Bolling Air Force Base, Washington, D.C. 20332
	9. PROCUREMENT INSTRUMENT IDENTIFICATION NUMBER: [illegible] AFOSR 84-0289
	10. SOURCE OF FUNDING NOS. — PROGRAM ELEMENT NO.: 61102F; PROJECT NO.: 2917; TASK NO.: 146; WORK UNIT NO.:
11. TITLE (Include Security Classification): "Equipment for Subpicosecond Extreme Ultraviolet Facility"	
12. PERSONAL AUTHOR(S): Rhodes, Charles K.	
13a. TYPE OF REPORT: Final/Scientific	13b. TIME COVERED: FROM 7/15/84 TO 7/14/85
14. DATE OF REPORT (Yr., Mo., Day): 1986, February, 5	15. PAGE COUNT: 137
16. SUPPLEMENTARY NOTATION: ---	

17. COSATI CODES		
FIELD	GROUP	SUB. GR.

18. SUBJECT TERMS (Continue on reverse if necessary and identify by block number): Ultraviolet and x-ray lasers.

19. ABSTRACT (Continue on reverse if necessary and identify by block number)

The research program underway at the University of Illinois at Chicago, whose main goal is the development of coherent x-ray sources in the kilovolt range, is described. The new femtosecond source developed under the equipment grant provided by the Air Force has been placed in operation.

DTIC FILE COPY

DTIC ELECTE JUN 13 1986 S D A

20. DISTRIBUTION/AVAILABILITY OF ABSTRACT: UNCLASSIFIED/UNLIMITED ☒ SAME AS RPT. ☐ DTIC USERS ☐	21. ABSTRACT SECURITY CLASSIFICATION: UNCLASSIFIED
22a. NAME OF RESPONSIBLE INDIVIDUAL: Dr Schlossberg	22b. TELEPHONE NUMBER (Include Area Code): (202) 767-4906
	22c. OFFICE SYMBOL: --- NP

DD FORM 1473, 83 APR — EDITION OF 1 JAN 73 IS OBSOLETE.

86 6 10 128

UNCLASSIFIED

SECURITY CLASSIFICATION OF THIS PAGE

DISCLAIMER NOTICE

THIS DOCUMENT IS BEST QUALITY PRACTICABLE. THE COPY FURNISHED TO DTIC CONTAINED A SIGNIFICANT NUMBER OF PAGES WHICH DO NOT REPRODUCE LEGIBLY.

THE UNIVERSITY OF ILLINOIS AT CHICAGO

Department of Physics (M/C 273)
College of Liberal Arts and Sciences
Box 4348, Chicago, Illinois 60680
(312) 996-3400

FINAL REPORT - Grant AFOSR-84-0289

For the Period: 7/15/84 - 7/14/85

"EQUIPMENT FOR SUBPICOSECOND EXTREME ULTRAVIOLET FACILITY"

by Charles K. Rhodes, Principal Investigator
Keith Boyer, Co-Investigator
Ting Shan Luk, Co-Investigator

Prepared for:

Dr. Howard Schlossberg
AFOSR/NP
Building 410, Room C219
Bolling Air Force Base
Washington, D.C. 20332

CONTENTS

ABSTRACT

The research program underway at the University of Illinois at Chicago, whose main goal is the development of coherent x-ray sources in the kilovolt range, is described. The new femtosecond source developed under the equipment grant provided by the Air Force has been placed in operation.

I. Discussion of Research Progress

A basic and long-standing problem in the field of coherent sources is that associated with the generation of coherent energy in the extreme ultraviolet and soft x-ray regions. During the last three years, picosecond rare gas halogen (RGH) excimer laser technology, on account of the very favorable scaling relationships governing the spectral brightness of these sources, has emerged as a key factor in new techniques useful for generation of coherent radiation below 100 nm. In the program discussed in this report, which has explored the research topics listed in Appendix A, the operation of RGH systems has been extended down into the femtosecond region, a development that will enable sources with peak powers P in the $1TW \leq P \leq 10TW$ range to be used in physical studies. Light sources of this kind should permit the generation of focal intensities above ~ 10^{20} W cm^2. Appendix B details the properties of the femtosecond KrF* (248 nm) source provided for under this grant.

Recent research findings[1] lead to the conclusion that the direct multiphoton excitation of appropriate amplifying media with high spectral brightness ultraviolet sources is the most promising choice for the generation of short wavelength radiation in the kilovolt range. In addition to satisfying the demanding energy density requirements generally called for to create amplification in the x-ray range, this method of excitation utilizes the coherence obtainable from RGH sources to enhance the coupling strength and provide selectivity in the energy flow[2,3]. No alternative method under study has this feature. The application of this technique to the x-ray region requires an extended study of the basic character of high order nonlinear processes in the ultraviolet in an intensity range corresponding to radiating

field strengths E greater than an atomic unit (e a). This class of physical mechanisms, which, under appropriate conditions, appears to involve ordered electronic motions in the atom, has been recently shown to exhibit surprising characteristics. These features suggest that entirely new approaches for the efficient production of x-rays are feasible.

Our work involves a program of activities, involving both experimental and theoretical components, to explore the physical processes relevant to the basic question of coherent x-ray production. This includes measurements of ions[4,5], electrons[6], and photons in addition to a theoretical effort concentrating on the character of high order multiquantum coupling in the intensity regime above 10^{17} W cm^2. In addition, attention is given to closely related issues involving the spectroscopy of multiply excited atomic states and the properties of electron collisions. Detailed discussions on the relevant technical issues are contained in Appendices C - H.

We believe that the results of these basic measurements will provide important information on the properties of inner-shell systems useful for high energy x-ray production. A three-year program of research is envisaged, the principal goal of which is the development of an x-ray laser in the kilovolt range. If the program of studies described in this document is successful and develops along the expected lines, the feasibility of laboratory scale coherent sources in the x-ray range will be established and a demonstration model will have been constructed and placed in operation. It is also anticipated that such a device will prove to be compact, rugged, and moderate in cost.

II. Conclusions

Experimental results obtained over the last several years demonstrate that bright tunable coherent radiation in the 10 nm to 100 nm spectral range can be generated with the use of high spectral brightness (RGH) laser systems. Strong evidence, consisting primarily of the known scaling properties of RGH systems, the discovery of anomalous nonlinear radiative coupling to certain heavy materials, and the availability of an atomic mechanism for selective inner-shell excitation, supports the conclusion that these results can be extended to the kilovolt spectral region. Elementary considerations led to the conclusion several years ago that peak powers in excess of 10^{12} W can be generated with relatively modest scale RGH systems of special high brightness design. The presently available femtosecond pulse technology, which is clearly applicable to the ultraviolet region, rigorously underlines this view and appears to make peak powers near 10 TW feasible. With instrumentation of that kind, a program of basic physical studies can be performed into an intensity range exceeding 10^{20} W cm^2. At such an intensity, the peak electric field of the coherent driving wave approaches the unprecedented value of ~ 100 e/a_0^2. In such an extreme environment, which is impossible to generate by any other known means, it is likely that physical processes never previously observed will be detected.

At energy densities of the scale stated above, an atom experiences a violent perturbation that has important features in common with certain well studied collisional phenomena such as ion-atom collisions,[7,8] electron-ion collisions, and beam-foil interactions. Indeed, in the case of beam-foil collisions, a radiative environment at an intensity of 3 x 10^{18} W cm^2 at an ultraviolet wavelength approximates, in several important respects, the

conditions associated with the passage of an argon ion through a carbon foil with a kinetic energy of ~ 1 GeV. This rough similarity leads to the consideration of the concept[9] of an "optical solid" in which stationary atoms in a sufficiently intense radiative field will experience an interaction comparable to that of energetic ions traversing solid matter. A natural expectation is an extreme level of excitation. In addition, the coherence of the radiative environment is expected to introduce a measure of control on the energy transfer that will markedly increase the efficiency of energy flow over that normally characteristic of incoherent means of excitation.

The work outlined in this report has as its goal the development of an x-ray laser in the kilovolt range. If this program is successful, the feasibility of laboratory scale coherent sources in the x-ray range will be established. Furthermore, in this event, we believe that the concepts we are exploring have the clear potential of being engineered into compact and rugged devices. This achievement will, perforce, serve an immense range of applications involving the micro-characterization of condensed matter, and may be as influential in our future understanding of the natural world as the discovery of the light microscope was in its day three hundred years ago.

III. Acknowledgements

The author wishes to acknowledge fruitful discussions with U. Johann, A. P. Schwarzenbach, I. A. McIntyre, A. McPherson, H. Jara, K. Boyer, and A. Szoke as well as the technical assistance of R. Slagle, J. Wright, T. Pack, and R. Bernico.

IV. References

1. C. K. Rhodes, Science 229, 1345 (1985).

2. K. Boyer and C. K. Rhodes, Phys. Rev. Lett. 54, 1490 (1985).

3. A. Szöke and C. K. Rhodes, "A Theoretical Model of Inner-Shell Excitation By Outer-Shell Electrons," Phys. Rev. Lett., in press.

4. T. S. Luk, H. Pummer, K. Boyer, M. Shahidi, H. Egger, and C. K. Rhodes, Phys. Rev. Lett. 51, 110 (1983).

5. T. S. Luk, U. Johann, H. Egger, H. Pummer, and C. K. Rhodes, Phys. Rev. A32,214 (1985).

6. U. Johann, T. S. Luk, H. Egger, and C. K. Rhodes, "Rare Gas Electron Energy Spectra Produced By Collision-Free Multiquantum Processes," submitted to Phys. Rev. A.

7. C. K. Rhodes, Fundamentals of Laser Interactions, Lecture Notes in Physics No. 229, edited by F. Ehlotzky (Springer-Verlag, Berlin, 1985) p. 111.

8. U. Johann, T. S. Luk, and C. K. Rhodes, "Multiphoton Inner-Shell Atomic Excitation and Multiple Ionization," XIVth International Conference on the Physics of Electronic and Atomic Collisions, edited by D. C. Lorents, W. E. Meyerhof, and J. R. Peterson, (North-Holland, Amsterdam, in press).

9. C. K. Rhodes, in Report on VUV and X-Ray Sources of Atomic and Molecular Sciences Workshop, (National Academy Press, Washington, D.C., in press).

V. Appendices

Appendix A: Compendium of Publications 1983 - 1985

"Generation of Extreme Ultraviolet Radiation at 79 nm by Sum Frequency Mixing," T. Srinivasan, H. Egger, H. Pummer, and C. K. Rhodes, IEEE J. Quantum Electron. QE-19, 1270 (1983).

"Progress in Dye and Excimer Laser Sources for Remote Sensing," T. Srinivasan, H. Egger, T. S. Luk, H. Pummer, and C. K. Rhodes, in Laser and Optical Remote Sensing, edited by D. Killinger and A. Mooradian (Springer-Verlag, Berlin, 1983) p. 269.

"Multiphoton Dissociation of $OCCl_2$ at 193 nm: Formation of Electronically Excited Cl_2," M. W. Wilson, M. Rothschild, and C. K. Rhodes, J. Chem. Phys. 78, 3779 (1983).

"Evidence for Laser Induced Surface Silanol Formation," D. F. Muller, M. Rothschild, and C. K. Rhodes, in Materials Research Society Symposium Proceedings Volume 17 (Elsevier, New York, 1983) p. 135.

"Generation of Vacuum Ultraviolet and Extreme Ultraviolet Radiation by Nonlinear Processes with Excimer Lasers," C. K. Rhodes, in Laser Interaction and Related Plasma Phenomena, Vol. 6, edited by H. Hora and G. H. Miley (Plenum, New York, 1984) p. 87.

"High-Power VUV Stimulated Emission from Two-Photon Excited H_2," H. Pummer, H. Egger, T. S. Luk, T. Srinivasan, and C. K. Rhodes, in AIP Conference Proceedings, Vol. 100, Excimer Lasers - 1983, edited by H. Egger, H. Pummer, and C. K. Rhodes (American Institute of Physics, New York, 1983) p. 151.

"Generation of Electronically Excited Products in the Multiphoton Dissociation of Phosgene at 193 nm," M. W. Wilson, M. Rothschild, and C. K. Rhodes, in AIP Conference Proceedings, Vol. 100, Excimer Lasers - 1983, edited by H. Egger, H. Pummer, and C. K. Rhodes (American Institute of Physics, New York, 1983) p. 317.

"Collision-Free Generation of Highly Ionized Atomic Species with 193 nm Radiation," T. S. Luk, H. Pummer, K. Boyer, M. Shahidi, H. Egger, and C. K. Rhodes, in AIP Conference Proceedings, Vol. 100, Excimer Lasers - 1983, edited by H. Egger, H. Pummer, and C. K. Rhodes (American Institute of Physics, New York, 1983) p. 341.

"Vacuum Ultraviolet Stimulated Emission from Two-Photon Excited Molecular Hydrogen," H. Pummer, H. Egger, T. S. Luk, T. Srinivasan, and C. K. Rhodes, Phys. Rev. A28, 795 (1983).

"Anomalous Collision-Free Multiple Ionization of Atoms with Intense Picosecond Ultraviolet Radiation," T. S. Luk, H. Pummer, K. Boyer, M. Shahidi, H. Egger, and C. K. Rhodes, Phys. Rev. Lett. 51, 110 (1983).

"Ultraviolet and X-Ray Lasers," H. Egger and C. K. Rhodes, in the 1984 Mcgraw-Hill Yearbook of Science and Technology (McGraw-Hill, New York, 1983) p. 245.

12. "Stimulated Vacuum Ultraviolet Emission Following Two-Photon Excitation of H_2," H. Egger, T. S. Luk, H. Pummer, T. Srinivasan, and C. K. Rhodes, in Laser Spectroscopy VI, Proc. 6th Intl. Conf., edited by H. P. Weber and W. Lüthy (Springer-Verlag, Berlin, 1983) p. 403.

13. "Collisionless Multiquantum Ionization of Atomic Species with 193 nm Radiation," T. S. Luk, H. Pummer, K. Boyer, M. Shahidi, H. Egger, and C. K. Rhodes, in Laser Spectroscopy VI, Proc. 6th Intl. Conf., edited by H. P. Weber and W. Lüthy (Springer-Verlag, Berlin, 1983) p. 369.

14. "Stimulated Extreme Ultraviolet Emission at 93 nm in Krypton," T. Srinivasan, H. Egger, T. S. Luk, H. Pummer, and C. K. Rhodes, in Laser Spectroscopy VI, Proc. 6th Intl. Conf., edited by H. P. Weber and W. Lüthy (Springer-Verlag, Berlin, 1983) p. 385.

15. "Vacuum Ultraviolet and Extreme Ultraviolet Generation with Excimer Lasers," C. K. Rhodes in Abstract Volume, Laser 83 Opto-Elektronik (6th International Congress, Munich, 1983) p. 114.

16. "Dye, Vacuum Ultraviolet, and Extreme Ultraviolet Lasers," C. K. Rhodes, Kodak Laboratory Chemicals Bulletin, 54, 1 (1983).

17. "Progress in Short Wavelength Sources," C. K. Rhodes, Laser Focus (Pennwell Publishing Co., Massachusetts, October 1983) p. 16.

18. "The Influence of the Optical Stark Shift on the Two-Photon Excitation of the Molecular Hydrogen E,F $^1\Sigma_g^+$ State," T. Srinivasan, H. Egger, T. S. Luk, H. Pummer, and C. K. Rhodes, IEEE J. Quantum Electron. QE-19, 1874 (1983).

19. "Optical Properties of Rare Gas Fluoride Dimers and Trimers Dissolved in Liquid Rare Gases," H. Jara, H. Pummer, H. Egger, and C. K. Rhodes, Phys. Rev. B30, 1 (1984).

20. "Interaction of Atomic and Molecular Systems with High Intensity Ultraviolet Radiation," K. Boyer, H. Egger, T. S. Luk, H. Pummer, and C. K. Rhodes, J. Opt. Soc. Am. B1, 3 (1984).

21. "Vacuum Ultraviolet and Extreme Ultraviolet Generation with Excimer Lasers," C. K. Rhodes in Physics News in 1983, edited by Philip F. Schewe (American Institute of Physics, New York, 1983) p. 121.

22. "Collision-Free Multiple Ionization of Atoms and XUV Stimulated Emission in Krypton at 193 nm," H. Egger, T. S. Luk, W. Müller, H. Pummer, and C. K. Rhodes, AIP Conference Proceedings Subseries on Optical Science and Engineering, Laser Techniques in the Extreme Ultraviolet (American Institute of Physics, New York, 1984) p. 64.

23. "High-Spectral-Brightness Excimer Systems," H. Pummer, H. Egger, and C. K. Rhodes, Topics in Applied Physics: Excimer Lasers, Vol. 30, Second Enlarged Edition, C. K. Rhodes, editor (Springer-Verlag, Berlin, 1984) p. 217.

24. "Applications of Excimer Systems," K. Hohla, H. Pummer, and C. K. Rhodes, Topics in Applied Physics: Excimer Lasers, Vol. 30, Second Enlarged Edition, C. K. Rhodes, editor (Springer-Verlag, Berlin, 1984) p. 229.

25. "Multiphoton Ionization and Short Wavelength Stimulated Emission Using Excimer Lasers," H. Egger, K. Boyer, T. S. Luk, W. Müller, H. Pummer, and C. K. Rhodes, SPIE Vol. 476, Excimer Lasers, Their Applications, and New Frontiers in Lasers (Society of Photo-Optical Instrumentation Engineers, Bellingham, Washington, 1984) p. 52.

26. "Stimulated VUV Radiation from HD Excited by a Picosecond ArF Laser," T. S. Luk, H. Egger, W. Müller, H. Pummer, and C. K. Rhodes, Ultrafast Phenomena IV, D. H. Auston and K. B. Eisenthal, editors (Springer-Verlag, Berlin, 1984) p. 42.

27. "Studies of Collision-Free Nonlinear Processes in the Ultraviolet Range," C. K. Rhodes, in Proceedings of the Third International Conference on Multiphoton Processes, P. Lambropoulos and S. J. Smith, editors (Springer-Verlag, Berlin, 1984) p. 31.

28. "The Generation of Radiation in the Extreme Ultraviolet and Soft X-Ray Range with Excimer Lasers," C. K. Rhodes, in Energy Technology XI, Richard F. Hill, editor (Government Institutes, Inc., Rockville, Maryland, 1984) p. 1459.

29. "Lasers in the Vacuum Ultraviolet and X-Ray Region," C. K. Rhodes, invited presentation at the Workshop on Vacuum Ultraviolet and X-Ray Sources held by the Committee on Atomic and Molecular Sciences at the National Academy of Sciences, Washington, D.C., November 9, 1984 (to be published).

30. "The Observation of Stimulated Emission in the 119 nm to 149 nm Range from HD Excited by picosecond 193 nm Radiation," T. S. Luk, H. Egger, W. Müller, H. Pummer, and C. K. Rhodes, J. Chem. Phys. 82, 4479 (1985).

31. Excimer Lasers, 2nd Enlarged Edition, C. K. Rhodes, editor (Springer-Verlag, Berlin, 1984) pp. 1-271.

32. "Atomic Inner-Shell Excitation Induced by Coherent Motion of Outer-Shell Electrons," K. Boyer and C. K. Rhodes, Phys. Rev. Lett. 54, 1490 (1985).

33. "Collision-Free Multiple Photon Ionization of Atoms and Molecules at 193 nm," T. S. Luk, U. Johann, H. Egger, H. Pummer, and C. K. Rhodes, Phys. Rev. A32, 214 (1985).

34. "Studies of Multiquantum Processes in Atoms," C. K. Rhodes, in Seminar on Fundamentals of Laser Interactions, invited presentation, February 24 - March 2, 1985, Bundessportheim, Obergurgl (Ötztal), Austria (Springer-Verlag, Berlin, 1985) p. 111.

35. "Multiphoton Ionization of Atoms," C. K. Rhodes, Science 229, 1345 (1985).

35. "Generation of VUV Radiation with Lasers," C. K. Rhodes, in Resonance Ionization Spectroscopy 1984, edited by G. S. Hurst and M. G. Payne (The Institute of Physics, Bristol and Boston, 1984) p. 333.

. "Properties of Stimulated Emission Below 100 nm in Krypton," T. Srinivasan, W. Müller, M. Shahidi, T. S. Luk, H. Egger, H. Pummer, and C. K. Rhodes, J. Opt. Soc. Am. B, to be published.

. "Optically excited XeF Excimer Laser in Liquid Argon," M. Shahidi, H. Jara, H. Pummer, H. Egger, and C. K. Rhodes, Opt. Lett. 10, 448 (1985).

. "Laser Excitation of Atomic Inner-Shells by Coherent Processes with Implications for X-Ray Lasers," K. Boyer and C. K. Rhodes, Southwest Conference on Optics, Vol. 540, Robin S. McDowell, editor (SPIE, 1985).

. "A Theoretical Model of Inner-Shell Excitation by Outer-Shell Electrons," A. Szöke and C. K. Rhodes, Phys. Rev. Lett., in press.

. "High Order Nonlinear Processes in the Ultraviolet," T. S. Luk, U. Johann, H. Egger, K. Boyer, and C. K. Rhodes, in Laser Spectroscopy VII, edited by T. W. Hänsch and T. R. Shen (Springer-Verlag, Berlin, in press).

. "Cryogenic XeF Excimer Laser," M. Shahidi, H. Jara, H. Pummer, H. Egger, and C. K. Rhodes, in Conference on Lasers and Electro-Optics '85, May 21-24, 1985, Baltimore, Maryland, ThZZ6-1 (Post-deadline Paper Supplement).

. "Ultraviolet Excitation of Cryogenic Rare-Gas Chlorine Solutions," H. Jara, M. Shahidi, H. Pummer, H. Egger, and C. K. Rhodes, in Conference on Lasers and Electro-Optics '85, May 21-24, 1985, Baltimore, Maryland, p. 154.

. "Evidence for Atomic Inner-Shell Excitation in Xenon from Electron Spectra Produced by Collision-Free Multiphoton Processes at 193 nm," U. Johann, T. S. Luk, H. Egger, H. Pummer, and C. K. Rhodes, in Conference on Lasers and Electro-Optics '85, May 21-24, 1985, Baltimore, Maryland, p. 152.

. "Multiphoton Inner-Shell Atomic Excitation and Multiple Ionization," U. Johann, T. S. Luk, and C. K. Rhodes, XIVth International Conference on the Physics of Electronic and Atomic Collisions, edited by D. C. Lorents, W. E. Meyerhof, and J. R. Peterson, (North-Holland, Amsterdam, in press).

46. "Multiphoton Ionization in Ultrahigh Optical Fields: A Statistical Description," H. Egger, U. Johann, T. S. Luk, and C. K. Rhodes, J. Opt. Soc. Am., in press.

47. "Rare Gas Electron Energy Spectra Produced by Collision-Free Multi-quantum Processes," U. Johann, T. S. Luk, H. Egger, and C. K. Rhodes, submitted to Phys. Rev. A.

APPENDIX B

SUB-PICOSECOND KrF* EXCIMER LASER SOURCE

A. P. Schwarzenbach, T. S. Luk, I. A. McIntyre, U. Johann, A. McPherson,
K. Boyer, and C. K. Rhodes
Department of Physics, University of Illinois at Chicago
P. O. Box 4348, Chicago, Illinois 60680

ABSTRACT

A KrF* laser system capable of producing 23 ± 2 mJ in pulses of 450 ± 150 fsec duration (59 ± 24 GW) is described. Efficient extraction of the stored energy in the final amplifier is demonstrated at ~ 10 mJ cm^{-2}, thus showing that nonlinear losses in the amplifying medium up to intensities of ~ 20 GW cm^{-2} are not significant.

Considerable interest exists in the development of high power ultraviolet (UV) sources for use in areas such as surface science,[1] the study of atomic nonlinear phenomena[2] and for use in multiphoton pumping of vacuum ultraviolet[3] and X-ray lasers.[4] Systems based on rare-gas halide (RGH) excimer amplifiers have been used in the past to produce high power UV pulses with picosecond durations (5 - 8). Recent advances in subpicosecond laser technology have now allowed researchers to more fully utilize the broad gain bandwidth of RGH excimer systems [e.g. ~ 3.4 nm (~ 550 cm^{-1}) in KrF^* (9)] in order to produce high power UV pulses in the subpicosecond regime. A system based on amplification in $XeCl^*$ at 308 nm was recently reported to have produced 10 mJ pulses of ~ 350 fsec duration (10).

This letter reports the operation of a subpicosecond high power laser system based on KrF^* amplifiers which has produced pulses of 23 $\pm$ 2 mJ and 450 $\pm$ 150 fsec duration at 248 nm. The method used to generate the 248 nm seed pulses is shown schematically in Figure (1). A mode-locked, frequency doubled Nd:YAG laser (Quantronix 416) operating in the cw-mode is used to pump synchronously a passively mode-locked dye laser (Coherent 702). The dye laser uses a 4×10^{-2} M solution of Pyridine 2 in ethylene glycol and the saturable absorber employed is a 2×10^{-5} M solution of HITCI, also in ethylene glycol. The dye laser is tuned to 745 nm using a single plate birefringent filter and is cavity dumped at a rate of 3.8 MHz. A continuous train of ~ 1 psec pulses is produced which has an average power of 40 mW.

These pulses are fed into a fiber-grating compressor which employs a 1 m length of single-mode, polarization-preserving fiber with a 3.2 μm core diameter (ITT 1605) and a 600 line mm^{-1} holographic grating which is double-passed using a prism retroreflector. Approximately 25% of the incident radiation is passed through the fiber, and with a grating efficiency of ~40%

per pass, the average power after compression is 1.5 mW. The compressed pulse shows an autocorrelation FWHM of 380 fsec (Fig. 2), a value corresponding to a duration of 250 fsec if a $sech^2$ pulse shape is assumed.

Single pulses are amplified in a two-stage dye amplifier which is transversely pumped by a frequency-doubled, Q-switched Nd:YAG laser (Quantel YG 580). The amplifier cells contain a 10^{-3} M solution of Oxazine 750 in propylene carbonate/methanol and a solid saturable absorber (Schott glass RG850, 1 mm) is placed between the cells to reduce amplified spontaneous emission (ASE). The amplified 745 nm pulse typically has an energy of around 130 μJ and the pulse length, measured using a noncollinear second harmonic technique (11,12), is ~ 270 fsec. The ASE content is about 5% of the energy. The averaged spectrum of 50 shots is shown in Figure (3a) and that of a single shot in Figure (3b). The single shot spectrum is found to vary considerably from pulse to pulse, but the pulse length remains between 260 - 290 fsec, about twice the transform limit.

The 745 nm radiation is converted to a wavelength suitable for excimer amplification by frequency doubling to 372 nm in KDP and then sum-frequency mixing the fundamental with its second harmonic in a second KDP crystal. Both crystals are cut for type I phase matching and an appropriate waveplate is used to orient the polarizations of the 372 nm and 745 nm beams parallel to one another before entering the mixing crystal. The lengths of the crystals were carefully chosen, since they have to meet conflicting requirements. In order to match the phase-matched bandwidth of the crystal with the broad bandwidth of the incident radiation and also to reduce the effects

of group velocity dispersion (the generated pulse falling behind the generating pulses), a short crystal is necessary. On the other hand, long crystal lengths are desired for efficient frequency conversion. The doubling crystal used is 3 mm long and the mixing crystal 0.5 mm long. The 745 nm radiation incident on the doubler has an intensity of 10 GW cm^2 without focussing which results in a 10% second harmonic generation efficiency. Conversion in the mixer is lower, around 5%, so the energy of the 248 nm seed pulse is about 500 nJ. No surface damage on either crystal has been observed while working with this intensity.

The 2 mm diameter 248 nm seed beam is then passed through the first of two KrF^* amplifier stages (a Lambda Physik MSC EMG 201 with the mirrors replaced by Brewster angle CsF_2 windows) in which the gain is measured to be about 1000. However, due to poor beam quality from the amplifier and distortion of the beam profile in the discharge, only about 80 μJ is passed by a spatial filter consisting of a 1 m focussing lens, a 250 μm pinhole and a 4 m collimating lens. The pinhole is placed in a 1 m evacuated tube in order to avoid the possibility of self-phase modulation in the focal region observed in (10). However, the signal to ASE contrast after the spatial filter is excellent, being > 600:1. Earlier measurements on the distortion introduced by the amplifier showed that the focussability of a diffraction limited beam would be reduced to twice the diffraction limit after passing through the EMG 201 amplifier (Figure 4).

The expanded beam (2 cm x 2 cm) is then passed through a second amplifier (Lambda Physik EMG 200) after which 23 ± 2 mJ are readily observed in a short pulse with up to 27 mJ being detected. An aperture is placed in front of the energy meter (a Gentec PRJ-M) to pass only the amplified beam. With the 248 nm seed beam blocked, this arrangement detects only 3 - 5 mJ ASE. Thus the energy contrast ratio is better than 5:1. Previous measurements on the EMG 200 showed that this amlifier introduced no beam distortion.

The linewidth of the amplified pulse is measured to be 5.8 Å. The pulse length of the amplified 248 nm beam was measured by using a single pulse, cross-correlation technique. An amplified 248 nm pulse was mixed with its 744 nm fundamental (τ ~ 270 fsec) in a 1 mm KDP crystal using a noncollinear geometry to obtain the difference frequency. The evaluation of the cross correlation signal (372 nm) showed a pulse duration of 450 ± 150 fsec for the 248 nm pulse after the first excimer amplifier.

Monitoring the amplified 248 nm output on a photodiode (Hamamatsu R 1328 and Tektronix 7912 AD transient digitizer) allows examination of the behavior of the ASE in the presence of the subpicosecond seed pulse. As can be seen in Figure (3), the ASE is clearly reduced after passage of the seed pulse, indicating that saturation of the second amplifier is taking place. The extracted energy density is ~ 10 mJ cm^{-2} and, significantly, the Brewster angle output window is exposed to an intensity of ~ 15 GW cm^{-2} without experiencing any damage. This is an important result since it indicates that the stored energy can be extracted efficiently from the gain medium, even on such short timescales, and therefore scaling upwards to larger aperture amplifiers will allow efficient amplification to terawatt power levels.

In conclusion, we have demonstrated the operation of a 25 mJ KrF^* source of high spectral brightness with a pulse duration of 450 $\pm$ 150 fsec, nominally delivering an optical peak power of ~ 60 GW. The ability to saturate the excited KrF^* medium has been proved and improvements to the beam peak power and focussability are in progress. Even without these improvements the beam has been focussed to ~ 10^{16} W cm^2 and used to yield new results in ion and electron spectra produced by multiphoton excitation of atomic species (13).

Acknowledgements

The authors wish to thank H. Egger for useful discussion, and R. Bernico, T. Pack, R. Slagle, and J. Wright for technical assistance. This work was supported by the Office of Naval Research, the Air Force Office of Scientific Research under contract number F49620-83-K-0014, the Innovative Science and Technology Office of the Strategic Defense Initiative Organization, the Department of Energy under grant number DE-AC02-83ER13137, the Lawrence Livermore Laboratory under contract number 5765705, the National Science Foundation under grant number PHY 84-14201, the Air Force Office of Scientific Research, Department of Defense University Research Instrumentation Program under grant number USAF 840289, the Defense Advanced Research Projects Agency, and the Los Alamos National Laboratory under contract number 9-X74-C6096-1.

References

1. R. Haight, J. Bokor, J. S. Stark, R. H. Storz, R. R. Freeman, and P. H. Bucksbaum, Phys. Rev. Lett. 54, 1302 (1985); C. K. Rhodes in Novel Materials and Techniques in Condensed Matter, edited by G. W. Crabtree and P. Vashishta (Elsevier Science Publishing Co., New York, 1982) p. 151.
2. T. S. Luk, U. Johann, H. Egger, H. Pummer, and C. K. Rhodes, Phys. Rev. A32, 214 (1985).
3. C. K. Rhodes, Science 229, 1345 (1985).
4. H. Egger, H. Egger, T. S. Luk, T. Srinivasan, and C. K. Rhodes, Phys. Rev. A28, 795 (1983).
5. P. A. Bucksbaum, J. Boker. R. H. Storz, and J. C. White, Opt. Lett. 7, 399 (1982).
6. P. B. Corkum and R. S. Taylor, IEEE J. Quantum Electron. QE-18, 1962 (1982).
7. H. Egger, T. S. Luk, K. Boyer, D. F. Muller, H. Pummer, T. Srinivasan, and C. K. Rhodes, Appl. Phys. Lett. 41, 1032 (1982).
8. S. Szatmari and F. P. Schäfer, Appl. Phys. B33, 219 (1984).
9. Ch. Wittau, Excimer Lasers, C. K. Rhodes ed. (Springer-Verlag, Berlin, 1979) p. 91.
10. J. M. Hownia, G. Arjavalingham, P. P. Sorokin, and J. E. Rothenburg, "Amplification of 350 fs Pulses in XeCl Excimer Gain Modules," (to be published).
11. J. Janszky, G. Corradi, and R. N. Gyuvalian, Opt. Comm. 23, 293 (1977).

12. C. Kolmedo, W. Zirth, and W. Kaiser, Opt. Comm. 30, 453 (1979).

13. U. Johann, T. S. Luk, I. A. McIntyre, A. P. Schwarzenbach, K. Boyer, and C. K. Rhodes, "Subpicosecond Studies of Collision-Free Multiple Ionization of Atoms at 248 nm" (Phys. Rev. Lett., submitted).

Figure Captions

1. Schematic showing the dye laser and amplification system used to generate the seed pulses at 248 nm.

2. Autocorrelation trace after pulse compression. The pulsewidth is deduced from the autocorrelator signal assuming a $sech^2$ pulse shape.

3. a) Average spectrum of 50 shots of the amplified 745 nm pulse, showing a linewidth of 60 Å.

   b) Single shot spectrum of an amplified 745 nm pulse. Horizontal scale the same as in a).

4. a) Showing the beam profile of the focus of a diffraction-limited beam on a Reticon after passing through an MSC EMG 201 amplifier without the discharge running.

   b) Showing the same as a) but with the amplifier switched on. Note the increased spot size.

5. Showing the output from the second amplifier. Note how the ASE is reduced after the short pulse, showing a depletion of the upper level.

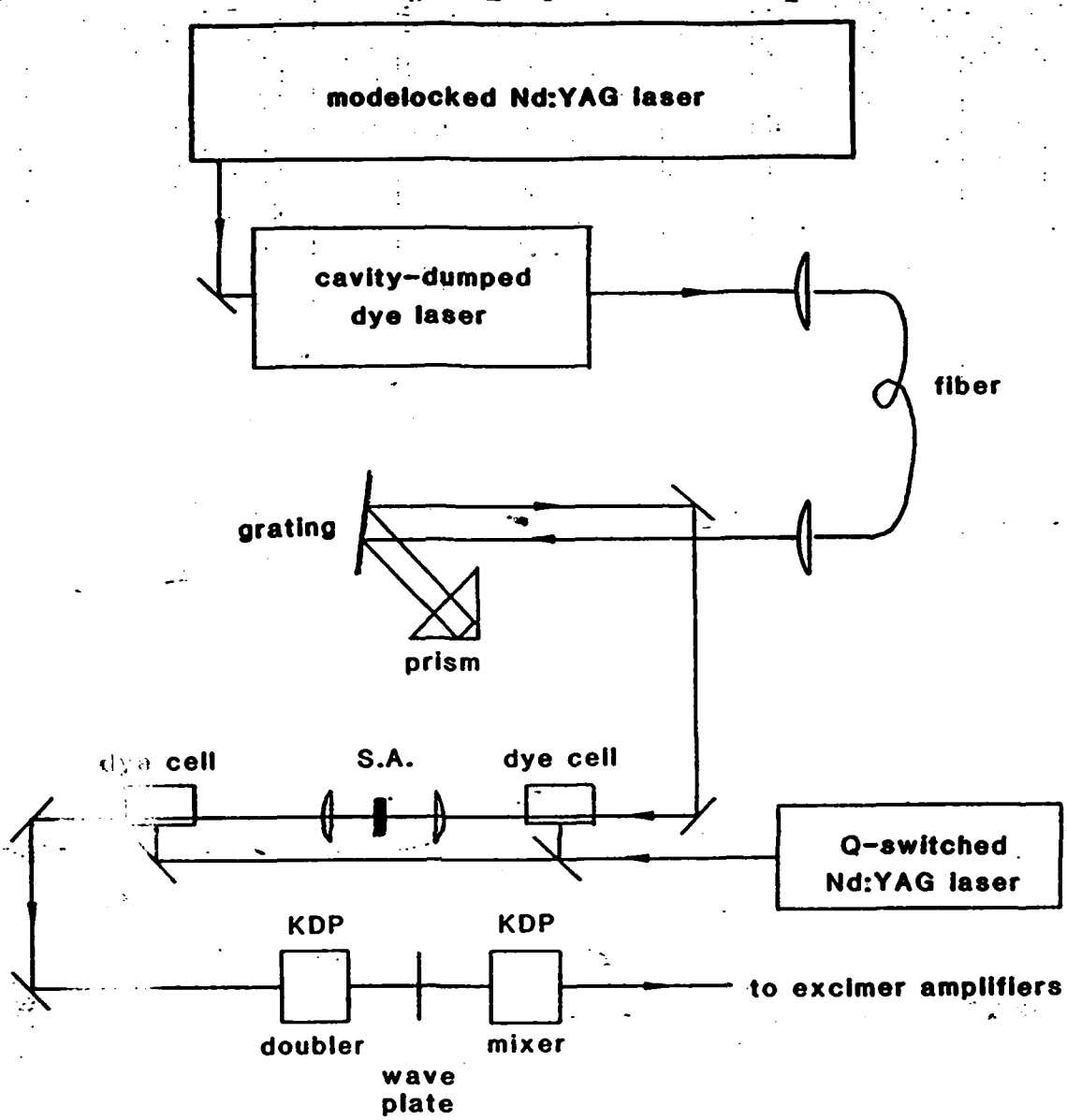
modelocked Nd:YAG laser
cavity-dumped dye laser
fiber
grating
prism
dye cell
S.A.
dye cell
Q-switched Nd:YAG laser
KDP
KDP
to excimer amplifiers
doubler
mixer
wave plate

fig. 1

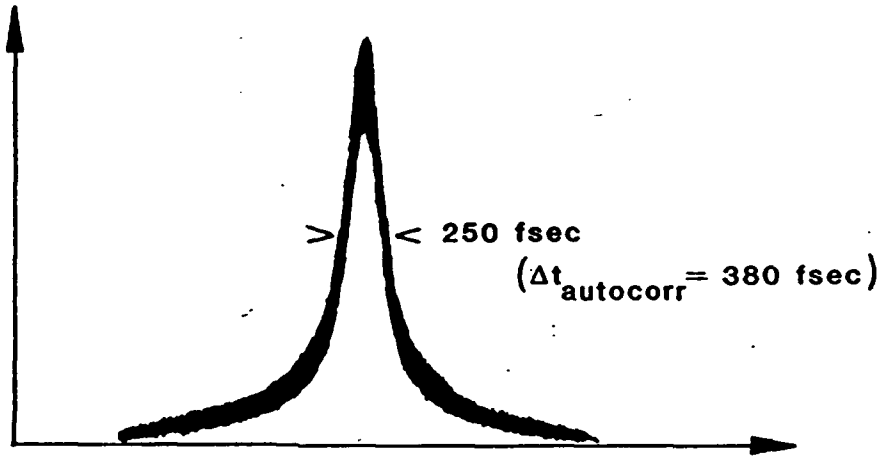

ig. 2

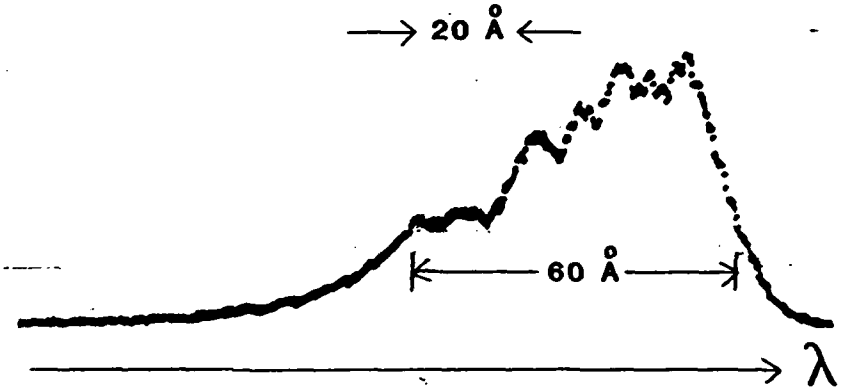

fig. 3a

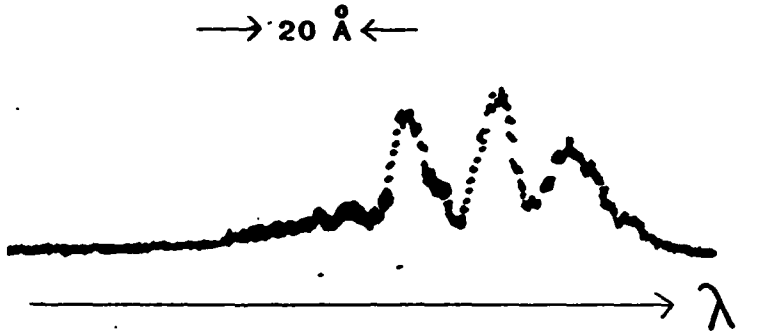

Fig.

(a) amplifier off

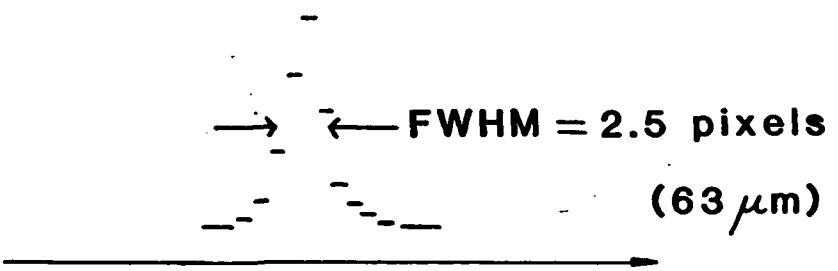

(b) amplifier on

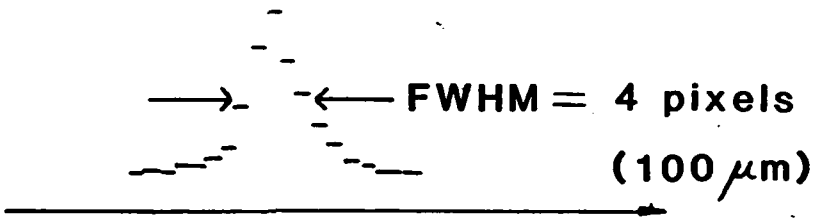

Fig 4

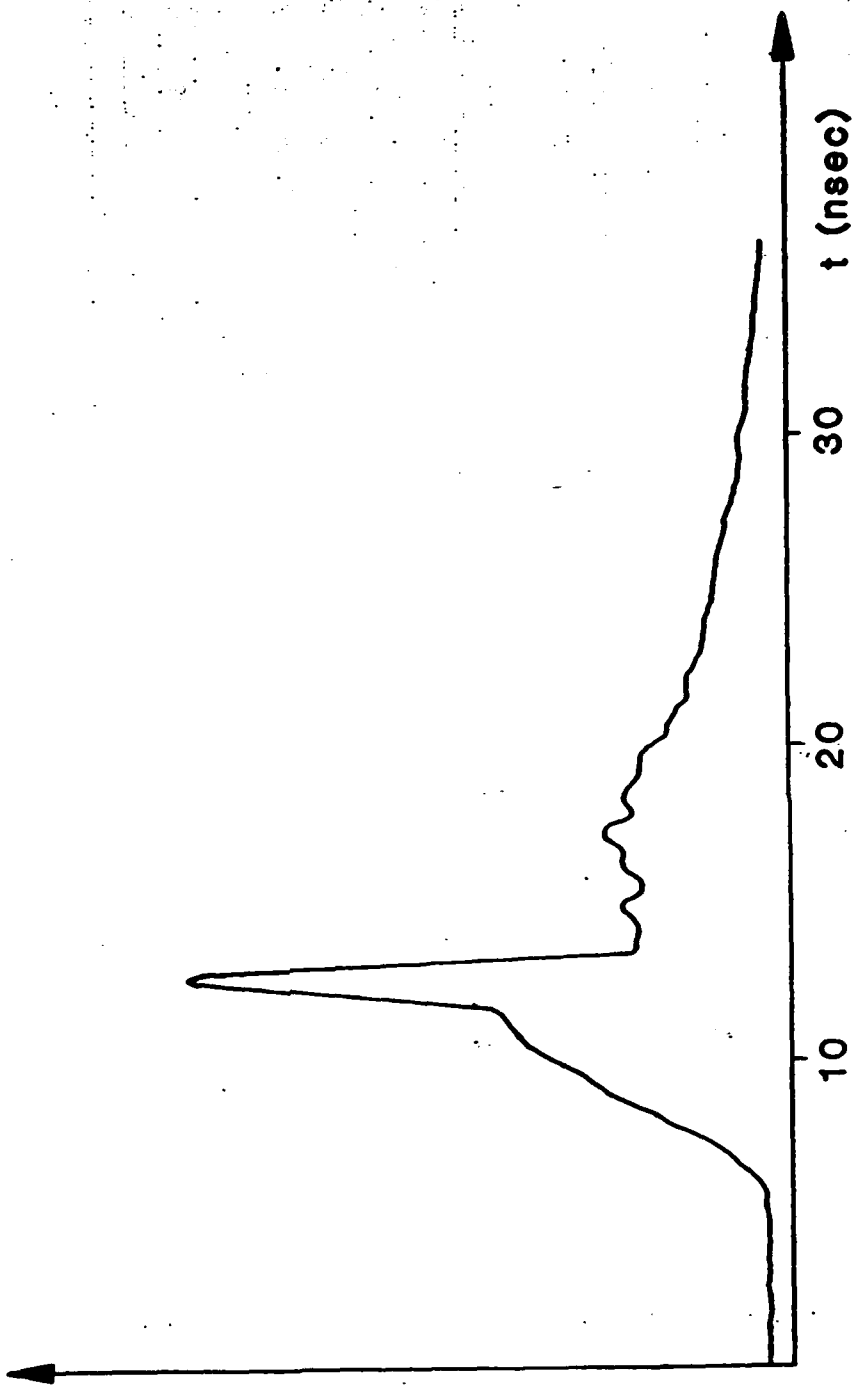

Fig. 5

APPENDIX C

27 September 1985, Volume 229, Number 4720 SCIENCE

Multiphoton Ionization of Atoms

Charles K. Rhodes

Summary. Studies of multiphoton ionization of atoms have revealed several unexpected characteristics. The confluence of the experimental evidence leads to the hypothesis that the basic character of the atomic response involves highly organized, coherent motions of entire atomic shells. The important regime, for which the radiative field strength is greater than an atomic unit (e/a_0^2), can be viewed in approximate correspondence with the physics of fast (approximately 10 MeV per atomic mass unit) atom-atom scattering. This physical picture provides a basis for the expectation that stimulated emission in the x-ray range can be produced by direct, highly nonlinear coupling of ultraviolet radiation to atoms.

The invention of the laser made possible the experimental study of the nonlinear interaction of radiation with matter. And, subsequently, over the last two decades, a considerable field of activity has developed around that basic problem, which can be represented generically by the process

$$N\hbar\omega + X \rightarrow X^* \qquad (1)$$

in which N photons lead to the excitation of a target atom or molecule X. For generality the excited product X^* can denote either bound or continuum motions of the constituent particles. This article will deal with certain recent findings concerning multiphoton ionization. The context of this physical study, however, relates directly to another problem of general fundamental significance and one that has had an important influence on the direction and purpose of work at the University of Illinois at Chicago. That problem concerns the development of a laser at x-ray wavelengths, a long-sought goal.

Historically, the initial discussions of coherent generation in the x-ray range (*1*) and nonlinear atomic emission (*2*) and absorption (*3*) all appeared more than 20 years ago in entirely independent circumstances. Recently, however, these two areas of inquiry have become strongly linked, and it now appears that the achievement of the former may depend, at least in one possible representation, on certain basic properties of the latter.

The significance of the x-ray laser goal is easily stated. A spectrally bright source of radiation in the x-ray region would be unsurpassed (*4*) in its ability to microvisualize condensed matter. There is little doubt that major areas of application would include basic materials research, microelectronics, biology, and, indeed, any field that requires structural information of solid matter on an atomic scale. Since the peak spectral brightness of an x-ray laser is expected to be on the order of one trillion times greater than any alternative means, it would be an ideal source of radiation for these purposes. At the same time, it is undisputed that matter, under appropriate conditions, can provide the amplification in the x-ray range ($\hbar\omega \sim 10^3$ to 10^4 eV) that is necessary to construct a coherent source. However, the achievement of those suitable conditions has proven to be a formidable task.

The difficulty in generating amplification at a quantum energy of 1 keV is apparent from the general requirement, established by basic physical reasoning, that extraordinarily high specific power densities, on the order of 10^{14} W/cm^3 or greater, be applied in a carefully controlled way (*1*, *5*). How can these necessary conditions best be produced? It is generally understood (*1*, *5*) that a high effective brightness source of excitation and an appropriate physical coupling mechanism are the key requirements for the successful creation of the conditions for amplification in the x-ray range. Although several alternative approaches are currently being evaluated, over the last few years our work has centered on the use of high-power ultraviolet lasers to serve as the source of excitation and nonlinear radiative processes to provide the needed physical coupling. In order to evaluate whether this idea could work, we began our study of multiple quantum ionization.

A simple representation of the overall process is illustrated in Fig. 1. Obviously, if $\hbar\omega_x$ is in the kilovolt range and if $\hbar\omega$ represents an ultraviolet quantum, processes with values of N exceeding 100 must occur with appreciable probability in order for this mechanism to be useful. Therefore, a single fundamental question emerges: What are the basic physical principles that establish the limit on N?

When we began to study this question, no relevant experimental data on this matter existed. This was particularly true for radiative field strengths (E) in the vicinity of an atomic unit, e/a_0^2, where a_0 is the smallest Bohr radius. Extant theoretical work, however, predicted ridiculously low rates for high-order processes and, if believed, would automatically lead to the conclusion that any proposal to utilize a mechanism, such as that shown in Fig. 1, is preposterous. These earlier theories, however, were based on rather restrictive assumptions concerning the basic nature of the electronic motions governing the nonlinear amplitudes. On the other hand, several years ago I found it possible to construct a class of high-order processes, involving certain types of atomic motions, in which the rates would be enormously enhanced. Are such motions possible? I now believe that the method used to calculate those original estimates

The author is in the Department of Physics, University of Illinois at Chicago, P.O. Box 4348, Chicago, Illinois 60680.

was in many ways incorrect, although the conclusion derived may not be. In any case, the basic question had been raised and resolution of the issue could only come from experiment.

Experimental Studies

Basically, there are three categories of fundamental physical measurement, founded respectively on the spectroscopy of (i) ions, (ii) electrons, or (iii) photons, that can be used to unravel the nature of the physical processes involved in the nonlinear interactions under study. In our work we have used ion charge-state spectra, photoelectron energy spectra, and the properties of scattered radiation. Among these, the measurement of ion charge-state spectra under collision-free conditions provides a simple, unambiguous experimental test that gives direct information on the scale of the energy-transfer rate between the radiation field and the atom. Therefore, as a first step, such experiments were performed. The results of these initial studies were surprising, for it was from measurements (*6*, *7*) of this kind that the first suggestions of an anomalously strong coupling for high-order processes ($N \sim 100$) were obtained.

The general class of physical processes studied in those experiments examining ion charge-state spectra (X^{q+}) was

$$N\gamma + X \rightarrow X^{q+} + qe^- \qquad (2)$$

Some of the apparatus used in the work described below is illustrated in Fig. 2, which shows the 193-nm ultraviolet laser system, the time-of-flight ion spectrometer, and the time-of-flight electron analyzer. Available ultraviolet laser technology makes the performance of such studies convenient, since extraordinarily high brightness and, therefore, unusually large focused intensities are possible with these laser sources. Initially, studies (*6*) of the process represented by Eq. 2, a subclass of the general reaction in Eq. 1, were conducted with 193-nm radiation at an intensity of approximately 10^{14} W/cm^2.

Figure 3 illustrates the range of intensity that has been explored over the past 2 years along with a projection of the experimental regime that should become available over a comparable period in the future. Currently, peak intensities in the range of 10^{16} to 10^{17} W/cm^2 can be produced with pulses having a duration of a few picoseconds at a wavelength of 193 nm. At this intensity, the electric field E_0 is comparable to an atomic unit. Furthermore, as shown in Fig. 3, it is believed

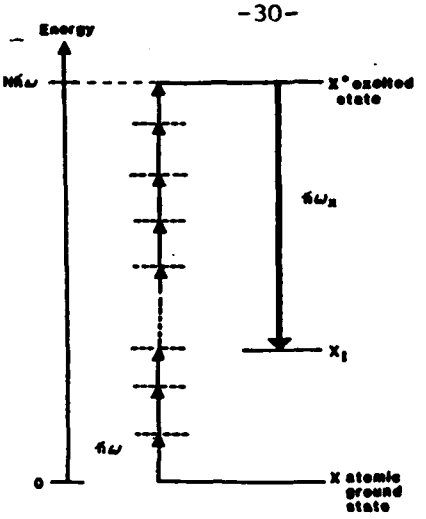

Fig. 1. Simple representation of an atomic multiquantum process involving the absorption of N ultraviolet quanta ($\hbar\omega$) to produce an appropriate upper state X^* that is inverted with respect to the population in a lower level X_f. Since a kilovolt energy scale is assumed for $\hbar\omega_n$, $N \gg 1$ and X^* and X_f will generally lie far above the ionization energy of the neutral atomic ground-state system X.

that technical advances in femtosecond ultraviolet laser technology should enable peak intensities, for coherent energy, to be produced in the range of 10^{20} to 10^{21} W/cm^2. This would represent a radiation field amplitude of about 100 E_0 and, in terms of energy density, would be equivalent to that produced by a blackbody with a temperature close to 10 keV, which is an environment characteristic of thermonuclear sources. Although all the experiments to date have been conducted in the range of $E \lesssim E_0$, considerable attention in the discussion below will be given to this interesting and important regime for which $E \gg E_0$.

A prominent feature of the studies of the ion-charge spectra was the unusually strong nonlinear coupling characteristic of certain heavy materials (*6–9*), a feature that was apparent even at intensities in the vicinity of 10^{14} W/cm^2. These experiments clearly demonstrated that standard theoretical techniques were incapable, by a discrepancy as great as several orders of magnitude, of describing the observed charge-state spectra. A resemblance was perceived between the observed ion charge-state spectra and those known to be characteristic of Auger cascades (*7–10*). In addition, subsequent work by us, as well as other studies (*11*, *12*) conducted at wavelengths of 1.06 and 0.53 μm, confirmed the anomalous nature of the coupling strength. There was no doubt that the findings of these experiments were clearly in contradiction to all theoretical treatments, of which there is a considerable number (*13*). This unexpected result, of course, stimulated further studies.

In experiments to determine the role of atomic structure on the coupling mechanism, the ionic spectra of several elements from He ($Z = 2$) to U ($Z = 92$) were studied (*6–9*). A typical ionic spectrum for Xe, produced by 193-nm radiation at an intensity of about 10^{16} W/cm^2 with pulses of about 5 psec in duration, is illustrated in Fig. 4. The presence of all charge states up to Xe^{8+}, the first five of which have approximately comparable abundances, is immediately noted. An overall summary of the ionic species registered in the survey of the atomic number dependence is presented in Fig. 5. Here, the maximum observed energy transfers are on a scale of several hundred electron volts for certain heavy materials.

One of the salient features of the data is the apparent influence of atomic shell structure (*6*) on the observed ion spectra. This dependence is manifested prominently in the behavior of the heavier rare gases. For Ar, Kr, and Xe, the maximum charge states observed correspond to the complete removal of certain outer atomic subshells. Indeed, for these materials they are the $3p$, the $4p$, and both the $5s$ and $5p$ shells, respectively.

The hint provided by the role of the shell structure led to the hypothesis that it was mainly the number of electrons in the outer subshells that governed the coupling. A measurement of the response of elements in the lanthanide region, with the use of a method involving laser-induced evaporation (*14*) to provide the material, enabled this view to be checked. From La ($Z = 57$) to Yb ($Z = 70$) in the lanthanide series, aside from slight rearrangements (*15*) involving the $5d$ shell for Gd ($Z = 64$), $4f$ electrons are being added to interior regions (*16*) of the atoms. The data illustrated in Fig. 5 for Eu ($4f^7 6s^2$) and Yb ($4f^{14} 6s^2$), which differ by seven $4f$ electrons, indicate that these inner electrons play a small role in the direct radiative coupling, a fact that is in rapport with the observed dependence on the outer-shell structure.

The intensity dependence of these ion spectra was also examined (*8*, *9*). Over the range of intensities studied (~10^{15} to 10^{17} W/cm^2), higher intensity generally translated into an increased yield of ions of a particular charge, although not necessarily an increase in the maximum charge state observed. For example, the ion Xe^{8+}, with closed-shell ground-state (*17*) configuration $4d^{10}$, was the greatest charge state detected at approximately 10^{16} W/cm^2 and, although its abundance

increased at about 10^{17} W/cm^2, no Xe^{9+} appeared at the higher intensity. This observation has led to the interpretation that the $3p$ and $5s$ electrons in Xe are the ones that govern the direct coupling of the atom to the ultraviolet radiation field.

It was also possible to obtain information on the frequency dependence of the coupling by comparing the results at 193 nm (*8*) with studies performed independently at 1.06 and 0.52 μm (*12*). This comparison, which was conducted for an intensity of about 10^{14} W/cm^2 for both Kr and Xe, indicated that the energy transfer rate was reduced at the longer wavelengths.

Overall, the ion studies showed (i) anomalously strong nonlinear coupling for certain heavy materials, (ii) an unmistakable signature of atomic shell effects, and (iii) that energy transfer rates were generally greater at shorter wavelengths of irradiation. Moreover, the experimental evidence strongly suggested, at least in a first approximation, that the greater the number of electrons in the outer shell, as designated solely by the principal quantum number, the greater the strength of the nonlinear coupling (*6–9*).

Since it is expected that the measurement of photoelectron energy distributions could provide valuable information on the detailed nature of the electronic motions occurring in reactions such as that shown in Eq. 2, experiments of that type, performed under collision-free conditions, have been conducted (*18*). This expectation, indeed, appears to be borne out. For example, substantial differences in the electron distributions produced by Ar and Kr were seen even though the ion spectra for these materials are similar and show that the outer p shell is completely stripped in both cases (*8, 9*).

The most significant results now available, however, appear in connection with the behavior of Xe. Indeed, in contrast to Ar and Kr, the Xe electron energy spectrum exhibits a dramatic change with increasing intensity of the 193-nm radiation in the range of 10^{14} to 10^{15} W/cm^2. The first ionization line, which corresponds to two-photon absorption with an attendant photoelectron energy of 0.7 eV, nearly disappears, while the three-photon process, arising from continuum-continuum transitions (*19*), becomes dominant. Furthermore, the final-state distribution of the ions generated for the three-quantum process has approximately 80 percent in the excited $5s^25p^5\ ^2P_{1/2}$ state, with the remaining 20 percent in the $5s^25p^5\ ^2P_{3/2}$ ground-level state.

In addition to the ladder of continuum-continuum lines, new sharp photoelectron features appear in the range from 8 to 22 eV at an intensity of about 10^{15} W/cm^2. These lines have been assigned to $N_{45}00$ Auger lines after excitation of the $4d$ inner shell. The most prominent lines are those associated with $N_{45}0_10_1$ transitions, which terminate in the $4d^{10}5s^05p^6$ double-hole state. This identification is predicated on the observation that their relative spacing, number, and, to a somewhat lesser extent, relative intensities fit well to values previously reported (*20*) for such Auger transitions. Moreover, a total of eight electron lines is observed, representing a quartet of pairs of transitions, all of which exhibit the known (*20*) $4d_{3/2}$ to $4d_{5/2}$ splitting in Xe of approximately 2 eV.

The general trend (*21, 22*) of the electron spectrum for Xe as a function of intensity is illustrated in Fig. 6. The appearance of a group of lines at an intensity of about 10^{15} W/cm^2 is attributed to Auger decay of $4d$ vacancies in the atom. This spectral region (*18*), which is believed to represent $N_{45}00$ Auger processes, is shown in higher resolution in Fig. 7.

Finally, further experimental evidence bearing on the mechanism of coupling is present in the characteristics of certain stimulated emission spectra that have been observed in Kr (*23*). In this case, the states believed to be involved are those having multiple excitations and inner-shell excitations (*24*) in closely coupled subshells, such as $4s4p^6nl$ and $4s^24p^4nln'l'$. As discussed below, this class of levels is of exactly the type expected to be strongly excited if certain highly organized atomic motions, which are consistent with both the ion charge–state and photoelectron spectra, are driven by the radiation field.

Mechanism of Coupling

We are now in a position to interpret the experimental findings in terms of a specific, although highly speculative, model for the atomic response. The main purpose of the description given below is

Fig. 2. Experimental apparatus used in the studies of multiphoton ionization at the University of Illinois at Chicago. (a) Output amplifier (left) of the gigawatt 193-nm picosecond laser system; (b) ion time-of-flight spectrometer; and (c) electron time-of-flight spectrometer.

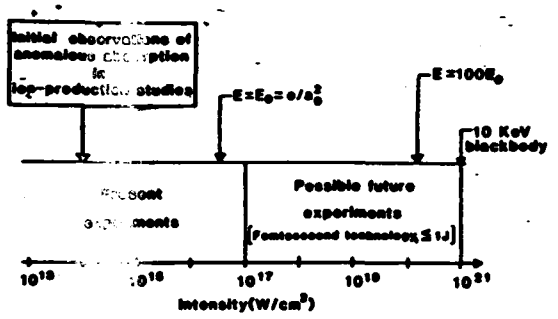

Fig. 3. Representation of present and possible future ranges of intensity of irradiation available with high-brightness ultraviolet laser technology. Initial observations of anomalous processes were made at approximately 10^{14} W/cm^2. Intensities comparable to thermonuclear environments ($\sim 10^{21}$ W/cm^2) appear to be possible with pulse lengths in the 100-fsec range containing about 1 J of energy.

not to provide an exact definitive analysis, which now obviously is impossible, but rather to furnish a framework for the process of physical reasoning that should reveal the true nature of these very nonlinear mechanisms.

From the analysis of the data now at hand, which include information on the dependence on the atomic number Z (6–8), the intensity, the frequency, and the polarization, the following hypothesis has emerged as an approximate description of the basic character of the electronic motions involved in these processes. Overall, the data strongly indicate that an organized motion of an entire shell or a major fraction thereof, is directly involved in the nonlinear coupling. With this picture, the outer atomic subshells are envisaged as being transiently *set in coherent oscillation* by the intense ultraviolet wave. With this type of electronic motion, the observed increase in the multiphoton coupling strength can be qualitatively related (*8*) with the larger magnitude of the effective charge involved in the interaction. In quantum mechanical language, an oscillating shell would be represented by a wave function of a multiply excited configuration. In this way, a *multielectron* atom undergoing a nonlinear interaction responds in a fundamentally different fashion than that of a single-electron counterpart. A class of multiply excited configurations, consisting of doubly excited states, is known (*25*) to play an important role in processes of single-quantum photoionization. With this interpretation, the results of our studies of multiquantum ionization simply indicate a nonlinear analog of this basic electronic mechanism.

In principle, the response of an atom to a pulsed external field with an amplitude approaching an atomic unit, if calculated with full rigor in the framework of a time-dependent many-body theory, would present the possibility of a nearly unbounded level of complication. Therefore, in order to advance our understanding of this problem, we must find a simpler approximate form of analysis. An appropriately formulated treatment that correctly represents the basic nature of electronic motions, however, should be able to describe qualitatively the principal characteristics of the experimental observations. These include the basic coupling strength and resulting energy transfer rate, the shell effects, the origin of the strong nonlinearity, the frequency characteristics, and the ability to produce atomic inner-shell excitation.

In order to achieve that goal, we can contemplate a relatively simple model (*8*, *9*) that is valid at sufficiently high intensity. In this case, we imagine an atom composed of two parts: an outer shell of electrons (*a*) driven in coherent oscillation by the radiative field, and a remaining atomic core (*b*) for which direct coupling to the radiation field is neglected (Fig. 8). In this picture, coupling between these two systems can occur, since the outer electrons could, through inelastic "collisions," transfer energy to the core. Simple estimates (*9*) indicate that, for intensities corresponding to an electric field $E \gg e/a_0^2$, enormous oscillating atomic current densities j on the scale of 10^{14} to 10^{15} A/cm^2 could be temporarily established in the outer regions of the atom. For ultraviolet radiation under these conditions, the electrons in the outer atomic shell can be accelerated to mean kinetic energies considerably higher than 10 KeV, a value far above their respective binding energies (*9*). Furthermore, in the limit of high intensity, it is possible to formulate an estimate of the coupling of the coherently driven outer electrons with the remaining atomic core by relatively simple procedures. This is now done at two levels of approximation, initially with the neglect of the influence of the coherence characterizing the motion of the outer electrons and, subsequently, with its inclusion.

An estimate can now be furnished based simply on the magnitude of the ambient current density j. Since the electron kinetic energies are considerably higher than their corresponding binding energies, it is possible to use a first-order Born approximation (*26*) in a manner similar to that used to study electron collisions for K- and L-shell ionization (*27*) and shell-specific ionization processes in highly charged ions (*28*). Indeed, in the case of Xe ions, measured cross sections for electron impact ionization are available (*29*).

In this elementary classical picture (*9*), the transition rate R can be written as

$$R \simeq j\sigma_e \qquad (3)$$

in which e is the electronic charge and σ_e is the cross section characterizing the excitation of the atomic core by inelastic electron collisions arising from the current density j. If $j \simeq 10^{14}$ A/cm^2 and $\sigma_e \simeq 10^{-19}$ cm^2, then $R \simeq 6 \times 10^{13}$ sec^{-1}. Furthermore, if the radiatively driven current density j is damped by electron emission in a time τ on the order of about 10^{-15} seconds, which is an approximate time scale characterizing autoionization, then the overall transition probability $P \simeq R\tau \simeq 6 \times 10^{-2}$, indicating a significant probability of energy transfer.

The characterization of the outer-shell motion as a simple current density j, however, does not take into account the fact that the electronic motions are gen-

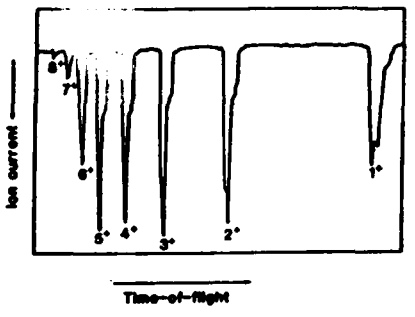

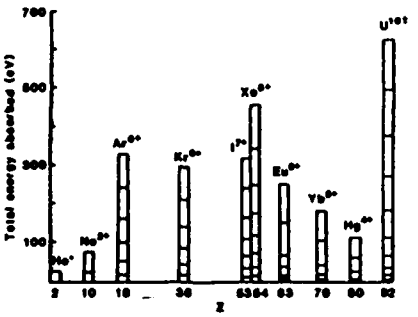

Fig. 4 (left). Collision-free ion time-of-flight spectrum of Xe produced by 193-nm irradiation at an intensity of about 10^{16} W/cm^2 with pulses having a duration of about 5 psec. The distortion of the charge-state peaks is caused by the naturally occurring isotopic distribution of Xe. The charge states of the Xe^{q+} species observed are indicated. Fig. 5 (right). Data concerning the multiple ionization of atoms produced by irradiation at 193 nm: plot of total ionization energies of the observed charge states as a function of atomic number Z. The coincidence of an H_2O^+ background signal prevented the I^{7+} species from being positively identified.

erated through interaction with a coherent wave. It is expected that the coherence associated with the motions of the outer-shell electrons induced by intense irradiation will have important consequences (*30*) for the coupling of energy to atomic inner shells that were ignored in the simple estimate given above. The influence of this type of coherent atomic motion is now described in relation to certain properties (*31*) of energetic (≳10 MeV/amu) atom-atom collisions.

The role of coherence in the motion of the outer electrons in the excitation of the core is readily described in terms of energetic atom-atom (*A-B*) collisions. In this comparison (*30*), a correspondence is established, as shown in Fig. 8, between the scattering of the coherently driven outer electrons *(a)* from the atomic core *(b)* and the respective interaction of the electrons in the projectile atom *A* with the target atom *B*. Consider the process

$$A + B(0) \xrightarrow{e} A + B^*(n) \qquad (4)$$

in which *A* is a ground-state neutral atom with atomic number Z_A and $B^*(n)$ represents an electronically excited configuration of the target system with quantum numbers collectively represented by *(n)*. In the plane-wave Born approximation (PWBA), the cross section σ_{n0} can be written in the form presented by Briggs and Taulbjerg (*31*) as

$$\sigma_{n0} = \frac{8\pi e^4}{v^2} \times \int_{K_{min}}^{K_{max}} |\epsilon_{n0}^B(\mathrm{K})|^2 \, [|Z_A - \textstyle\sum_j \omega_j < \phi_j^A| \exp(i\mathrm{K}\cdot s_A)\, |\phi_j^A> |]^2 \frac{dK}{K^3} \qquad (5)$$

in which

$$\epsilon_{n0}^B(\mathrm{K}) = \int dr_B^3 \psi_{nB}^*(r_B) \exp(i\mathrm{K}\cdot r_B) \psi_{0B}(r_B) \qquad (6)$$

In Eqs. 5 and 6, *e* is the electron charge; Z_A is the atomic number of the projectile atom; *v* is the relative atom-atom velocity; ϕ_j^A are orthonormal spin orbitals representing the electrons on the projectile atom with spatial coordinate s_A; ω_j is the statistical weight of the shell; K is the momentum transfer in the collision; and ψ_{0B} and ψ_{nB} represent the electron wave functions of the target system as a function of the spatial variable r_B. The summation over the index *j* appearing in Eq. 5 extends over all occupied orbitals so that, in the limit $\mathrm{K} \to 0$, the summation tends to the number of electrons N_A associated with the projectile atom (*31*). In the low-momentum transfer limit, in which complete screening occurs, the amplitudes of the electrons combine coherently, and the contribution to the cross section σ_{0n} arising from the motion of the electrons in atom *A* is increased by a factor of N_A^2 over that of a single electron at the same collision velocity *v*. Equivalently, for sufficiently low momentum transfer such that $Ka_0 \ll \hbar$, the electron cloud acts as a coherent scattering center with a mass $N_A m_e$, a charge $N_A e = Z_A e$, a velocity *v*, and a kinetic energy $N_A(1/2\ m_e v^2)$. Significantly, because of the coherence, the single-particle energies $(1/2\ m_e v^2)$ add so that, in principle, this value could be below the magnitude required to produce the excitation of the target atom *B*.

In sufficiently high field strengths, it appears that coherently accelerated electrons in outer atomic shells *(a)* can interact with the remaining atomic core system *(b)* in a manner closely analogous to the atom-atom scattering described above. If a PWBA description is used, the cross section representing energy transfer can be written by inspection from Eq. 5 with $Z_A = 0$. The basic physical concepts are simply represented in the high field limit ($E \gg e/a_0^2$), a regime in which the driven electronic velocities correspond approximately to those characteristic of atom-atom collisions at a collision energy of approximately 10 MeV/amu. *Therefore*, the motion of these electrons can simulate the electronic collisional environment that would occur in fast atom-atom encounters but with the

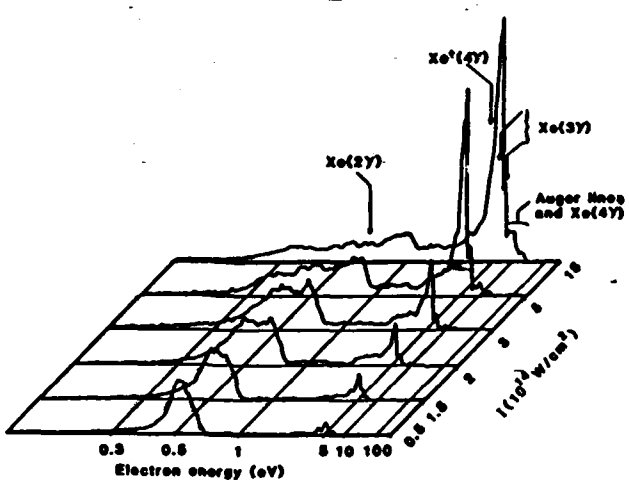

Fig. 6. Overall time-of-flight photoelectron spectrum for Xe from approximately 0.1 to 100 eV. The uncertainty in the intensity scale is approximately a factor of 2. Irradiation was at 193 nm with a pulse duration of about 5 psec and a lens with a focal distance of 20.5 cm. Electron lines originating from Xe and Xe^+ arising from two 2γ and three 3γ and 4γ processes are indicated along with a group tentatively assigned as Auger features.

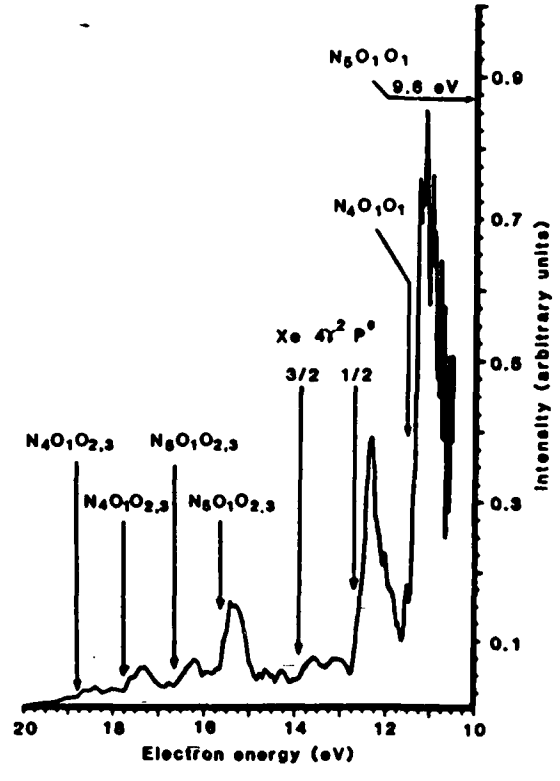

Fig. 7. Prominent transitions observed in the electron spectrum of Xe irradiated at 193 nm and approximately 10^{15} W/cm². Both continuum-continuum ($4\gamma \rightarrow Xe^+_{3/2}, Xe^+_{1/2}$) and tentatively assigned Auger ($N_{45}00$) features are apparent. The splittings between the three N_4–N_5 pairs, two of which are shown by horizontal arrows, have the common value of about 2 eV, which is the known $4d_{5/2}$ to $4d_{3/2}$ separation in Xe. The vertical arrows indicate the high-energy edges of the observed features that represent the true energies of the lines.

important absence of the nuclear contribution arising from the Z_A term in Eq. 5.

In order to see how this mechanism would scale with the basic physical parameters involved, we can now estimate the contribution of σ_{0n} for inner-shell excitation arising from coherently excited atomic shells. For this, Eq. 5 is taken with $Z_A = 0$ and K_{max} restricted to $\leq \hbar/a_0$ to fulfill the condition for complete shielding. Further, Z_1 can be taken to denote the number of electrons in the outer shells and Eq. 6 expanded for $\epsilon_{n0}^2(\mathbf{K})$ in the customary fashion, so that only the leading dipole term x_{0n} is retained. Finally, for a core excitation energy ΔE we put $K_{min} \simeq \Delta E/v$, which is the condition that holds for ΔE much less than the collision energy. With these modifications, the full coherent piece σ_{0n}^c can be written as

$$\sigma_{0n}^c \simeq \frac{8\pi e^4 x_{0n}^2 Z_1^2}{v^2\hbar^2} \int_{\Delta E/v}^{\hbar/a_0} \frac{dk}{K} \qquad (7)$$

a result that, with the exception of the restriction on K_{max} and the Z_1^2 factor, is exactly the form of the well-known result for inelastic scattering of electrons on atoms developed by Bethe (*32*). The final result, valid for

$$\alpha\left(\frac{v}{c}\right)\left(\frac{m_e c^2}{\Delta E}\right) > 1 \qquad (8)$$

is

$$\sigma_{0n}^c \simeq \left(\frac{c}{v}\right)^2 Z_1^2 x_{0n}^2 \ln\left[\alpha\left(\frac{v}{c}\right)\left(\frac{m_e c^2}{\Delta E}\right)\right] \qquad (9)$$

in which α is the fine-structure constant.

Obviously, all types of possible excited configurations cannot fully benefit from this type of coherent motion, regardless of the field strengths used. Indeed, the limitation can be estimated from Eq. 8. At sufficiently high intensity in the limit $v \to c$, the maximum value of ΔE_{max} is given by

$$\Delta E_{max} \sim \alpha m_e c^2 = 3.73 \text{ KeV} \qquad (10)$$

The physical picture presented above also enables a statement concerning the frequency of irradiation ω to be formulated. For the excitation of inner-shell states in the kilovolt range by the quasi-free coherently driven motion of outer-shell electrons, two basic assumptions are involved. The first, as noted above, concerns the field strength E such that the condition

$$E \gg E_0 = e/a_0^2 \qquad (11)$$

holds, enabling the electrons to be regarded as approximately free. The second consideration involves the energy scale of the motion, ϵ_e, which in this case is taken to be sufficiently great to excite readily the inner-shell states in the desired kilovolt range. With the neglect of relativistic corrections, the electron energy can be expressed as

$$\epsilon_e \simeq 1/2 m_e v_e^2 \qquad (12)$$

with the quantity v_e representing the velocity of induced electronic motion. For a free electron, the maximum value of v_e, commonly known as the quiver velocity, is given by

$$v_e = \frac{eE}{m_e\omega} \qquad (13)$$

for a field with angular frequency ω (*33*).

For stated values of E and ϵ_e that fulfill the assumptions of the model, a frequency scale generally characteristic of those physical conditions is now defined by combination of Eqs. 11, 12, and 13. If we take $E \simeq 3E_0$ to satisfy Eq. 11 and $\epsilon_e \sim 10^3$ eV as reasonable values, then

$$\omega \simeq 30\alpha^3 \frac{c}{\lambda_c} \qquad (14)$$

which is a frequency that corresponds to an ultraviolet wavelength of approximately 200 nm. With this result, we are led to the conclusion that ultraviolet wavelengths naturally match the physical conditions characteristic of the coherent atomic motions envisaged in this description. Experimental results are in agreement with this conclusion because, as shown by the ion charge-state studies described above, the observed energy transfer rates for infrared and visible radiation were reduced with respect to those characteristic of the ultraviolet range.

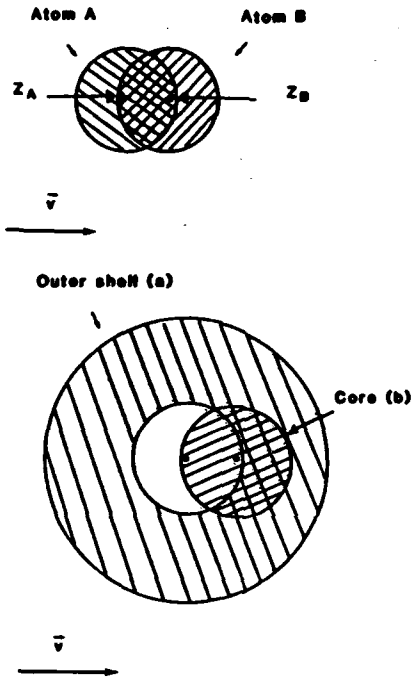

Fig. 8. Approximate correspondence between (top) *A-B* atom-atom collision at relative velocity v and (bottom) coherent relative motion of outer-shell electrons *(a)* with respect to core *(b)*. For simplicity, the electrons in the bottom half of the figure are depicted as undistorted, mutually displaced charge distributions moving with relative velocity v. The nuclear charges of the projectile and target systems, Z_A and Z_B, respectively, are denoted in the atom-atom collisions.

This simple model can also be used to estimate the threshold condition for 4*d* vacancy production in Xe. Although these initial results (*18*) do not constitute a proof of the mechanism involved, it is simply observed that energy transfer from coherently driven valence-shell electrons could produce such inner-shell excitation. Furthermore, with the model presented above, along with consideration of the known (*29*) inelastic electron scattering cross sections for Xe ions, an estimate can be made of the intensity at which such Auger lines should appear. Inelastic scattering studies (*29*) show that the 4*d* excitation in Xe has a threshold at about 67.6 eV that is closely followed by a broad maximum at about 100 eV. If the motion of the N_A outer electrons in Xe is approximated as that of free electrons, the maximum electronic kinetic energy ϵ_e can be written, in a form that reexpresses Eq. 12, as

$$\epsilon_e = (1.79 \times 10^{-13})\lambda^2 I \qquad (15)$$

with units of electron volts for ϵ_e, micrometers for λ, and watts per square centimeter for I. The 4*d* threshold at approximately 67.6 eV corresponds to an intensity I for single-electron motion of about 10^{16} W/cm^2, a value somewhat above that used in the actual experimental studies (*18, 21*) for photoelectron production. However, if the picture of the coherent motion is valid, the single-particle energy can be reduced, for a fixed threshold requirement, by a factor of Z_1, which is the number of electrons participating in the coherent outer-shell motion. For Xe, previous ion studies (*6, 8, 9*), data from which are shown in Fig. 4, indicated that $Z_1 = 8$ is a reasonable value, which is the total number of electrons in the $n = 5$ shell ($5s^25p^6$). This reduces the threshold intensity for 4*d* vacancy production to approximately 1.2×10^{15} W/cm^2, a value quite close to that ($\sim 10^{15}$ W/cm^2) corresponding to the experimental appearance of the electron lines presumed to arise from Auger decay shown in Figs. 6 and 7.

Conclusions

Basic physical studies of collision-free nonlinear atomic processes, through an analysis involving combined measurements of ion charge-state distributions, photoelectron energy spectra, and pho-

ton spectra arising from intense ultraviolet irradiation, have produced data that strongly indicate that multielectron atoms respond in a manner fundamentally different from single-electron counterparts. The confluence of the evidence suggests that, under appropriate circumstances, the outer atomic subshells can be driven in coherent oscillation, and this ordered electronic motion can, by direct intra-atomic coupling, lead to the rapid excitation of atomic inner-shell states. Quantum mechanically, such states of motion for the outer-shell electrons would be described by multiply excited configurations. Two direct consequences of this type of motion are (i) that the maximum magnitude of the oscillating intra-atomic electric field can approach several atomic units, since the fields of all the participating outer electrons combine constructively, and (ii) that the harmonic content of the resulting field can, because of the nonlinear character of the electron-electron $1/r^2$ coulombic interaction, become large. A strong, highly nonlinear intershell coupling results, and enhanced rates of nonlinear absorption are expected.

An elementary atomic model, formulated to take advantage of certain simplifications that appear to be characteristic of the high-intensity regime ($E \gg e/a_0^2$), has enabled qualitative comparisons to be made among several of the most prominent experimentally observed properties. Although this representation is only at the hypothetical stage, the five points of contact are (i) the basic coupling strength, (ii) the shell effects, (iii) the origin of the strong nonlinearity, (iv) the frequency characteristics, and (v) the ability to produce atomic inner-shell excitation. This general, although approximate, form of analysis has additional merit, since it enables us to estimate the response of atoms throughout the periodic table and thereby provides a set of testable hypotheses for comparison with future experiments. It is important to add that, since the original preparation of this article, results obtained by much more quantitative calculations (*34*) involving the time-dependent Hartree-Fock method basically confirm the fundamental character of atomic motion (represented as the analogy with fast atom-atom collisions) even for field strengths approaching E_0 (*22, 30*) and provide remarkable quantitative agreement as well. For the latter, the intensity levels at which 4*d* Auger electrons should be observable in Xe correspond, within a factor of approximately 2, for both theoretical approaches. These results are also in accord with experimental figures (*18*) to within the same rather small level of uncertainty.

An atom in a radiative field whose amplitude is significantly greater than an atomic unit experiences a violent perturbation that has important features in common with certain well-studied collisional phenomena, such as ion-atom collisions, electron-ion collisions, and beam-foil interactions (*35*). Indeed, in the case of beam-foil collisions, a radiative environment at an intensity of 3×10^{18} W/cm^2 and an ultraviolet wavelength approximates (*22*), in several important respects, the conditions associated with the passage of an Ar ion through a carbon foil with a kinetic energy of about 1 GeV. This similarity leads to the concept (*36*) of an "optical solid," in which stationary atoms in a sufficiently intense radiative field will experience an interaction comparable to that of energetic ions traversing solid matter. The consequence is an extreme level of excitation on the scale required to establish the conditions needed to produce stimulated emission in the kilovolt range. In addition, the coherence of the radiative environment can act to introduce a measure of control on the energy transfer that will enable considerable selectivity in the energy flow to be achieved. If this speculative hypothesis survives, a synthesis of many areas of atomic physics and an unexpected nexus between the original research concerning coherent x-ray production and nonlinear processes may result.

References and Notes

1. A. L. Schawlow and C. H. Townes, *Phys. Rev.* 112, 1949 (1958).
2. M. Goppert-Mayer, *Ann. Physik* 9, 273 (1931).
3. I. D. Abella, *Phys. Rev. Lett.* 9, 453 (1962).
4. C. K. Rhodes, in *Proceedings of the 11th Energy Technology Conference and Exposition*, Washington, D.C., 19 to 21 March 1984; in *Workshop on Vacuum Ultraviolet and X-Ray Sources*, Washington, D.C., 9 November 1984.
5. P. W. Hoff and C. K. Rhodes, in *Excimer Lasers*, C. K. Rhodes, Ed. (Springer-Verlag, Berlin, 1979), p. 175; K. Hohla *et al.*, in *Topics in Applied Physics*, C. K. Rhodes, Ed. (Springer-Verlag, Berlin, ed. 2, 1984), vol. 30, p. 230; R. C. Elton *et al.*, Naval Research Laboratory Report 7412 (May 1972); R. W. Waynant and R. C. Elton, *Proc. IEEE* 64, 1059 (1976).
6. T. S. Luk *et al.*, *Phys. Rev. Lett.* 51, 110 (1983).
7. T. S. Luk *et al.*, *Am. Inst. Phys. Conf. Proc.* 100, 341 (1983).
8. T. S. Luk *et al.*, *Phys. Rev. A* 32, 214 (1985).
9. C. K. Rhodes, in *Proceedings of the Third International Conference on Multiphoton Processes*, P. Lambropoulos and S. J. Smith, Eds. (Springer-Verlag, Berlin, 1984), p. 31.
10. T. A. Carlson, W. E. Hunt, M. O. Krause, *Phys. Rev.* 151, 41 (1966).
11. A. L'Huillier *et al.*, *Am. Inst. Phys. Conf. Proc.* 119, 79 (1984).
12. A. L'Huillier *et al.*, *Phys. Rev. Lett.* 48, 1814 (1982); A. L. Huillier *et al.*, *Phys. Rev. A* 27, 2503 (1983); A. L'Huillier *et al.*, *J. Phys.* 44, 1247 (1983).
13. P. Lambropoulos, *Adv. Atom. Mol. Phys.* 12, 87 (1976); H. B. Bebb and A. Gold, *Phys. Rev.* 143, 1 (1966); Y. Gontier and M. Trahin, *J. Phys. B* 13, 4384 (1980); Y. Gontier and M. Trahin, *Phys. Rev.* 172, 83 (1968); H. R. Reiss, *Phys. Rev. A* 1, 803 (1970); *Phys. Rev. Lett.* 25, 1149 (1970); *Phys. Rev. D* 4, 3533 (1971); *Phys. Rev. A* 6, 817 (1972); H. S. Brandi and L. Davidovich, *J. Phys. B* 12, L615 (1979); L. V. Keldysh, *Sov. Phys. J. Exp. Theor. Phys.* 20, 1307 (1965).
14. T. S. Luk and U. Johann, personal communication.
15. T. D. Cowan, *The Theory of Atomic Structure and Spectra* (Univ. of California Press, Berkeley, 1981); I. I. Sobel'man, *Introduction to the Theory of Atomic Spectra* (Pergamon, Oxford, 1972).
16. F. Herman and S. Skillman, *Atomic Structure Calculations* (Prentice-Hall, Englewood Cliffs, N.J., 1963).
17. J. Blackburn *et al.*, *J. Opt. Soc. Am.* 73, 1325 (1983).
18. U. Johann *et al.*, Conference on Lasers and Electro-Optics '85, Baltimore, Maryland, 21 to 24 May 1985.
19. P. Kruit and F. H. Read, *J. Phys. E* 16, 373 (1983); H. G. Muller and A. Tip, *Phys. Rev. A* 30, 3039 (1984); P. Kruit *et al.*, *ibid.* 28, 248 (1983).
20. S. Southworth *et al.*, *Phys. Rev. A* 28, 261 (1983); L. O. Werme, T. Bergmark, K. Siegbahn, *Phys. Scr.* 6, 141 (1972).
21. U. Johann, personal communication.
22. C. K. Rhodes, *Seminar on Fundamentals of Laser Interactions*, Bundessportheim, Obergurgl (Otztal), Austria, 24 February to 2 March 1985.
23. T. Srinivasan *et al.*, in *Laser Spectroscopy*, H. P. Weber and W. Lüthy, Eds. (Springer-Verlag, Berlin, 1983), vol. 6, p. 385; H. Egger *et al.*, *Am. Inst. Phys. Conf. Proc.* 119, 64 (1984); H. Pummer *et al.*, *SPIE J.* 476, 52 (1984); K. Boyer *et al.*, *J. Opt. Soc. Am. B* 1, 3 (1984); T. Srinivasan *et al.*, unpublished results.
24. K. Codling and R. P. Madden, *J. Res. Natl. Bur. Stand.* 76A, 1 (1972); *Phys. Rev. A* 4, 2261 (1971); D. L. Ederer, *ibid.*, p. 2263; M. Boulay and P. Marchand, *Can. J. Phys.* 60, 855 (1982); J. A. Baxter, P. Mitchell, J. Comer, *J. Phys. B* 15, 1105 (1982).
25. A. F. Starace, in *Fundamental Processes in Energetic Atomic Collisions*, H. O. Lutz, J. S. Briggs, H. Kleinpoppen, Eds. (Plenum, New York, 1983), p. 69; A. F. Starace, *Handb. Physik* 31, 1 (1982).
26. N. F. Mott and H. S. W. Massey, *The Theory of Atomic Collisions* (Oxford Univ. Press, London, 1965); H. S. W. Massey and E. H. S. Burhop, *Electronic and Ionic Impact Phenomena* (Oxford Univ. Press, London, 1969), vol. 1; N. M. Kroll and K. M. Watson, *Phys. Rev. A* 8, 804 (1973).
27. J. H. Scofield, *Phys. Rev. A* 18, 963 (1978).
28. L. B. Golden, P. H. Sampson, K. Omidvar, *J. Phys. B* 11, 3235 (1978); *ibid.* 13, 2645 (1980).
29. D. C. Griffen *et al.*, *Phys. Rev. A* 29, 1729 (1984); D. C. Gregory and P. H. Crandall, *ibid.* 27, 2338 (1983); C. Achenback *et al.*, *J. Phys. B* 17, 1405 (1984).
30. K. Boyer and C. K. Rhodes, *Phys. Rev. Lett.* 54, 1490 (1985).
31. J. S. Briggs and K. Taulbjerg, in *Structure and Collisions of Ions and Atoms*, I. A. Sellin, Ed. (Springer-Verlag, Berlin, 1978), p. 105.
32. H. A. Bethe, *Ann. Phys.* 5, 325 (1930).
33. T. P. Hughes, *Plasmas and Laser Light* (Wiley, New York, 1975).
34. A. Szöke and C. K. Rhodes, unpublished results.
35. I. A. Sellin and D. J. Pegg, Eds., *Beam-Foil Spectroscopy* (Plenum, New York, 1976), vols. 1 and 2; U. Littmark and J. F. Ziegler, *Handbook of Range Distributions for Energetic Ions in All Elements* (Pergamon, New York, 1980), vol. 6.
36. *Report on VUV and X-Ray Sources of Atomic and Molecular Sciences Workshop* (National Academy Press, Washington, D.C., in press).

37. We wish to acknowledge fruitful discussion with T. S. Luk, H. Egger, U. Johann, A. P. Schwarzenbach, K. Boyer, A. Szöke, A. Pagnamenta, A. F. Starace, G. Wendin, and H. R. Schlossberg. Supported by the Office of Naval Research, the Air Force Office of Scientific Research (contract number F49620-83-K-0014), the Department of Energy (grant DE-AC02-83ER13137), the Lawrence Livermore National Laboratory (contract 5765705), the National Science Foundation (grant PHY81-16626), the Air Force Office of Scientific Research, Department of Defense—University Research Instrumentation Program (grant USAF 840289), the Defense Advanced Research Projects Agency, and the Los Alamos National Laboratory (contract 9-X54-C6096-1).

APPENDIX D

VOLUME 54, NUMBER 14 PHYSICAL REVIEW LETTERS 8 APRIL 1985

Atomic Inner-Shell Excitation Induced by Coherent Motion of Outer-Shell Electrons

K. Boyer and C. K. Rhodes
Department of Physics, University of Illinois at Chicago, Chicago, Illinois 60680
(Received 28 January 1985)

Outer-shell electrons coherently driven by intense radiation can transfer energy in a direct intra-atomic process to inner-shell excitations. Provided that the effective momentum transfer Δq is sufficiently low ($\Delta q \lesssim \hbar/a_0$), the amplitudes governing the coupling of the outer electrons to the atomic core constructively sum. The effective cross section, which can be related to fast atom-atom collisions ($\gtrsim 10$ MeV/u), is evaluated in a limiting form closely resembling the Bethe result for inelastic electron scattering from atoms.

PACS numbers: 32.80.-t, 34.50.Fa, 34.80.-i

Recent experiments[1,2] examining the nature of multiquantum ionization of atoms in intense ultraviolet fields have exhibited several anomalous characteristics. Among them are (1) reactions of unexpectedly high order, involving as many as 99 photons, and (2) a clear statement, from the atomic-number dependence, that the shell structure of the atom is the main determinant of the strength of the interaction. All the conspicuous characteristics of the experimental findings could be consolidated by that single principle. From the standpoint of this Letter, the main implication of these results[2] is that, at a sufficiently high intensity, the electrons in the outer atomic shells can be *coherently* driven by the incident wave to produce extremely high localized current densities j on the order of $10^{14} \leq j \leq 10^{15}$ A/cm^2. A multielectron atom undergoing a nonlinear interaction of this type responds in a *fundamentally different fashion* from that of a single-electron atom. It is expected that this ordered motion, which represents a very high level of atomic excitation corresponding quantum mechanically to a multiply excited configuration in which all the electrons in a shell are in excited orbitals, would have a lifetime τ given approximately by that characteristic of autoionization. This would place the lifetime in the range of $10^{-14} \geq \tau \geq 10^{-15}$ sec, a time scale approximately comparable to the period of the ultraviolet frequencies used in the studies of ionization.[1,2] In consideration of the outermost shells, an ultraviolet electric field strength E on the order of an atomic unit $E_0 = e/a_0^2$ is the regime in which the envisaged motion is expected to become an important factor in the dynamics. This corresponds to an electromagnetic intensity $I_0 \sim 7 \times 10^{16}$ W/cm^2.

The coherent oscillation of the electrons in outer atomic shells induced by irradiation at ultraviolet frequencies at intensities $I \gtrsim I_0$ has important consequences for the coupling of energy to atomic inner shells. Moreover, as described below, the influence of this type of atomic motion can be related to certain characteristics[3] of high-energy ($\gtrsim 10$ MeV/u) atom-atom collisions. At sufficiently high intensity, a relatively simple physical model can be envisaged which illustrates these effects. For simplicity, consider an intensity above $\sim 10^{19}$ W/cm^2, for which the peak electric field is more than ten times e/a_0^2, so that loosely bound outer electrons can be approximately modeled as completely free particles. Therefore, for those electrons, we can represent their motion as that of free electrons accelerating in intense coherent fields.[4,5] In this limiting case, we imagine that the atom is composed of two parts: (a) an outer shell of electrons driven in coherent oscillation by the radiative field, and (b) a remaining atomic core for which direct coupling to the radiation field is neglected. Coupling between these two systems can occur, since the outer electrons can, through inelastic "collisions," lead to the production of electronically excited core states. Indeed, since the outer electrons could acquire relativistic velocities at intensities on the order of 10^{21} W/cm^2, the production of electron-positron pairs by an *intra-atomic* process analogous to the well-known trident graph[6,7] becomes possible.

The role of coherence in the motion of the outer electrons in the excitation of the core is readily described by appeal to descriptions of energetic atom-atom (A/B) collisions. In this comparison, a correspondence is established between the scattering of the coherently radiatively driven outer electrons from the atomic core and the respective interaction of the electrons in the projectile atom A with the target atom B. Consider the process

$$A + B(0) \xrightarrow{\sigma_{n0}} A + B^*(n) \qquad (1)$$

in which A is a ground-state neutral atom with atomic number Z_A and $B^*(n)$ represents an electronically excited configuration of the target system with quantum numbers collectively represented by (n). In the plane-wave Born approximation, the cross section σ_{n0} can be written in the form presented by Briggs and Taulbjerg[3] as

$$\sigma_{n0} = (8\pi e^4/v^2)\int_{K_{min}}^{K_{max}} |\epsilon_{n0}^{B}(\mathbf{K})|^2 [|Z_A - \textstyle\sum_j \omega_j \langle \phi_j^A | \exp(i\mathbf{K}\cdot\mathbf{s}_A) | \phi_j^A \rangle|]^2 dK/K^3 \quad (2)$$

in which

$$\epsilon_{n0}^{B}(\mathbf{K}) = \int d\mathbf{r}_B^3 \psi_{nB}^*(\mathbf{r}_B) \exp(i\mathbf{K}\cdot\mathbf{r}_B) \psi_{0B}(\mathbf{r}_B). \quad (3)$$

In expressions (2) and (3), v is the relative atom-atom velocity, the ϕ_j^A are orthonormal spin orbitals representing the electrons on the projectile atom, ω_j is the statistical weight of the shell, K is the momentum transfer in the collision, and ψ_{0B} and ψ_{nB} represent the electron wave functions of the target system. The summation over the index j appearing in Eq. (2) extends over all occupied orbitals so that in the limit $K \to 0$, the summation tends to the number of electrons N_A associated with the projectile atom.[3] Since $N_A = Z_A$ for a neutral atom, complete screening[3] occurs in the low-momentum-transfer limit and the nuclear and electronic contributions cancel exactly. Therefore, in this limit, the amplitudes of the electrons combine coherently and the contribution to the cross section σ_{0n} arising from the motion of the *electrons* in atom A is increased by a factor of N_A^2 over that of a single electron at the same collision velocity v. Alternatively, for sufficiently low momentum transfer such that $Ka_0 \ll \hbar$, the electron cloud acts as a coherent scattering center with a mass $N_A m_e$, a charge $N_A e = Z_A e$, a velocity v, and a kinetic energy $N_A(\frac{1}{2}m_e v^2)$. Significantly, on account of the coherence, the single-particle energies ($\frac{1}{2}m_e v^2$) add so that, in principle, this value could be *below* the magnitude required to produce the excitation of the target atom.

In sufficiently high-field strengths, coherently accelerated electrons in outer atomic shells can interact with the remaining atomic core system in a manner closely analogous to the atom-atom scattering described above. If a plane-wave Born-approximation description is used, the cross section representing energy transfer can be derived directly from expression (2) with $Z_A = 0$. We now describe an example illustrating the circumstances under which this may occur. Since the basic physical concepts can be very simply represented in the high-field limit ($E \gg E_0$), we consider a peak electric field strength $E \sim 0.5 \times 10^{12}$ V/cm such that an electron acquires an energy of ~ 10 keV in a distance comparable to an atomic dimension (~ 2 Å). At this field strength, which corresponds to an intensity of $\sim 3 \times 10^{20}$ W/cm^2, the electron accelerates to the 10-keV energy in a time which is approximately 1% of an optical cycle for an ultraviolet wave length of ~ 200 nm, a condition consistent with the validity of the assumption of a constant field strength for accelerations on the scale of atomic dimensions. The resulting velocity of $\sim 8 \times 10^9$ cm/sec corresponds, for atom-atom collisions, to a collision energy of ~ 20 MeV/u. Therefore, the motion of these electrons simulates the *electronic* collisional environment that would occur in fast atom-atom encounters, but with the important *absence* of the nuclear contribution arising from the Z_A term in expression (2). In this case, no shielding is present in the low-momentum-transfer limit.

It is now possible to estimate the contribution to σ_{0n} for an inner-shell excitation arising from coherently excited atomic shells. For this we take expression (2) with $Z_A = 0$ and restrict K_{max} to $\lesssim \hbar/a_0$, to fulfill the condition for full shielding which, for this situation, corresponds to totally *constructive* interference of the electron amplitudes. We further take Z_1 to denote the number of electrons in the outer shells and expand Eq. (2) for $\epsilon_{n0}^{B}(\mathbf{K})$ in the customary fashion so that only the leading dipole term x_{0n} is retained. Finally, for a core excitation energy ΔE we put $K_{min} \simeq \Delta E/v$, the condition that holds for ΔE much less than the collision energy. With these modifications, the coherent piece $\sigma\delta_{0n}$ can be written as

$$\sigma\delta_{0n} \simeq \frac{8\pi e^4 x_{0n}^2 Z_1^2}{v^2\hbar^2}\int_{\Delta E/v}^{\hbar/a_0} \frac{dK}{K}. \quad (4)$$

a result which, with the exception of the restriction on K_{max} and the Z_1^2 factor, is exactly the form of the well-known result for inelastic scattering of electrons on atoms developed by Bethe.[8] The final result, valid for

$$\alpha\left(\frac{v}{c}\right)\left(\frac{m_e c^2}{\Delta E}\right) > 1, \quad (5)$$

is

$$\sigma\delta_{0n} \simeq 8\pi\alpha^2\left(\frac{c}{v}\right)^2 Z_1^2 x_{0n}^2 \ln\left|\alpha\left(\frac{v}{c}\right)\left(\frac{m_e c^2}{\Delta E}\right)\right|. \quad (6)$$

in which α is the fine-structure constant. For the example considered, the restriction on the logarithmic factor limits ΔE to a maximum value of approximately 1 keV, an energy corresponding to the region near the M edge of xenon,[9] a case which serves as a suitable numerical example. If we take the charge radius[10] of the M shell of xenon as the scale for x_{0n}, then $x_{0n} \sim 0.2a_0$, and if we assume that $Z_1 = 18$, accounting for the three outermost xenon shells ($5p^6 5s^2 4d^{10}$), then the resulting cross section is on the order of $\sigma\delta_{0n} \sim 7 \times 10^{-18}$ cm^2 with the weakly varying logarithmic term taken as a factor of $O(1)$. This value is somewhat greater than the total photon cross section[11,12] in the region near the M edge of xenon. Furthermore, since expression (4) respects dipole

selection rules, considerable state selectivity is present as only odd-parity excited core levels would be produced.

The upper limit in the integral in expression (4) can be extended to $K_{max}=2Z_1 m_e v$ if appropriate projectile-atom wave functions ϕ_f^A are used. This procedure produces a final cross section σ_{0n} with a magnitude of the same scale as that represented by Eq. (6), but with a somewhat different detailed dependence on v and ΔE. This refinement leaves the principal conclusion unchanged.

The coherent interaction described above can be viewed as a form of dynamic configuration interaction in which the fields of the participating electrons sum constructively. Constructive addition naturally results if the scale of the momentum transfer Δq communicated in the interaction is sufficiently small so that the length $\hbar/\Delta q$ is greater than the spatial scale of the scattering system. The physical origin of this effect is the same as that which generates the coherent forward scattering[13] observed in nuclear collisions.[14]

Obviously, all types of possible excited configurations cannot fully benefit from this type of coherent motion regardless of the field strengths used. For example, the coherence is unimportant in the amplitude for intra-atomic electron-positron pair production by the trident diagram shown in Fig. 1, since the momentum transfer Δq associated with the propagator for pair production in this interaction is such that

$$\hbar/\Delta q \sim \lambda\!\!\!^{-}_c \ll a_0. \tag{7}$$

Indeed, from Eq. (5), at sufficiently high intensity in the limit $v \to c$, the maximum value of ΔE_{max} is given by

$$\Delta E_{max} \sim \alpha m_e c^2 = 3.73 \text{ keV}. \tag{8}$$

Therefore, the cross section[6] for pair production in the field of a nucleus is easily shown to be

$$\sigma_t = (28/27\pi) Z_1 (Z\alpha)^2 r_0^2 (\ln\gamma)^3 \tag{9}$$

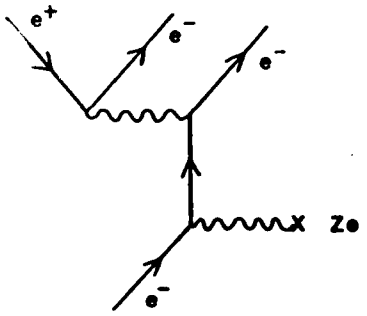

FIG. 1. Trident graph representing electron-positron pair production by collision on an energetic electron with a fixed center of charge Ze.

in which r_0 is the classical radius of the electron and γ is the customary relativistic factor

$$\gamma = [1-(v/c)^2]^{-1/2}. \tag{10}$$

At sufficiently high intensity ($\gtrsim 10^{21}$ W/cm^2), for $Z_1=50$ and $Z_2=90$, and with $\gamma \simeq 5$, $\sigma_t \simeq 2\times 10^{-24}$ cm^2, a value that would, under reasonable experimental conditions with an ultraviolet laser of 1–10-J output and $\sim$ 100-fs pulse length, make possible the generation of $\sim$ 100 pairs/pulse by this mechanism.

Coherently driven motions in outer electron shells can generate an enhanced intra-atomic coupling for the excitation of inner shells. The interaction, which can be viewed alternatively as a form of configuration interaction or electron scattering, has, on account of the constructive addition of amplitudes, a cross section which scales as the square of the number (Z_1) of outer electrons participating in the motion. A strong and highly nonlinear coupling arises as a direct consequence. Coherent motions of this type should enable the selective excitation of atomic inner-shell states in the kiloelectronvolt energy range to be produced by intense irradiation of atoms at ultraviolet wave lengths. The physical nature of this process of intra-atomic energy transfer bears a direct relationship with energetic atom-atom collisions. Similar conclusions can be reached by alternative theoretical approaches, such as those involving the time dependent Hartree-Fock method.[15]

The authors wish to acknowledge fruitful discussions with T. S. Luk, H. Egger, U. Johann, A. P. Schwarzenbach, and A. Szöke. This work was supported by the Office of Naval Research, the Air Force Office of Scientific Research under Contract No. F49630-83-K-0014, the Department of Energy under Grant No. DeAS08-81DP40142, the Lawrence Livermore National Laboratory under Contract No. 5765705, the National Science Foundation under Grant No. PHY 81-16626, the Defense Advanced Research Projects Agency, and the Avionics Laboratory, Air Force Wright Aeronautical Laboratories, Wright Patterson Air Force Base, Ohio.

[1]T. S. Luk, H. Pummer, K. Boyer, M. Shahidi, H. Egger, and C. K. Rhodes, Phys. Rev. Lett. 51, 110 (1983).

[2]C. K. Rhodes, in *Proceedings of the International Conference on Multiphoton Processes III*, edited by P. Lambropoulos and S. J. Smith (Springer-Verlag, Berlin, to be published).

[3]J. S. Briggs and K. Taulbjerg, in *Structure and Collisions of Ions and Atoms*, edited by I. A. Sellin (Springer-Verlag, Berlin, 1978), p. 105.

[4]Marc J. Feldman and Raymond Y. Chiao, Phys. Rev. A 4, 352 (1971).

[5]E. S. Sarachik and G. T. Schappert, Phys. Rev. D 1, 2738 (1970).

[6]A. I. Akhiezer and V. B. Berestetskii, *Quantum Electrodynamics* (Wiley-Interscience, New York, 1965).

[7]J. W. Shearer, J. Garrison, J. Wong, and J. E. Swain, Phys. Rev. A 8, 1582 (1973).

[8]H. A. Bethe, Ann. Phys. (Leipzig) 5, 325 (1930).

[9]K.-N. Huang, M. Aoyagi, M. H. Chen, B. Crasemann, and H. Mark, At. Data Nucl. Data Tables 18, 243 (1976).

[10]F. Herman and S. Skillman, *Atomic Structure Calculations* (Prentice-Hall, Englewood Cliffs, New Jersey, 1963).

[11]Wm. J. Veigele, At. Data Tables 5, 51 (1973).

[12]R. D Hudson and L. J. Kieffer, At. Data Tables 2, 205 (1971).

[13]J. L. Rosen, in *High-Energy Physics and Nuclear Structure—1975*, edited by D. E. Nagle, A. S. Goldhaber, C. K. Hargrave, R. L. Burman, and B. G. Storms, AIP Conference Proceedings No. 26 (American Institute of Physics, New York, 1975), p. 265.

[14]J. M. Blatt and V. F. Weisskopf, *Theoretical Nuclear Physics* (Wiley, New York, 1952).

[15]A. Szöke and C. K. Rhodes, "A Semiclassical Model of Inner-Shell Excitation by Outer-Shell Electrons," to be published.

APPENDIX E

A THEORETICAL MODEL OF INNER-SHELL EXCITATION BY OUTER-SHELL ELECTRONS*

A. Szöke
Lawrence Livermore National Laboratory
P.O. Box 808, Livermore, California 94550

and

C. K. Rhodes
Department of Physics, University of Illinois at Chicago
P.O. Box 4348, Chicago, Illinois 60680

(Received 8 July 1985)

ABSTRACT

An analysis is presented which shows that atomic inner-shell states can be strongly excited by outer-shell electrons driven coherently at ultraviolet frequencies. A semi-quantitative analysis, based on the time-dependent Hartree-Fock method, is formulated to illustrate the basic character of this extremely nonlinear inter-shell coupling. The results indicate that a substantial fraction of the absorbed energy can be channeled into inner-shell excitation.

---

* to be published, Phys. Rev. Lett.

Recent experimental studies[1-3] on the nonlinear coupling of intense ultra-violet radiation to atoms have indicated that it may be possible to excite atomic inner-shell levels through radiatively driven motions in outer-shells. Specifically, it has been suggested[4,5] that the outer-shell motions that could produce a substantial amplitude for inner-shell excitation are those involving ordered coherent motions of the outer electrons.

An approximate analysis of inner-shell excitation[5], based on an analogy with atomic interactions in energetic ($v/c \sim 1/10$) atom-atom collisions,[6,7] has recently been presented. That result, which is valid for very strong incident fields that give rise to comparable electronic velocities, is stated in a form resembling the well known cross section for inelastic scattering of electrons by atoms.[8] Closely related phenomena involving multiphoton excitation, and the ionization of many-electron atoms in strong electromagnetic fields have been formally treated on the basis of time-dependent Hartree Fock (TDHF) theory.[9] This communication extends that theory to describe inner-shell excitation. Specifically, we show that assuming coherent (collective) nonlinear motion of an electronic (outer-) shell produced by interaction with an external driving field, both the probability for excitation of inner-shell electrons and the quantum state specificity can be estimated.

In the following we give a simplified derivation of the theory using neutral xenon as an example. The $n = 5$ shell ($5s^2 5p^6$) of xenon will be designated as the outer-shell, and its $4d^{10}$ shell, to which it is closely coupled,[10-12] will be denoted as the inner-shell. The remaining strongly bound electrons that form the [Kr] - like core will be treated as an equivalent potential. In the TDHF formalism, the many-body wave function describing the outer- and the inner-shells is restricted to be an

antisymmetrized product of single electron orbitals, a single Slater determinant of the form,

$$\Psi_{TDHF} = \sum_{p} (-1)^{p} \prod_{i=1}^{K} \psi_i(\bar{r}_{p(i)},t) \qquad (1)$$

in which p is a permutation of the indices i of the K (= 18) electrons. The single particle wave functions satisfy equations which are, in the dipole approximation with the neglect of spin-orbit and other relativistic effects, written as

$$i\hbar \frac{\partial \psi_i(\bar{r},t)}{\partial t} = \left[\frac{\hbar^2}{2m}\nabla^2 + V(r) + V_c(\bar{r},t) + V_{xc}^{LDA}(\bar{r},t) - e\bar{r}\cdot\bar{E}(t)\right]\psi_i(\bar{r},t) \qquad (2)$$

In these equations, the laser field is assumed to be a nearly monochromatic classical field, given by

$$\bar{E}(t) = \bar{E}_0(t)\cos\omega t, \qquad (3)$$

and the self-consistent Coulomb V_c and exchange V_{xc}^{LDA} potentials are defined, in the local density approximation,[13] by

$$V_c(\bar{r},t) = \int d\bar{r}' \frac{e^2}{|\bar{r}-\bar{r}'|} n(\bar{r},t) \quad ; \quad n(\bar{r},t) = \sum_{i=1}^{K} |\psi_i(\bar{r},t)|^2 \qquad (4)$$

$$V_{xc}^{LDA}(\bar{r},t) = \frac{\partial}{\partial n(\bar{r})}\left[n(\bar{r})\,\varepsilon_{xc}(n(\bar{r}))\right] \qquad (5)$$

in which $E_{xc}(n(r))$ is the exchange energy of the uniform electron gas with the same density. In Eq. 1 above, V(r) is the potential produced by the ionic [Kr]-like core. In principle, these equations are nonlinear in the applied electromagnetic field.

We observe that the incident electromagentic field has a slowly varying envelope which means that both its amplitude $E_0(t)$ and its frequency ω remain approximately constant over many light periods. Thus, the Hamiltonian, Eq. 2, is almost periodic with period $T = (2\pi/\omega)$ and its corresponding stationary states satisfy the quantum mechanical Floquet theorem.[14-16] In particular, in the TDHF approximation the single electron wave functions do so individually: thus

$$\varphi_i(\bar{r},t) = \exp(-i\Omega_i t)\, \varphi_i(\bar{r},t); \quad \varphi_i(\bar{r},t+T) = \varphi_i(\bar{r},t) \tag{6}$$

in which Ω_i are the Floquet exponents with corresponding quasi-energies given by $\hbar\Omega_i$. The periodic functions φ_i can be expanded in a time-dependent Fourier series as

$$\varphi_i(\bar{r},t) = \sum_n \varphi_i^n(\bar{r}) \exp(-in\omega t)\,, \tag{7}$$

a form which clearly shows that Ψ_{TDHF} depends on time as a sum of exponential terms

$$\exp\left[-i\left(\sum_{i=1}^{K} \Omega_i + n\omega\right)t\right] \text{ with n an integer.}$$

We now introudce an important approximation and adopt a "shell model" which separates the treatment of the outer-shell electrons from those of the

inner-shell. It will be assumed that in the first approximation the $4d^{10}$ inner-shell electrons remain frozen in their ground state. It then follows that the TDHF Eqs. 1-5 have to be written for K = β with the inner-shell electrons counted as core electrons. We know that for a weak incident field this is a good approximation in xenon from detailed calculations using linear response theory.[17-18] [Note: This calculation was performed by C. Cerjan at the Lawrence Livermore National Laboratory using the computor program kindly provided by D. Liberman.[19]]

The response of the inner-shell will now be treated by perturbation theory. In this analysis, the potentials V_c, V_{xc} in Eq. 4 and Eq. 5 are calculated using only the outer-shell wave functions and are represented as an external potential U given by

$$U(\bar{r},t) = V(r) - e\bar{r}\cdot\bar{E}(t) + V_c(\bar{r},t) + V_{xc}^{LDA}(\bar{r},t) \quad . \tag{8}$$

This potential can be Fourier analyzed in time as

$$U(\bar{r},t) = \sum_{k=1}^{\infty} U^k(\bar{r})\cos(k\omega t + \theta_k) \quad . \tag{9}$$

It is important to note that in the TDHF analysis the Floquet exponent disappears; the time dependence comes directly from the various components Eq. 7. In particular, if ψ_i^n has large Fourier components for indices n = 0 and M; V_c and V_{xc} have correspondingly large Fourier components for integral indices occurring between -M and +M. Therefore, this potential will cause transitions in the inner-shell when the excitation energy E satisfies the condition $E = n\hbar\omega$ for $n \leq M$. The resulting transition rate, from perturbation theory, is

$$w(E) = \frac{2\pi}{\hbar} |S_n(E)|^2 \delta(E - n\hbar\omega) \tag{10}$$

in which the transition amplitude, $S_n(E)$ is calculated below.

Let us denote the inner-shell matrix elements of U^k by

$$U^k_{ij} = \int d\bar{r} \langle \Psi_j(\bar{r}) | U^k(\bar{r}) | \Psi_i(\bar{r}) \rangle \tag{11}$$

in which Ψ_i are a complete set of properly antisymmetric Hartree-Fock wavefunctions for the inner-shell, including levels in the continuum, with r symbolizes all inner-shell coordinates. In n^{th} order perturbation theory we obtain

$$S_n(E) = U^n_{oE} + \sum_{k_1+k_2=n} \sum_i \frac{U^{k_1}_{oi} U^{k_2}_{iE}}{E_o - E_i - k_1\hbar\omega}$$

$$+ \ldots + \sum_{i,j\ldots s} \frac{U^1_{oi} U^1_{ij} \ldots U^1_{sE} \text{ [n terms]}}{(E_i - E_o - \hbar\omega)(E_j - E_i - \hbar\omega) \ldots (E_s - E_r - \hbar\omega)} \tag{12}$$

with the summations denoting the customary sum over bound levels and integral over continuum states. In general, all orders in this expression must be retained, since the terms U^k are of k^{th} order in the external field and, consequently, all terms are of n^{th} order overall. Furthermore, it is clear by inspection that the first term corresponds to "internal n^{th}-order harmonic generation" while the last one corresponds to "lowest order perturbation theory" with the external field screened by the outer electron motion. In perturbation theory, consecutive orders of U^k are related by

$$U^k / U^{k-1} \approx \mu_{os} E / \Delta E_{os}; \qquad (13)$$

in which μ_{os} is a typical outer-shell dipole matrix element and ΔE_{os} is an energy scale characterising outer-shell excitations. Therefore, transition amplitudes in consecutive orders are related approximately by $\Delta E_{os}/(E_{n_i l_i} - k\hbar\omega)$. Since inner-shell energy spacings are typically larger than those in the outer-shell, consecutive orders in the perturbation treatment are generally diminishing except in cases possibly involving intermediate resonances. It is significant to note that, if there is an intermediate resonance at $k\hbar\omega$, a large dipole moment can be produced at that harmonic frequency.

The behavior of the single electron wave functions of the outer-shell, $\psi_i(r,t)$, are now investigated. Since we are interested in the behavior of the atom in a nearly monochromatic field that is applied adiabatically, we seek the solution of the TDHF equations (Eqs. 1-7, K = 8) that correlates adiabatically to the $5s^2 5p^6\ ^1S_0$ ground state. For weak fields and sufficiently low frequencies, the response of each electron is similar to that of an harmonic oscillator with a resonance energy equal to that of the first excited state $\hbar\omega_0$ (8 - 9 eV in xenon).[20] Therefore, the perturbation parameter, as given in Eq. 13, is

$$B = \frac{1}{4}\frac{\mu_{os} E_0}{\Delta E} = \frac{1}{4}\frac{\alpha(\omega) E_0^2}{\hbar\omega_0}\left(\frac{\omega_0^2}{\omega_0^2 - \omega^2}\right) \qquad (14)$$

in which $\alpha(\omega)$ is the measured atomic polarizability (per electron), a quantity which can also be calculated by linear response theory with a self-

sistent potential.[17,18] In reality, however, the potential is anharmonic. Therefore, the harmonic oscillator model must be used with caution, since a single excited electron ionizes if it gets excited above the ionization potential V_o. In xenon those values of V_o are 12.13 eV and 13.44 eV for J = 3/2 and J = 1/2 states of Xe^+, respectively. For simplicity, in the following we ignore possible complications arising from autonionizing resonances. Considering the form of the wave functions in the presence of the field as given by Eq. 6 and Eq. 7, we can see that if $\hbar(\Omega_i + n\omega) \geq V_o$, $\varphi_i^n(r)$ is a continuum wave function. However, we note that this relation has to be modified in strong fields, as discussed both below and in Ref. 21.

The atomic behavior in strong fields is now discussed. In an harmonic oscillator model, the amplitudes $|\varphi_i^n|^2$ are proportional to B^n for $B \ll 1$, the standard perturbation theory result. Therefore, in this regime, the probability of ionization in accordance with lowest order perturbation theory is obtained. For sufficiently strong field, $B > 1$, the higher harmonic components acquire large magnitudes, the self-consistent potential becomes appreciably modified, and the ionization of the lowest φ_i^n states can be suppressed.[3,9,21,22] The criterion[21] for the disappearance of the n^{th} channel for ionization, due to electron trapping by the ponderomotive potential is

$$n\hbar\omega - V_o(E_o) < \frac{1}{4}\frac{E_o^2 e^2}{m\omega^2}, \qquad (15)$$

in which $V_o(E_o)$ is the ionization energy of the atom modified by the AC-Stark effect. Significantly, both the disappearance of the lowest energy electrons and the persistence of the higher energy peaks have been observed[3,23]

in good agreement with Eq. 15. In the experiments of Johann el al.[3] in xenon at 193 nm, electron trapping of the two-photon (n = 2) peak occurs at an intensity of 2×10^{14} W/cm^2 according to Eq. 15. However, the onset of strong non-linearity arises at an intensity of 1.2×10^{15} W/cm^2, the value for which B = 1 in Eq. 14. The combined result of these effects is that the single electron wave function, described by Eq. 6 and Eq. 8, will have sizeable n = 2 component that does <u>not</u> ionize. The n > 2 components, of course, will still consist, at least partly, of outgoing waves. If we <u>assume</u> a coherent outer-shell motion, a reasonable approximation for the bound part of the TDHF wave function that correlates to the ground state is a symmetric product of wave functions for the six 5p electrons of the form[9]

$$\psi_i(\bar{r},t) = \exp(-i\Omega_i t)\left[\varphi_i^0(\bar{r}) + \varphi_i^1(\bar{r})e^{-i\omega t} + \varphi_i^2(\bar{r})e^{-2i\omega t}\right]. \qquad (16)$$

the norms of the Fourier components,

$$P_n = \int |\varphi_i^n(\bar{r})|^2 d\bar{r}, \qquad (17)$$

were calculated for a one dimensional harmonic oscillator with polarizability and resonance frequency similar to that of xenon; for an intensity of 4.5×10^{14} W/cm^2 and frequency $\omega = 0.7\omega_0$ the values are $P_0 = 0.246$, $P_1 = 0.330$, $P_2 = 0.234$, $P_3 = 0.116$ respectively.

Two important conclusions emerge. First, if we interpret P_n as the probability of an individual electron being "dressed" by n photons, the $5p^6$ shell of xenon has a sizeable amplitude for being dressed with, or virtually excited with, 12 photons,[24] an energy sufficient to ionize a 4d electron, at an incident 193 nm laser intensity in the range of $\sim 4 \times 10^{14}$ W/cm^2.

Significantly, this range of intensity agrees, to within a factor of two, with the intensity observed[3,4] in the electron spectrum of xenon for the onset of strong nonlinear coupling. Second, substituting Eq. 16 into Eqs. 4 and 8, we see that the potential produced by these electrons contains predominantly the first and second harmonic components. This is <u>exactly</u> the expected characteristic of a coherent ordered motion of the outer-shell electrons.

An estimate can be made of the inner-shell excitation due to the potential U, Eq. 8, in perturbation theory. The xenon $4d^{10}$ ionization thresholds are 67.55 eV ($4d_{5/2}$) and 69.52 eV ($4d_{3/2}$). When the $n = 2$ terms get large, the dominant lowest order terms in the pertubation analysis represented by Eq. 12 can be cast in a form in which the individual terms are written as $(\mu E_2/\hbar\Delta\omega)^2$, in which μ is an inner-shell dipole matrix element, E_2 is the field at 2ω induced by the outer shell, and $\hbar\Delta\omega$ is an appropriate energy denominator. Using $\mu^2 = f(ea_0)^2(Ry/\hbar\omega_1)$, in which Ry = 13.6 eV, $\hbar\omega_1$ is an inner-shell excitation energy, and f is the oscillator strength of the transition, we can estimate the square of the matrix elements of Eq. 11 as

$$|\langle|U|\rangle|^2 \approx \left(\frac{E_2}{E_a}\right)^2 \frac{4f(Ry)^3}{(\hbar\Delta\omega)^2(\hbar\omega_1)} \qquad (18)$$

with the atomic electric field denoted as $E_a = e/a_0^2$.

We now provide bounds for (E_2/E_a). A high estimate, $E_2/E_a = 1.4$, is derived if we assume an oscillating charge of 2e at $2\omega_1$ corresponding to the parameters $P_0 = P_1 = P_2 = 1/3$ for the six 5p electrons and a mean distance of $1.2a_0$ between the outer- and inner-shell. The latter is an unweighted average from a density functional calculation of xenon.[18] Conversely, a low estimate of $E_2/E_a = 0.17$ is obtained if we scale the

static shielding field calculated in Ref. 18 (Fig. 1), around the position of the peak density of the 4d shell ($0.8a_0$) with $P_2 = 1/3$. We believe that a better estimate of this quantity is the highest theoretical priority and its experimental determination is the most significant means for a comparison of theory and experiment. Fortunately, in the case of xenon, the structure of the excited levels of the $4d^{10}$ shell is well known.[25,26] We have to consider in Eq. 18 two different classes of terms, namely, (a) those in the continuum with $f = 11$ and $\hbar\omega_1 \sim 100$ eV and (b) one resonant level at 65.1 eV corresponding to the $4d^{10}5s^25p^6 \rightarrow 4d^95s^25p^2(^2D_{5/2})6p$ transition with $f = 0.02$. The latter transition can experience shifts due to outer-shell "vacancies" and the (shielded) external field. Taking the higher estimate for E_2, we get for $|\langle|U|\rangle|^2 = 0.29$ with the continuum as the intermediate state and $|\langle|U|\rangle|^2 = 7.6$ for the resonant level which corresponds to 10 photons absorbed. The latter value simply signifies that this particular step of the transition is saturated and that the appropriate magnitude to use is unity.

The simplest kind of perturbation calculation relates the probability of inner-shell ionization P (Auger) to that of the absorption $P(4\omega)$ corresponding to the absorption of four photons by a single electron, an outer-shell "above threshold" ionization process,[23] with the latter being calculated in lowest order perturbation theory. In this comparison, we assume that both these processes have the same density of final states, and the same bound-continuum matrix elements. This ratio then reduces to a product of four expressions of the type $|\langle|U|\rangle|^2$. Using the estimates given in the previous paragraph, we obtain for the ratio of probabilities, $P(\text{Auger})/P(4\omega) = 0.15$. The magnitude of this ratio indicates that an appreciable fraction of the absorbed energy can be channeled into the excitation of inner-shell states.[2]

In this letter a theoretical framework has been presented that allows the calculation of the probability of inner-shell excitation that arises when an outer-shell of an atom is driven coherently by a strong, non-resonant electromagnetic field. Naturally, in future analyses, it is important to examine more thoroughly the range of physical conditions[3] necessary for the validity of the central assumption of this work, namely, the existence of a coherent multi-electron excitation of an atomic outer-shell. For this question, TDHF calculations can set a limit. In the regime for which those calculations predict single electron excitations, in particular, close to a resonance, no coherent excitation will occur in a real atom. Of course, the residual interaction among the outer-shell electrons represents a mechanism for damping of the coherent motion that requires further investigation. Although a theoretical framework is known[27,28] which can be used to appraise these effects, the calculation falls outside the domain of TDHF theory.

ACKNOWLEDGEMENTS

The authors thank C. Cerjan for making his calculations available to us, and for fruitful discussion with T. S. Luk, H. Egger, U. Johann, A. P. Schwarzenbach, and K. Boyer. This work was supported in part by the Office of Naval Research, the Air Force Office of Scientific Research under contract number F49620-83-K-0014, the Innovative Science and Technology Office of the Strategic Defense Initiative Organization, the Department of Energy under grant number DE-AC02-83ER13137, the Lawrence Livermore National Laboratory under contract number 5765705, the National Science Foundation under grant number PHY 84-14201, the Air Force Office of Scientific Research, Department

opf Defense University Research Instrumentation Program under grant number USAF 840289, the Defense Advanced Research Projects Agency, and the Los Alamos National Laboratory under contract number 9-X54-C6096-1. This work was performed partially under the auspices of the U.S. Department of Energy by the Lawrence Livermore National Laboratory under contract W-7405-ENG-48.

REFERENCES

1. T. S. Luk, U. Johann, H. Egger, H. Pummer, and C. K. Rhodes, Phys. Rev. A32, 214 (1985).

2. U. Johann, T. S. Luk, and C. K. Rhodes, "Multiphoton Inner-Shell Atomic Excitation and Multiple Ionization," XIVth International Conference on the Physics of Electronic and Atomic Collisions, edited by D. C. Lorents, W. E. Meyerhof, and J. R. Peterson, (North-Holland, Amsterdam, in press).

3. U. Johann, T. S. Luk, H. Egger, and C. K. Rhodes, "Rare Gas Electron Energy Spectra Produced by Collision-Free Multiquantum Processes," submitted to Phys. Rev. A.

4. C. K. Rhodes, Science 229, 1345 (1985).

5. K. Boyer and C. K. Rhodes, Phys. Rev. Lett. 54, 1490 (1985).

6. J. Briggs and K. Taulbjerg in Structure and Collisions of Ions and Atoms, edited by I. A. Sellin (Springer-Verlag, Berlin, 1978) p. 105.

7. C. Bottcher, J. Phys. B10, L445 (1977).

8. H. A. Bethe, Ann. Phys. 5, 325 (1930).

9. A. Szöke, "On the Theory of Multiphoton Ionization of Many-Electron Atoms," submitted to Phys. Rev. A.

10. M. J. van der Wiel and T. N. Chang, J. Phys. B11, L125 (1978).

11. M. Ya. Amusia in Advances in Atomic and Molecular Physics, Vol. 17, edited by D. R. Bates and B. Bederson (Academic Press, New York, 1981) p. 1.

12. G. Wendin, "Breakdown of the One-Electron Pictures in Photoelectron Spectra," Structure and Bonding, Vol. 45 (Springer-Verlag, Berlin, 1981).

13. W. Kohn and P. Vashishta, "General Density Functional Theory," in Theory of the Inhomogeneous Electron Gas, edited by S. Lundqvist and N. H. March, (Plenum, New York, 1983)p. 79.

14. Ya. B. Zel'dovich, Usp. Fiz. Nauk 110, 139 (1973); Sov. Phys. -Uspekhi 16, 427 (1973).

15. S.-I. Chu, Adv. At. Mol. Phys. 21, xxx (1984).

16. This was treated in detail in Ref. 9, In addition, the first diabatic correction term was explicitly calculated.

17. M. J. Stott and E. Zaremba, Phys. Rev. A21, 12 (1980).

18. A. Zangwill and P. Soven, Phys. Rev. A21, 1561 (1980).

19. A. Zangwill and D. A. Liberman, Comp. Phys. Comm. 32, 63 (1984).

20. More precisely, this statement means that for weak, non-resonant excitation of a single particle, the wave function of the two-level system has the same coefficient of the excited state mixed in with its ground state, as an harmonic oscillator with the identical resonant frequency and matrix element.

21. A. Szöke, J. Phys. B18, L427 (1985).

22. H. G. Muller, A. Tip, and H. J. van der Wiel, J. Phys. B16, L679 (1983); H. G. Muller and A. Tip, Phys. Rev. A30, 3039 (1984).

23. P. Kruit, J. Kimman, H. G. Muller, and M. J. van der Wiel, Phys. Rev. A28, 248 (1983).

24. The equivalence of P_n with the probability of "dressing" or "virtual absorption" of n photons is discussed e.g. by L. Rosenberg, Advances in Atomic and Molecular Physics, Vol. 18, edited by D. Bates and B. Bederson (Academic Press, New York, 1982) p.1.

25. S. Southworth, U. Becker, C. M. Truesdale, P. H. Kobrin, D. W. Lindle, S. Owaki and D. A. Shirley, Phys. Rev. A28, 261 (1983).

26. D. L. Ederer and M. Manalis, JOSA 65, 634 (1975).

27. T. N. Chang and U. Fano, Phys. Rev. A13, 263, 282 (1976).

28. M. Baranger and I. Zahed, Phys. Rev. C29, 1005, 1010 (1984).

0051s

APPENDIX F

VOLUME 51, NUMBER 2 PHYSICAL REVIEW LETTERS 11 JULY 1983

Anomalous Collision-Free Multiple Ionization of Atoms with Intense Picosecond Ultraviolet Radiation

T. S. Luk, H. Pummer, K. Boyer, M. Shahidi, H. Egger, and C. K. Rhodes
Department of Physics, University of Illinois at Chicago, Chicago, Illinois 60680

(Received 27 April 1983)

Collisionless multiphoton absorption, resulting in multiple atomic ionization and exhibiting anomalously strong coupling, has been studied in the region spanning atomic number $Z = 2$ (He) to $Z = 92$ (U). The highest ion state identified is U^{16+}, corresponding to absorption of 99 quanta (~633 eV). Models of stepwise ionization using standard theoretical techniques are incapable of describing these results. A mode of interaction involving radiative coupling to a collective motion of an atomic shell is proposed.

PACS numbers: 32.80.Kf, 32.80.Fb, 33.80.Kn

The availability of spectrally bright picosecond ultraviolet light sources enables the study of nonlinear coupling mechanisms in that spectral range under experimental circumstances unaffected by collisional perturbations. In this Letter, the results of the first experiments examining the atomic-number dependence of processes of multiple ionization of atoms X with intense ($\lesssim 10^{14}$ W/cm^2) picosecond 193-nm radiation under *collision-free* conditions are reported.

The general physical process studied is

$$N\gamma + X \rightarrow X^{q+} + qe^- \qquad (1)$$

for which observed values of N and q range as high as 99 and 10, respectively. Of particular significance is the behavior of the amplitude for Reaction (1) as a function of atomic number (Z). Accordingly, the response of materials spanning the range in atomic number from He ($Z=2$) to U ($Z=92$) has been measured. Similar processes involving the irradiation of Kr at 1.06 μm have recently been described by L'Huillier *et al.*,[1] in addition to other studies concerning the characteristics[2] of Xe and Hg.

The experiments reported herein exhibit two salient features. These are (1) an unexpectedly strong coupling for extraordinarily high-order processes, and (2) a coupling strength which is dramatically enhanced at higher Z values.

The experimental arrangement used to detect the production of the highly ionized species consists of a double-focusing electrostatic energy analyzer (Comstock) operated as a time-of-flight mass spectrometer. The analyzer is positioned in a vacuum vessel which is evacuated to a background pressure of ~10^{-7} Torr. The materials to be investigated are introduced into the chamber in a controlled manner at pressures typically from ~3×10^{-7} to 10^{-5} Torr. The 193-nm ArF* laser used for irradiation[3] (~10 psec, ~4 GW) is focused by a $f=50$-cm lens in front of the entrance iris of the electrostatic analyzer, producing an intensity of $\lesssim 10^{14}$ W/cm^2 in the experimental volume. The number of atoms in the focal volume is estimated to be ~10^4 at 10^{-6} Torr. Therefore, any ion produced with a probability less than ~10^{-4} cannot be detected without extensive signal averaging. Ions formed in the focal region are collected by the analyzer with an extraction field in the range of 50–500 V/cm and detected with a microchannel plate at the exit of the electrostatic device.

Representations of the experimental results are given in Figs. 1(a) and 1(b) and Table I. Figure 1(a) shows a sample of typical time-of-flight ion current data for Xe. Table I contains the normalized relative abundances of the observed ion charge states for Xe, derived from Fig. 1(a) and uncorrected for detector sensitivity. Experiments indicate that the detector is about four times as sensitive for Xe^+. Similar data have been recorded for He, Ne, Ar, Kr, I, Hg, and U. In Fig. 1(b), the observed ions and the total energies required for their generation in the electronic ground state are given.

A remarkable feature of the data is the magnitude of the total energy which can be communicated to the atomic systems, especially for high-Z materials. The total energy investment[4-7] of ~633 eV, a value equivalent to 99 quanta, needed to generate U^{10+} from the neutral atom, with neglect of the small contribution associated with molecular binding[8] in the experimental material UF_6, represents the highest energy value reported for a collision-free nonlinear process. The removal of the tenth electron from uranium, which requires[5] ~133 eV if viewed as an independent process, requires a minimum of 21 quanta. The coupling strength implied by this scale of energy transfer at an intensity of ~10^{14} W/cm^2 very sub-

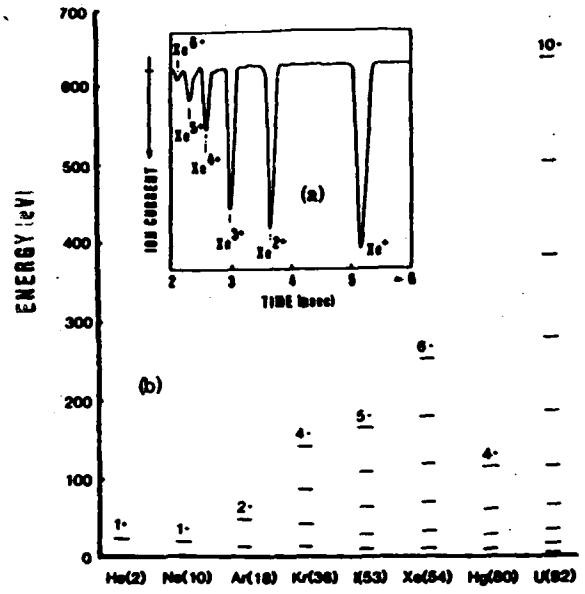

FIG. 1. Data concerning multiple ionization of atoms for 193-nm irradiation at $\sim 10^{14}$ W/cm^2. (a) Inset: typical time-of-flight ion current signal for xenon. (b) Plot of total ionization energies of the observed charge states as a function of atomic number (Z).

substantially exceeds that anticipated from conventional theoretical formulations describing multiquantum ionization.

Aside from the magnitude of the observed excitation energies, the general and strong tendency for increased coupling for materials heavier than argon and the similarity in the response of I and Xe, for which the maximum charge state observed in both cases corresponds to complete loss of the $5p$ shell, are significant. An examination of the ionization energies[4,5] for the species involved fails to suggest any consistent picture for this behavior. For example, the ionization of the second electron from He, which is not detected, requires an energy of ~54.4 eV, a value less than that necessary to remove the fifth electron from Xe. We are led to the conclusion that some factor other than the magnitude of the ionization potentials corresponding to the different species, or equivalently, the order of the nonlinear process, governs the strength of the coupling.

An explanation based simply on the density of states is also unconvincing. A comparison of the excited-state structures[9,10] for He and Ne quickly shows that the density of levels for Ne is very large in comparison to that for He, but only singly ionized species are observed for both materials. Likewise, the comparison of Xe and Hg leads to the conclusion that the density of states is not a key factor in determining the coupling strength.

TABLE I. Charge-state distribution of xenon derived from Fig. 1(a).

Charge state	Relative abundance
1+	44
2+	26
3+	20
4+	7
5+	5
6+	1

Conversely, all the conspicuous characteristics of Fig. 1(b) can be consolidated if the shell structure of the atom is the principal physical property determining the magnitude of the coupling. The considerable change seen in the atomic response observed between Ar and Kr implicates a role for the $3d$ shell which is filled in that region. A very similar variation between Ar and Kr, that has been observed in the amplitude for single-quantum multiple photoionization,[11] has been attributed to correlation effects arising from the d shell. A significant shell-dependent effect is also suggested by the comparative behavior of I and Xe, since complete removal of the valence $5p$ shell is observed in both cases although the total energies required differ substantially. We note that I and Xe exhibit similar and unusually intense $4d$ absorptions[12,13] in the region ~100 eV, strongly implicating correlated[14-16] motions in that shell.

The most elementary mechanism that could lead to the production of the observed ionic charge states is the stepwise removal of the individual electrons by conventionally described multiphoton ionization. A given charge state (e.g., Xe^{6+}) then requires the generation of all lower charge states, thereby linking the probability for its occurrence directly to the rates of production of these other species. The appearance of Xe^{6+} would require a sequence of 2-, 4-, 6-, 8-, 10-, and 12-photon processes of ionization.

The probabilities for multiphoton transitions calculated with standard perturbative approaches[17] and procedures valid in the high-field limit[18] have been discussed for single-electron systems. From these calculations, it can be shown that, at the 193-nm intensity of $\sim 10^{14}$ W/cm^2 used in these experiments, the transition rates for N-

photon processes decrease very rapidly with increasing N. An estimate shows that for $N=3, 5, 7$, the relative transition probabilities scale as $1:\sim 10^{-4}:\sim 10^{-8}$. On this basis, the expected ionic distributions should decrease very sharply towards higher charge states. Indeed, the abundances of ions in charge states $q > 3$ would fall below the detection limit of the apparatus used. It follows that the results obtained from single-electron models for multiquantum processes of this nature do not represent the observed experimental findings involving charge states $q > 3$. This conclusion holds for all materials studied that are heavier than Ar. Conversely, inspection of the experimental data indicates that the low-Z materials, essentially up to Ar, exhibit behavior in reasonable accord with that predicted by conventional theory. This interpretation can be reconciled with the presence of two different coupling mechanisms, one dominating in the low-Z region and the other providing enhanced coupling in the higher-Z materials. From our data, the division between these two regimes appears to occur between Ar and Kr.

The very substantial underestimate provided by standard theoretical models of the coupling strength observed and the envelope of the Z dependence both conspire to support an interpretation involving an alternative mode of coupling. The enhanced and anomalous strength of the radiative interaction points to a collective response of the atom. Such a collective response, or atomic plasmon,[19] is anticipated to be favored in the outer subshells of high-Z materials for which the correlation energy becomes a more substantial fraction of the total electronic energy.[4,20] The coherent motion envisaged has a counterpart in nuclear matter known as the giant dipole,[21] although giant multipoles higher than the dipole are known.[22]

All aspects of the experimental findings can be unified if an important mode of nonlinear coupling involves a direct multiquantum interaction with an atomic shell which undergoes a collective response. In this picture, it would follow naturally that the shell structure of the material would be reflected as an important property governing the coupling to the radiation field. Collective inner-shell responses have been discussed in relation to processes of single-photon ionization.[23] It is generally found that in cases for which the electronic correlations are important, the single-particle spectrum is very greatly altered, leading to a collectively enhanced many-electron process. In this regard, the xenon $4d^{10}$ shell[24,25] and the lanthanides[26] have been studied extensively. Recent analyses of collective responses in atomic and molecular systems have been given by Brandt and co-workers,[27-29] Wendin,[14,16,24] and Amusia and co-workers.[15,30] The results of our current studies simply indicate a nonlinear analog of this basic electronic mechanism. In the present experiments, the implication of the d-shell electrons seems particularly strong given the sharp change in behavior seen between Ar and Kr. Naturally, f electrons[31] would be expected to behave similarly, a consideration that clearly motivates study of the lanthanide sequence. Finally, the spatial dependence of the self-consistent field experienced by the atom[23] is expected to give rise to a complex Z dependence of the atomic response, an aspect that may be related to the relatively low value of maximum energy indicated in Fig. 1(b) for Hg.

In summary, studies examining the nonlinear coupling of intense ultraviolet radiation to atomic systems, spanning the atomic number range $Z=2$ to $Z=92$, reveal several important characteristics of this interaction. It is concluded that the conventional treatments of multiquantum ionization do not correspond to our experimental findings for high-Z materials. The essential findings are (1) an unexpectedly large amplitude for collision-free coupling, (2) a strong enhancement in the coupling strength for the heavy elements, and (3) the inference, based on the atomic-number dependence and the anomalous coupling strength, that a collective motion of d and f shells may play an important role in these phenomena. With this physical picture, selectivity in the population of excited ionic states is expected on the basis of photoelectron studies.[32]

Support for these studies was provided by the U. S. Office of Naval Research, the U. S. Air Force Office of Scientific Research through Grant No. AFOSR-79-0130, the National Science Foundation through Grant No. PHY81-16636, and the Avionics Laboratory, U. S. Air Force Wright Aeronautical Laboratories, Wright Patterson Air Force Base, Ohio. Fruitful discussions concerning atomic ionization energies with R. L. Carman and the skillful assistance of J. Wright and M. Scaggs are gratefully acknowledged.

[1]A. L'Huillier, L. A. Lompre, G. Mainfray, and C. Manus, Phys. Rev. Lett. 48, 1814 (1982).

[2]T. S. Luk, H. Pummer, K. Boyer, M. Shahidi, H. Egger, and C. K. Rhodes, in *Excimer Lasers—1983*, edited by C. K. Rhodes, H. Egger, and H. Pummer, AIP Conference Proceedings No. 100 (American Institute of Physics, New York, 1983).

[3]H. Egger, T. S. Luk, K. Boyer, D. R. Muller, H. Pummer, T. Srinivasan, and C. K. Rhodes, Appl. Phys. Lett. 41, 1032 (1982).

[4]R. D. Cowan, *The Theory of Atomic Structure and Spectra* (Univ. of California Press, Berkeley, 1981).

[5]T. A. Carlson, C. W. Nestor, Jr., N. Wasserman, and J. D. McDowell, At. Data 2, 63 (1970).

[6]F. T. Porter and M. S. Freedman, J. Phys. Chem. Ref. Data 7, 1267 (1978).

[7]J. Bearden and A. F. Burr, Rev. Mod. Phys. 39, 125 (1967).

[8]G. L. DePoorter and C. K. Rofer-Depoorter, Spectrosc. Lett. 8, 521 (1975).

[9]R. P. Madden and K. Codling, Astrophys. J. 141, 364 (1965); J. W. Cooper, U. Fano, and F. Prats, Phys. Rev. Lett. 10, 518 (1963); U. Fano, in *Photoionization and Other Probes of Many-Electron Interactions*, edited by F. J. Wuilleumier (Plenum, New York, 1976), p. 11.

[10]K. Codling, R. P. Madden, and D. L. Erderer, Phys. Rev. 155, 26 (1966).

[11]J. A. R. Samson and G. N. Haddad, Phys. Rev. Lett. 33, 875 (1974); J. A. R. Samson, in *Photoionization and Other Probes of Many-Electron Interactions*, edited by F. J. Wuilleumier (Plenum, New York, 1976), p. 419.

[12]F. J. Comes, U. Nielsen, and W. H. E. Schwarz, J. Chem. Phys. 58, 2230 (1973).

[13]D. L. Erderer, Phys. Rev. Lett. 13, 760 (1964).

[14]G. Wendin, Phys. Lett. 37A, 445 (1971).

[15]M. Ya. Amusia, V. K. Ivanov, and L. V. Chernysheva, Phys. Lett. 59A, 191 (1976).

[16]G. Wendin, in *Photoionization and Other Probes of Many-Electron Interactions*, edited by F. J. Wuilleumier (Plenum, New York, 1976), p. 61.

[17]Y. Gontier and M. Trahin, Phys. Rev. 172, 83 (1968).

[18]H. R. Reiss, Phys. Rev. A 1, 803 (1970), and Phys. Rev. Lett. 25, 1149 (1970), and Phys. Rev. D 4, 3533 (1971), and Phys. Rev. A 6, 817 (1972).

[19]F. Bloch, Z. Phys. 81, 363 (1933).

[20]*Correlation Effects in Atoms and Molecules*, edited by R. Lefebvre and C. Moser, Advances in Chemical Physics Vol. 14 (Wiley, New York, 1969); O. Sinanoglu and K. A. Brueckner, *Three Approaches to Electron Correlation in Atoms* (Yale Univ. Press, New Haven, Conn., 1970); A. Hibbert, Rep. Prog. Phys. 38, 1217 (1975); A. W. Weiss, Adv. At. Mol. Phys. 9, 1 (1973).

[21]G. C. Baldwin and G. S. Klaiber, Phys. Rev. 71, 3 (1947), and 73, 1156 (1948); M. Goldhaber and E. Teller, Phys. Rev. 74, 1046 (1948).

[22]*Giant Multipole Resonances*, edited by F. E. Bertrand (Harwood Academic, London, 1980).

[23]A. Zangwill and P. Soven, Phys. Rev. A 21, 1561 (1980); W. Ekardt and D. B. Tran Thoai, Phys. Scr. 26, 194 (1982).

[24]G. Wendin, J. Phys. B 3, 455, 466 (1970), and 4, 1080 (1971), and 5, 110 (1972), and 6, 42 (1973).

[25]D. J. Kennedy and S. T. Manson, Phys. Rev. A 5, 227 (1972); J. B. West, P. R. Woodruff, K. Codling, and R. G. Houlgate, J. Phys. B 9, 407 (1976); G. R. Wight and M. J. Van der Wiel, J. Phys. B 10, 601 (1977); D. M. P. Holland, K. Codling, J. B. West, and G. V. Marr, J. Phys. B 12, 2465 (1979).

[26]J. P. Connerade and D. H. Tracy, J. Phys. B 10, L235 (1977).

[27]W. Brandt and S. Lundquist, Phys. Rev. 132, 2135 (1963).

[28]W. Brandt, L. Eder, and S. Lundquist, J. Quant. Spectrosc. Radiat. Transfer 7, 185 (1967); G. Wendin and M. Chno, Phys. Scr. 14, 148 (1976).

[29]W. Brandt and S. Lundquist, J. Quant. Spectrosc. Radiat. Transfer 7, 411 (1967).

[30]M. Ya. Amusia, N. A. Cherepkov, and L. V. Chernysheva, Zh. Eksp. Teor. Fiz. 60, 160 (1971) [Sov. Phys. JETP 33, 90 (1971)].

[31]A. Zangwill and P. Soven, Phys. Rev. Lett. 45, 204 (1980).

[32]R. A. Rosenberg, M. G. White, G. Thomson, and D. A. Shirley, Phys. Rev. Lett. 43, 1384 (1979).

APPENDIX G

PHYSICAL REVIEW A VOLUME 32, NUMBER 1 JULY 1985

Collision-free multiple photon ionization of atoms and molecules at 193 nm

T. S. Luk, U. Johann, H. Egger, H. Pummer, and C. K. Rhodes
Department of Physics, University of Illinois at Chicago, P.O. Box 4348, Chicago, Illinois 60680
(Received 4 February 1985)

The nonlinear coupling of 193-nm radiation to a range of atomic and molecular materials has been experimentally explored up to a maximum intensity on the order of $\sim 10^{17}$ W/cm^2. Studies of collision-free ion production clearly exhibit anomalous behavior which strongly implies that the atomic shell structure is the principal determinant in the observed response. On the basis of the observed coupling strength and the measured atomic-number (Z) dependence, the experimental evidence points to a coherent atomic motion involving several electrons, possibly an entire shell, as the main physical mechanism enabling the scale of energy transfers seen. Therefore, states representing multiple excitations appear to play a central role in the coupling, a consideration that fundamentally distinguishes the nonlinear interaction of a multielectron atom from that of a single-electron system. Comparison of the experimental findings with standard theoretical treatments, of either a perturbative or nonperturbative nature, does not produce satisfactory agreement. Conversely, the formulation of a simple classical estimate qualitatively conforms to several features of the observed behavior including the shell character of the interaction, the maximum energy transfer, the dependence of the average energy transfer on the intensity of irradiation, the frequency dependence of the observed energy transfer, and the weak influence of polarization.

I. INTRODUCTION

The initial studies[1,2] of the Z dependence of collision-free multiphoton ionization of atoms at 193 nm clearly exhibited anomalous behavior in terms of the gross rate of energy transfer. The general class of physical processes studied was

$$N\gamma + X \rightarrow X^{q+} + qe^- . \quad (1)$$

A prominent feature of these studies was the unusually strong nonlinear coupling found characteristic of certain heavy materials such as Xe and U. In the case of U, the maximum observed values of N and q were found to be 99 and 10, respectively. By comparison with theoretical approaches based on perturbation theory,[3–5] these experiments clearly demonstrated that standard theoretical techniques were incapable, by a discrepancy as great as several orders of magnitude, of describing the observed results. Subsequent work,[6] conducted at a wavelength of 1.06 μm, has confirmed the anomalous nature of the coupling strength.

II. EXPERIMENTAL CONSIDERATIONS

For the studies of multiple ionization conducted since the earlier studies[1,2] were completed, the 193-nm ArF* laser used for irradiation[7] ($\sim$5 psec, $\sim$3 GW) was focused by an appropriate lens to generate intensities in the range of 10^{15}–10^{17} W/cm^2 in the experimental volume. In order to produce the highest intensities used, an $f/2$ aspheric focusing element was necessary. The ions are created in a vacuum vessel which is evacuated to a background pressure of $\sim 10^{-9}$ Torr.

In contrast to the earlier work,[1,2] the ion analyzer had a greatly extended time-of-flight drift region which permitted significantly superior mass and charge discrimination.[8] In this case, the isotopic signature of heavy atoms was readily distinguished.[9] This aspect provided a clear identification of the signal and enabled unambiguous separation of the desired ion current from any spurious signals originating from the background gas.

Figure 1 illustrates the characteristic isotopic pattern observed for Xe^{5+}. Note the close correspondence of the individual isotopic peaks to the strengths expected on the basis of the isotopic natural abundance.[10] Under typical experimental conditions, the ions formed in the focal region were collected by the analyzer with an extraction field in the range of 100–5000 V/cm, and a microchannel plate located at the exit of the time-of-flight region served as the ion detector. In addition, a laser-evaporation technique has been incorporated[11] into the apparatus to enable the study of elements, such as the lanthanides, which are not conveniently available in gaseous form, and preliminary experiments involving Eu and Yb have been conducted.

III. EXPERIMENT RESULTS ON ION PRODUCTION

The basic information obtained by observation of the ion spectra pertains to the scale of the energy transfer, for both average and peak values, communicated to the target atom X by the radiation field. An examination of the Z dependence of the average energy transfer is informative. Figure 2 illustrates the dependence observed at 193 nm for an intensity of irradiation in the range of 10^{15}–10^{16} W/cm^2. The comparison in the average energy absorbed for the adjacent elements, I ($Z=53$) and Xe ($Z=54$), is remarkable. This difference, which is approximately a factor of 4, cannot reasonably be attributed to experimental error, since only the strong, easily registered ion-signal

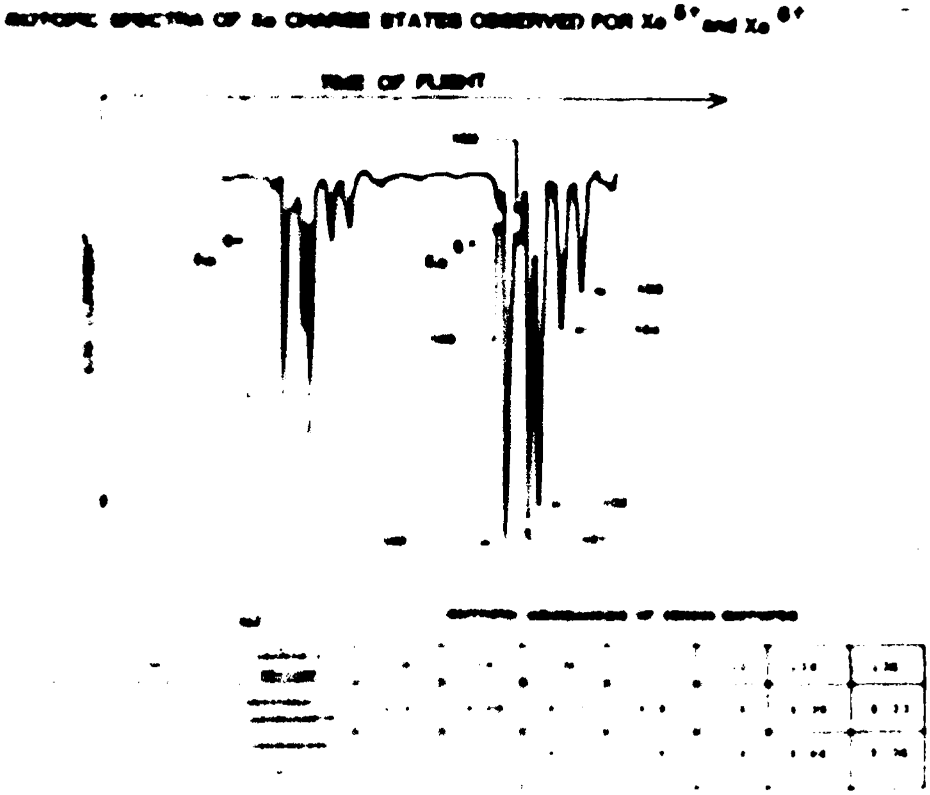

[illegible] with the natural abundance

[illegible]

[illegible] has been studied [illegible] spanning He ($Z = 2$) to U [illegible] the initial [illegible] spectrum for xenon is illustrated [illegible] the clear presence of eight [illegible] of which are seen to have approximately comparable abundances. An overall summary [illegible] is presented in Fig. 4. As [illegible] the maximum observed energy [illegible] of several hundred electron volts

[illegible]

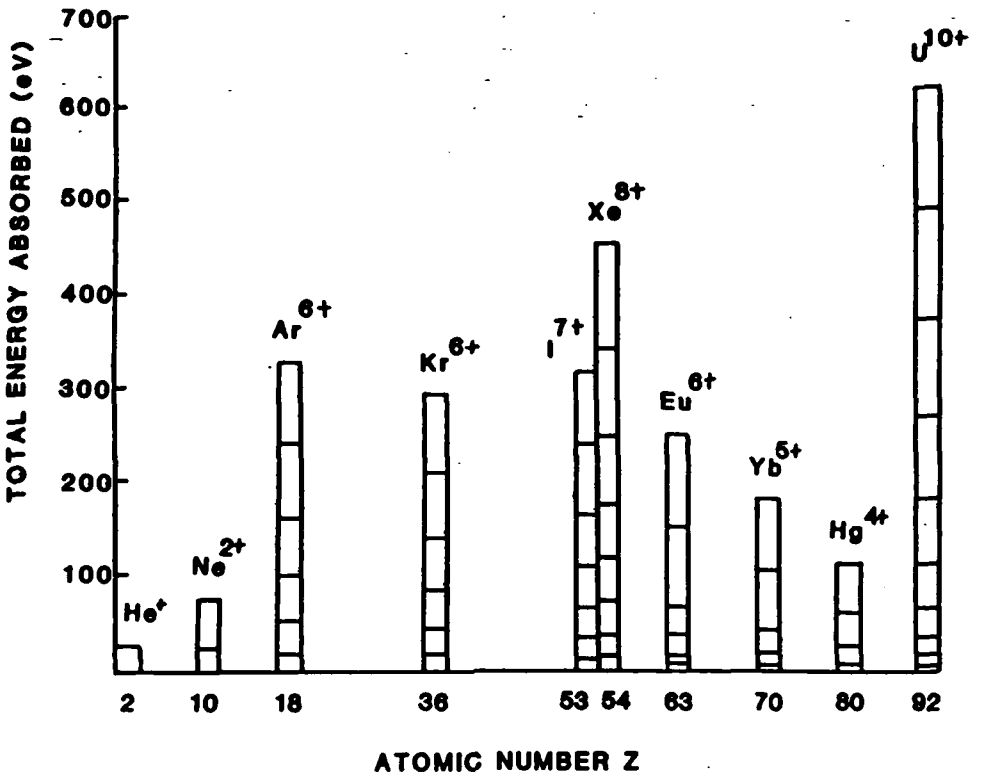

FIG. 4. Data concerning the multiple ionization of atoms for irradiation at 193 nm. Plot of total ionization energies of the observed charge states as a function of atomic number (Z). $_{53}I^{7+}$ was not positively identified because it coincides with an H_2O^+ background signal.

for the heavy materials. In the earlier experiments[1] conducted at $\sim 10^{14}$ W/cm^2, an examination of the ionization energies[12,13] of the species involved failed to suggest any consistent picture for the understanding of the stages of ionization produced. Furthermore, the subsequent work reported herein shows that this situation continues to exist at intensity levels as high as the 10^{16}–10^{17} W/cm^2 range. For example, the ionization of the second electron from He, which is not detected, requires an energy of $\sim$54.4 eV, a value less than that necessary to remove the fifth electron from Xe, a process which is clearly seen. We are led to the conclusion that some factor other than the magnitude of the ionization potentials corresponding to the different species, or equivalently, the order of the nonlinear process, governs the strength of the coupling. Clearly, this strong variation in coupling strength cannot be explained by standard perturbative and unperturbative theories.

Another clear characteristic of these data is the shell dependence manifested in the behavior of the heavier rare gases. For Ar, Kr, and Xe, the maximum charge states observed would correspond to the complete removal of atomic subshells. For these materials they are the $3p$, the $4p$ and both the $5s$ and $5p$ shells, respectively. Similarly, if the I^{7+} signal is present under the H_2O^+ peak, then that also implies complete removal of the $5s$ and $5p$ shells.

The hint provided by the role of the shell structure described above led to the hypothesis that it was mainly the number of electrons in the outer subshells that governed the coupling. A measurement of the response of elements in the lanthanide region, with the use of a method involving laser-induced evaporation to provide the material, enabled this view to be checked. As one moves from La ($Z=57$) to Yb ($Z=70$) in the lanthanide sequence, aside from slight rearrangements involving the $5d$ shell for Gd ($Z=64$), $4f$ electrons are being added to interior regions of the atoms. The data illustrated in Fig. 4 for $_{63}$Eu ($4f^7 6s^2$) and $_{70}$Yb ($4f^{14}6s^2$), which differ by seven $4f$ electrons, indicated that these inner electrons play a small role in the direct radiative coupling, a fact that is in rapport with the observed dependence on the outer-shell structure.

The intensity dependence of these ion spectra, corrected for the relative sensitivity of different charge states,[14] has also been examined, and Fig. 5 illustrates the nature of this response for xenon. Over the range of intensities studied ($\sim 10^{15}$–10^{17} W/cm^2), higher intensity translates generally into an increased yield of ions of a particular charge, although not necessarily an increase in the maximum charge state observed. For example, the ion $_{54}Xe^{8+}$, with ground-state[15] configuration $4d^{10}$, is the greatest charge state detected at $\sim 10^{16}$ W/cm^2, and although its abundance increases at $\sim 10^{17}$ W/cm^2, no $_{54}Xe^{9+}$ appears at the higher intensity. The average energy communicated to the atom also increases at the higher intensities, although clearly not as rapidly as the intensity. In the case of xenon, as shown in Fig. 5, the average ener-

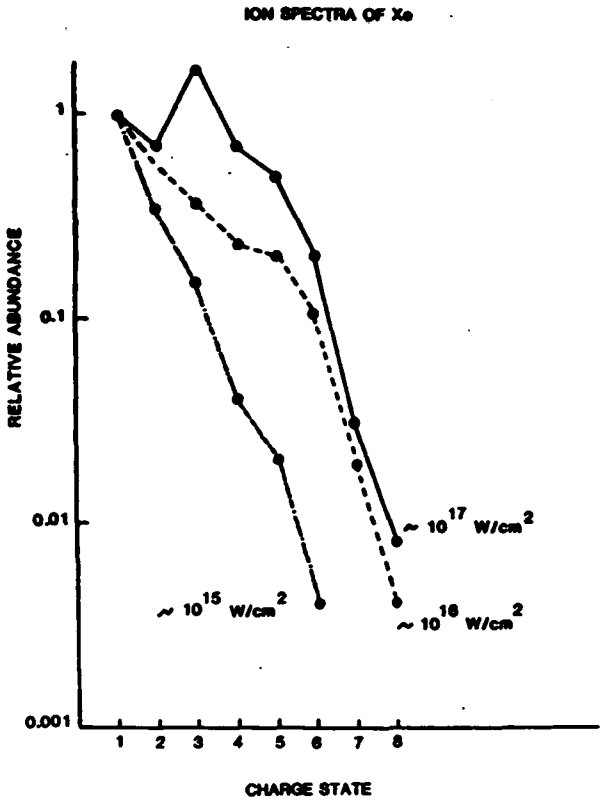

FIG. 5. Relative abundance of charge-state distributions observed in the ion spectra of xenon in the intensity range 10^{15}–10^{17} W/cm^2 at 193 nm.

gy increased by only approximately a factor of 7 when the intensity was increased 100-fold. It is important, however, to be aware of the experimental uncertainty involved in the intensity dependence, since low-charge states can be disproportionately produced in the outer regions of the focal volume. This particular effect is expected to be somewhat more significant for materials, such as $_{63}$Eu and $_{70}$Yb, which can be ionized by a single 193-nm photon. Nevertheless, the data illustrated in Fig. 5 clearly show a relatively weak intensity scaling for the high-order (N) process that produces the higher-charge-state species observed.

Several existing types of nonperturbative calculations predict a variety of different laws governing the intensity (I) scaling of the transition probabilities. For a field strength comparable to or greater than the binding field E_b of the electrons, Pert[16] and Mittleman[17] derived $I^{-1/2}\ln(I/I_0)$ and a I_0/N^2I relationships, respectively, in which I_0 represents the intensity corresponding to the value of the electronic-binding field E_b. Moreover, under conditions for which the radiative-field strength is small compared to the electronic-binding field E_b, Keldysh[18] obtained a $I^{1/4}$ scaling. Furthermore, for the experiments under consideration, it is not apparent that the analyses of Pert[16] and Mittleman[17] can be validly applied to the production of the higher observed charge states, since the intensity I is much less than the corresponding I_0 for those species. Finally, we note that, in the weak-field limit corresponding to applicability of the Keldysh[18] approach, the model predicts a substantial abundance of He^{2+}, a conclusion that stands in contrast to the experimentally observed absence of this charge state.

The frequency dependence of the coupling has also been examined by comparison of our results at 193 nm with other studies performed[19,20] at 1.06 μm and 0.53 μm. The comparison, conducted at an intensity of $\sim 10^{14}$ W/cm^2 for both krypton and xenon, indicates that the average energy absorbed is reduced at the longer wavelengths. Figures 6 and 7 illustrate these comparative differences for krypton and xenon, respectively.

The influence of laser polarization has been studied for xenon. With the use of a quarter-wave plate, the linearly polarized radiation normally produced by the 193-nm source[7] can be conveniently transformed into circularly polarized radiation. The ion spectra observed for xenon were found to be negligibly modified by the change from linear to circular polarization. This result is in contrast to that expected on the basis of perturbation theory analysis[3] in the single-electron picture of the interaction. In that case, for high-order processes, the much greater abundance of available channels for linear polarization produces a substantially greater ionization rate in comparison to that characteristic of circular polarization. Nonperturbative treatments[21] also indicate that greater ionization rates are commonly associated with linear polarization.

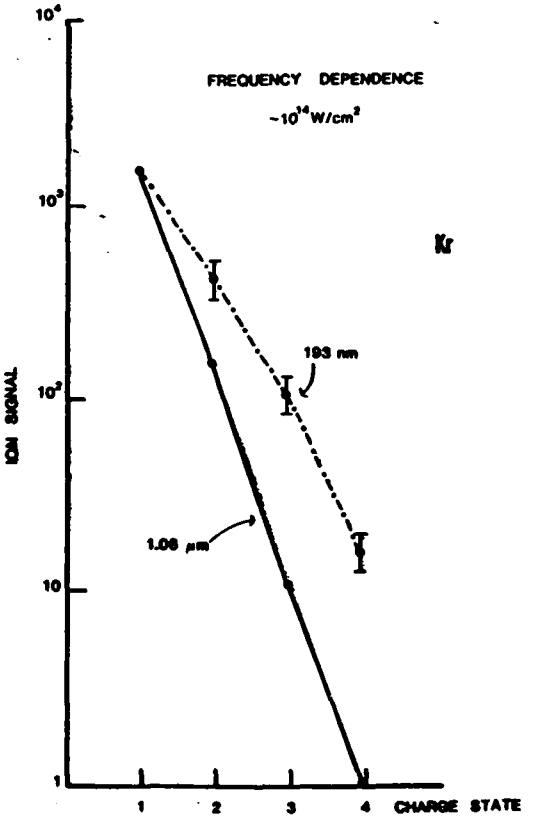

FIG. 6. Comparison of charge-state spectra observed for krypton at an intensity of $\sim 10^{14}$ W/cm^2 at 1.06 μm and 193 nm. The data shown for 1.06 μm irradiation is taken from Ref. 19.

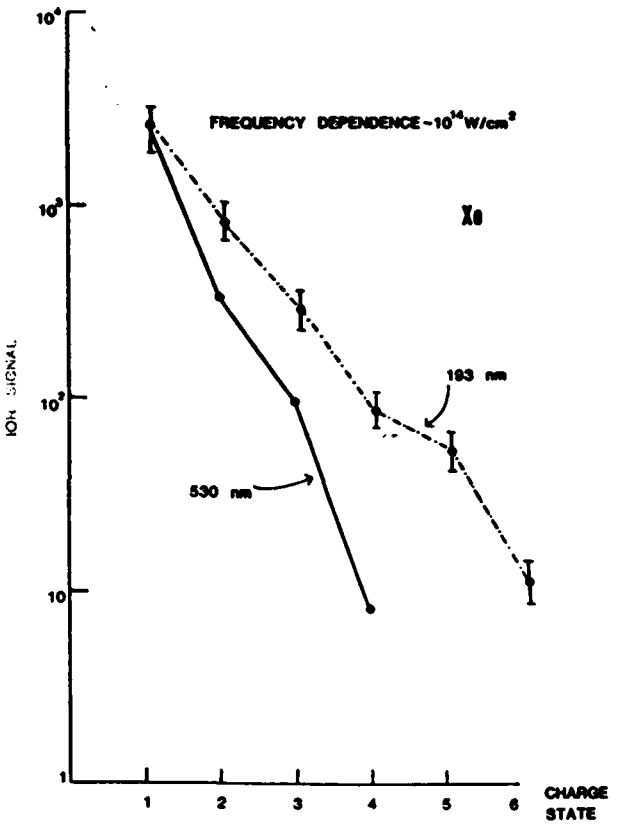

FIG. 7. Comparison of charge-state spectra observed for xenon at an intensity of $\sim 10^{14}$ W/cm^2 at 0.53 μm and 193 nm. The data shown for 0.53 μm irradiation is taken from Ref. 20.

We comment further that, at sufficiently high electromagnetic fields, all angular momentum states become accessible,[22] a fact that will certainly alter the polarization dependence.[17]

IV. DISCUSSION OF RESULTS

A. Ion production

In broad terms, we now discuss and interpret these experimental findings. In the data represented in Figs. 2, 4, and 5, two salient characteristics exhibited by the experiments involving ion production are (i) the large coupling strength for heavy materials and (ii) the sharp variations present in the average energy transfer as a function of Z, such as that illustrated by the comparison of iodine and xenon in Fig. 2.

Qualitatively, several aspects of the basic interaction emerge clearly. With reference to xenon, for example, a 100-fold increase in 193-nm intensity from $\sim 10^{15}$–10^{17} W/cm^2 does not drastically increase either the maximum charge state observed or the average energy transferred. Over this range of intensity, the charge state q advances from $q=6$ to 8, and the average energy transferred in the interaction increases by approximately a factor of 7. Within the experimental uncertainty over this range of intensity, the average energy appears to grow approximately linearly to the magnitude of the radiative electric field, a fact we comment on further below. Furthermore, since the charge state does not increase beyond the apparent removal of the full $5p$ and $5s$ subshells, tentatively we can conclude that the $n=5$ shell is an important agent coupling the xenon atom to the 193-nm radiation field. It is also known, however, particularly from photoionization studies involving multiple-electron ejection,[23,24] that the $5p$, $5s$, and $4d$ shells exhibit substantial intershell coupling and behave in a collective fashion in a manner resembling a single supershell.[25] In this connection it is also known that the spatial dependence of the self-consistent field[26] experienced by the atom is expected to contribute to the Z dependence of the atomic response.

In this picture, the increase in multiphoton coupling strength results directly from the larger magnitude of the effective charge involved in the interaction. In this way, a multielectron atom undergoing a nonlinear interaction responds in a *fundamentally different fashion* from that of a single-electron atom.[18,27,28] This interpretation involving a collective atomic response with several coupled atomic shells is exhibited most prominently for Xe, but is also apparent in the nature of the Ar and Kr spectra.

We now briefly consider the magnitude of the coupling strength. A strong implication of the studies reported initially[1] and noted above, and which is reinforced by the additional data illustrated in Figs. 2 and 4, is that the atomic-shell structure is a principal determinant in the atomic response. Indeed, all the conspicuous characteristics of the experimental findings can be consolidated by this single principle. Surprisingly, the order N of the nonlinear process appeared as relatively unimportant. Furthermore, the data strongly indicated that a collective response of an entire shell, or a major fraction thereof, was directly involved in the nonlinear coupling. Collective responses of atomic shells, as noted above, have been discussed in relation to the mechanism of single-photon photoionization. The present studies simply point to a *nonlinear analog* of this basic electronic mechanism. With this picture, the outer atomic subshells are envisaged as being driven in *coherent* oscillation by the intense ultraviolet wave. Of course, such a model can only be valid if the damping rate, presumably by electron emission, is sufficiently low. Consequently, that assumption is naturally implied in this description. We note that an oscillating atomic shell, quantum mechanically, would be represented by a *multiply* excited configuration. The simplest examples are doubly excited levels of the type commonly observed in the extreme ultraviolet spectra of the rare gases such as argon.[29] Naturally, higher stages of multiple excitation can be considered such as those discussed in the context of planetary atoms.[30]. Therefore, if this type of description is a valid representation of the radiative coupling, then it would follow that multiply excited configurations would be prodigiously generated and, therefore, be prominent features in any excited-state populations produced. We shall see below that additional evidence supports this interpretation in the case of xenon and krypton.

Within the framework of the above picture, it is possible to make a simple estimate of the energy absorbed by an atom and the corresponding scaling law describing the intensity dependence. For this we imagine an atom com-

posed of two parts: (i) an outershell of n electrons driven by the radiative field at frequency ν and (ii) an atomic core. The outer electrons could, through "inelastic collisions" at frequency ν_c, transfer energy to the core. Assuming a mean free path δ for the electrons between two collisions, and for large collision frequencies ($\nu_c > \nu$), the work done by the radiative field between two collisions is $neE\delta$. The total energy transferred to the core during the lifetime τ of the highly excited atomic configuration represented by the coherently driven outer shell is then given by

$$neE\,\delta\nu_c\,\tau=\hbar\omega_x\ . \tag{2}$$

Here, this energy is written in the form of a quantum with magnitude $\hbar\omega_x$. Using $\delta\nu_c=v$ and estimating the average velocity v by equating the kinetic energy of an electron with the potential energy lost between two collisions

$$\tfrac{1}{2}mv^2=eE\delta\ , \tag{3}$$

one obtains for the optical electric field

$$E=\frac{1}{e}\left[\frac{\hbar\omega_x}{n\tau}\sqrt{m/2\delta}\right]^{2/3}\ . \tag{4}$$

As an example, if we take $\hbar\omega_x=1$ keV, $n=6$ representing a closed p shell, $\delta=0.1$ A, and $\tau=10^{-15}$ sec, then $E=2.0\times10^9$ V/cm, corresponding to an intensity $I=10^{16}$ W/cm^2.

The value taken for the mean free path δ requires some discussion. It is predicted on the mean free path associated with the scattering of an electron, having an energy considerably above the Fermi energy, interacting through a screened Coulomb potential in an electron gas. The cross section σ_0 for this process, estimated, for example, in the case of sodium,[31] by Pines,[32] to have a value $\sigma_0\sim17\pi a_0^2$, in combination with the electron density ρ_e characteristic of the xenon $n=5$ shell, yields a scale length $\delta\sim(\rho_e\sigma_0)^{-1}\sim10^{-9}$ cm. Interestingly, if we examine the data for xenon in Figs. 4 and 5, we observe that the maximum charge state Xe^{8+}, which corresponds to $\sim$450 eV total energy,[13] was seen for an intensity in the range of 10^{16}–10^{17} W/cm^2, figures not far from those represented by Eq. (4). Finally, since Eq. (4) is independent of the frequency ν, a weak dependence on frequency is expected. As shown in Figs. 6 and 7 frequency does not appear to exert a strong influence on the average energy transfer. Certainly, no quantitative accuracy can be claimed for the estimate made above; its only significance is that the general nature of the atomic response and the qualitative scales of the physical quantities, for what appear to be reasonable choices of atomic parameters, are roughly that observed in actual experiments.

It is informative to consider the case representing the high-intensity limit.[17,22] At an intensity of $\sim10^{19}$ W/cm^2, which we anticipate will be available soon with the use of subpicosecond rare-gas halogen lasers, the peak ultraviolet electric field is more than tenfold e/a_0^2, so that loosely bound outer electrons can be approximately modeled as free particles. In this case, the problem reduces to that of the acceleration of electrons in focused laser fields,[33] an issue that, incidentally, is related to the acceleration of cosmic rays by rotating neutron stars.[34] Simple estimates indicate that for intensities of that magnitude, the outer electrons would approach relativistic velocities ($\sim$50–80 keV) and that oscillating atomic-current densities on the order of 10^{14}–10^{15} amps/cm^2 could be established as a result. Actually, in this high-intensity limit it appears to be possible to estimate the coupling of the coherently driven outer electrons with the remaining atomic core by a relatively simple procedure. Since the electron-kinetic energies are considerably above their corresponding binding energy, it appears possible to use a first-order Born approximation[35] in a manner similar to that used to the study of electron collisions for K- and L-shell ionization[36] and shell specific ionization processes in highly charged ions.[37,38] Indeed, in the case of xenon ions, cross sections for electron-impact ionization are available.[39] It also seems possible to account for the transition from adiabatic to sudden excitation of core electrons with a rather simple procedure.[40]

The results illustrated in Fig. 2 indicate a complex and rapidly varying Z dependence for heavy materials. It has not been possible to formulate a reasonable explanation of this behavior solely on the basis of the systematics of valence-shell properties.[1,2,9] These results again point to the significance of intershell couplings. Such couplings are manifested in an obvious way, for example, in Coster-Kroning processes.[41] Indeed, if we consider, as specific cases, giant Coster-Kronig (GCK) processes of the type

$$n\underline{s}\rightarrow n\underline{p}^2nd,\epsilon d \tag{5}$$

and super Coster-Kronig (SCK) processes like

$$n\underline{p}\rightarrow m\underline{f},\epsilon f\ , \tag{6}$$

it is well established that strong perturbations[42] are present and that the single-electron picture seriously breaks down.[43] These processes are sensitive to systematics of the shell-energy levels and, therefore, can exhibit sharp variation in their dependence on atomic number. In particular, many-electron effects are prominent when there is a degeneracy between single- and double-vacancy states that are strongly coupled. These requirements are commonly fulfilled and strong collective behavior arises, for example, in single-photon photoionization.[25,44,45] Significantly, in comparison with the results illustrated in Figs. 2 and 4 these effects are known to be of importance[43,46] over certain regions of the atomic number from argon to the heavier part of the Periodic Table. A particular case involves double photoionization of Ga in the energy region near the $3d$ ionization threshold.[47]

The degeneracies of single- and double-hole states occur at particular values of the atomic number. Figure 8, which was derived from calculations[48] of neutral-atomic binding energies performed with a relaxed-orbital relativistic Hartree-Fock-Slater analysis, illustrates the region from $_{29}$Cu to $_{40}$Zr. Near degeneracies in the $n=3$ shell are indicated for $_{32}$Ge, $_{36}$Kr, and $_{37}$Rb. Moreover, since the $3p$ and $3d$ orbitals both have their maximum charge densities at nearly identical radii,[49] strong coupling between these subshells is expected to occur. Indeed, such couplings are known[50] to produce discontinuous behavior in the L_α and $L_{\beta1}$ satellite fractions as well as in the

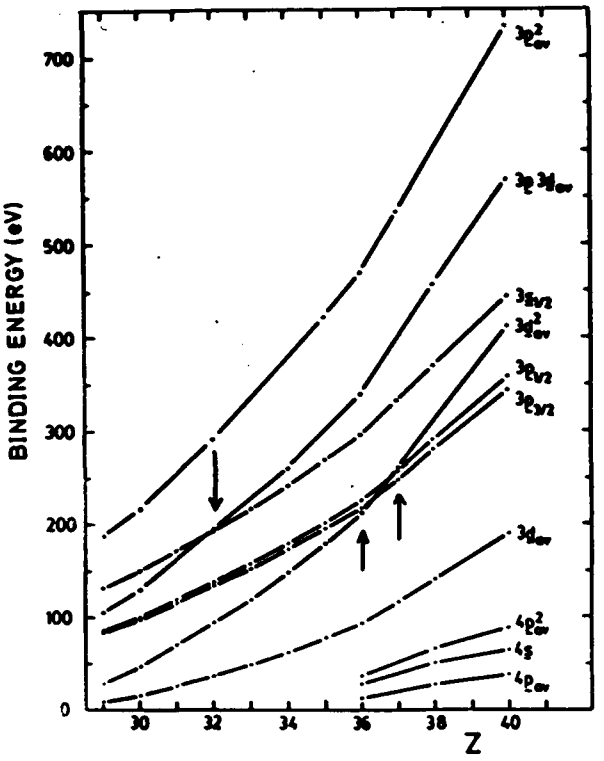

FIG. 8. Atomic, relativistic ΔSCF single- and double-hole levels for $_{29}$Cu to $_{40}$Zr. The energies were obtained from Ref. 48 and the figure has been adapted from Fig. 17 of Ref. 43 appearing on p. 28. The arrows indicate the locations of near degeneracies between single- and double- vacancy states. Figure reprinted by permission.

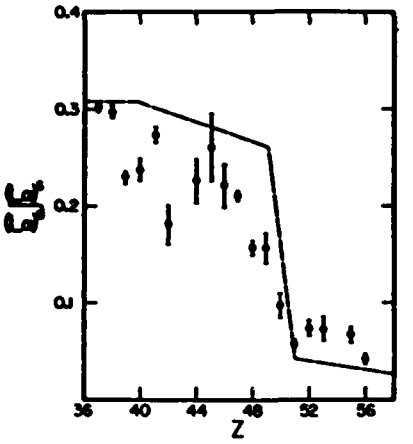

FIG. 9. $L\alpha$ satellite $(L\alpha)^s$ to diagram $(L\alpha)^d$ line ratio as a function of atomic number Z. The data are taken from Ref. 50. The dashed curve corresponds to a theoretical treatment adapted from a calculation performed in Ref. 51. Figure reprinted by permission.

$L_{\beta 3,4}/L_\alpha$ and $L_{\beta 1}/L_\alpha$ intensity ratios as a function of atomic number Z. The data illustrated in Fig. 9 convey this effect for the L_α features for atomic number in the vicinity of $Z=50$. In this case, the observation[50] is consistent with a critical atomic number of $Z\simeq 50$ for the L_1-L_3M_{45} Coster-Kronig transition. The dashed line appearing in Fig. 9 is a theoretical curve related to the calculation of Krause *et al.*[51] The discontinuous behavior in Z characteristic of the data shown in Fig. 9 has a striking similarity to that exhibited in Fig. 2. Similarly sharp variations in atomic number have been calculated in the Auger width associated with a $2s$ vacancy.[52] Interestingly, it has been predicted[52] that plasma-shielding effects can have a strong influence on autoionizing widths by causing an energetic closing of the channel for Coster-Kronig transitions, although no such behavior has ever been actually observed. For a $2s$ vacancy with an argon-like configuration, a sharp change in the $2s$ width is estimated for $Z=22$ at an electron density of $\sim 5\times 10^{20}$ cm^{-3}. It should be possible to achieve such a plasma density, under controlled conditions, with the use of a subpicosecond rare-gas halogen source. We note that several informative accounts of vacancy distributions[53] and the behavior of autoionizing widths are available.[54,55]

Normally, relaxation mechanisms involving intershell coupling, such as Coster-Kronig and Auger processes, are experimentally observed by initially producing an inner-shell vacancy which subsequently relaxes, generally producing multiple vacancies and excitation in outer shells. In principle, the initial vacancy can be produced with radiative excitation,[56,57] electron collisions,[58,59] beam-foil methods,[60] ion collisions,[61] and nuclear-decay processes such as K capture.[62,63] To these alternatives, the results of these experiments suggest that multiquantum processes may now conceivably be added. Furthermore, the nature of Coster-Kronig processes provides a hint at the mechanism that could make this possible. In simple terms, this can be viewed as a *reverse* Coster-Kronig process[43] in which *multiple* excitations in outer shells generate excitations in more tightly bound shells. In this fashion we use the term "excitation" in a broad sense to include both bound excited levels and continuum states (vacancies). For double and single excitations or vacancies, this mechanism is basically represented by the reverse reactions of processes (5) and (6), namely,

$$n\underline{s}\leftarrow n\underline{p}^2 nd,\epsilon d\ , \tag{5'}$$

$$n\underline{p}\leftarrow n\underline{d}^2 mf,\epsilon f\ . \tag{6'}$$

Indeed, since these intershell couplings are sensitive to the systematics of the shell binding energies, resonance effects[43,64] are expected in certain regions of atomic number Z for the reasons stated above. In summary, the similarity of the discontinuous character of the data represented in Figs. 2 and 9 mentioned above plainly, although tentatively, suggest a common origin for this general type of behavior, namely, the possibility that the electrons involved in the nonradiative relaxation of an atom in the forward reaction (5) could, in the *reverse* process (5'), if driven by coupling to a sufficiently intense radiation field, generate a corresponding transfer of energy *into* an atom.

Finally, we comment on some aspects of this general line of inquiry which deserve exploration. It is of natural and fundamental interest to further examine the properties of the ionization process (i) with different ultraviolet

frequencies, specifically 248 nm, since it is readily available at high intensities, (ii) over a greater variation in Z, particularly in regions for which the intershell couplings are believed to be large, and (iii) at intensities above 10^{17} W/cm^2. Studies of this nature, therefore, are obviously an important element of our current activity. Examples of specific materials which appear as promising candidates for study are Ba, on account of the known[65–67] sensitivity of the $4f$ orbital to the state of ionization; the lanthanides, on account of the unusual systematics associated with the filling of the $4f$ shell and the effects of configuration interaction[68,69] prominent for certain members of that sequence; and $_{90}$Th and $_{92}$U, the heaviest materials[70] available for practical study. Finally, since molecular binding is known to have an influence on the behavior of inner-shell transitions, sometimes with rather dramatic effects, such as that known for the $5d$-f absorption of uranium,[71] a comparison of the ionization properties of certain molecular and atomic species is planned.

B. Radiative properties

Measurements of emission produced by the highly excited states provide important information on the nature of the coupling mechanism involved. Specifically, if the interpretation discussed above in Sec. IV involving a collective atomic response with coupled atomic shells has any validity, detectable emission at short wavelengths or energetic electrons would be expected.

Indeed, in a recent, although preliminary, experiment examining the properties of the xenon ions produced in the ion studies discussed in Secs. III and IV A which was designed to detect extreme ultraviolet radiation, significant levels of spontaneous radiation and/or energetic electrons have been observed.[72] The spectral width observed in the radiation channel was determined by the 1500-Å aluminum filter (10–80 eV) used. The schematic of the apparatus employed in these studies and the signal observed are shown in Fig. 10. The signal occurs precisely

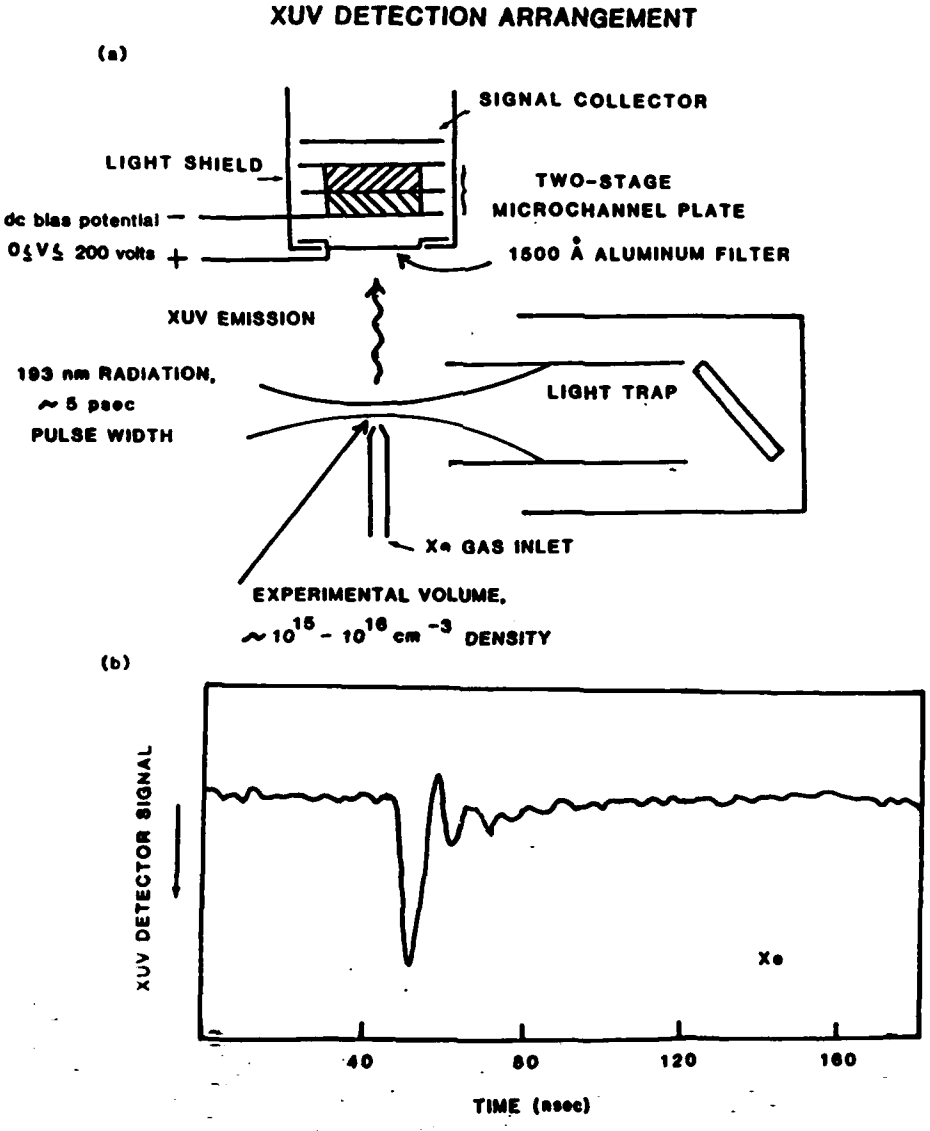

FIG. 10. (a) Experimental arrangement used to detect xuv radiation from highly excited atoms excited by 193-nm radiation at an intensity of $\sim 10^{16}$–10^{17} W/cm^2. (b) xuv signal observed from xenon in the 10–100 eV range with ~100-V bias between the aluminum filter and the microchannel plate; some ringing of the detector circuit is evident.

at the time of irradiation of the gas with the 5-psec 193-nm radiation, vanishes if the xenon flow is terminated, and is not observed if the xenon is replaced by other materials, such as krypton or hydrogen. In order to eliminate the influence of electrons that could be produced by photoemission from the surface of the aluminum filter facing the microchannel plate from reaching the detector, a dc electrical bias of 200 V was applied to retard the motion of electrons moving in that direction. Some evidence of an electron-induced signal was observed if no negative-bias potential was used. Judging from the spectral transmission and the electron stopping power of the 1500-Å Al filter, we conclude that only xuv photons in the region of 10–100 eV and energetic electrons exceeding a few hundred electron volts could possibly contribute to the observed signal. This observation is consistent with the excitation of an inner-shell electron state, presumably the $4d$ level in xenon, by atomic processes of the nature described above. Significantly, recent experiments[73] measuring the photoelectron spectra under identical experimental conditions have ruled out the presence of electrons with sufficient energy to produce the observed signal. In addition, the photoelectron measurements[73] reveal the presence of several lines in the xenon spectrum which closely match the pattern expected from $N_{4,5}$-OO Auger transitions, a finding which strongly reinforces the interpretation given above. Naturally, further experiments are being prepared to determine the electron and photon spectra of the observed emission more accurately.

Another class of experiments, intended to observe stimulated emission from highly excited states, has also been performed.[74–77] In the experiment designed to observe amplification in Kr in the extreme ultraviolet range, intense stimulated emission was detected on five transitions spanning the range from 91.6–100.3 nm. An examination of the linewidths and tuning behavior of these transitions led to a possible identification of the upper levels as autoionizing neutral levels involving both singly excited inner-shell excitations[75] and doubly excited configurations.[74,76,77] This is the first indication of stimulated emission arising from such electronically unstable states. Finally, if we reason that the anomalous increase in this coupling is connected with the presence of multiply excited configurations and if we recall that coherently excited shells, in quantum-mechanical language, are described in terms of multiple excitations,[78,79] then the results of the ion-production experiments and the observation of stimulated emission in krypton can be viewed in a unified manner.

V. CONCLUSIONS

The nonlinear coupling of 193-nm radiation to a range of atomic systems has been studied up to a maximum intensity on the order of $\sim 10^{17}$ W/cm^2. Studies of ion production, under collision-free conditions, exhibit anomalous behavior which implicate the atomic-shell structure as the principal determinant in the observed response. On the basis of the coupling strength observed and the measured Z dependence, the experimental evidence points to a collective coherent atomic motion involving several electrons, possibly an entire shell, as the main physical mechanism enabling the scale of the energy transfers seen. In quantum-mechanical language, states representing multiple excitations appear to play a central role in the coupling, a consideration that *fundamentally* distinguishes the nonlinear interaction of a multielectron atom from that of a single-electron system.

Comparison with standard theoretical treatments of nonlinear processes, of either perturbative or nonperturbative nature, does not produce agreement with the experimental findings. Conversely, the formulation of a simple classical estimate qualitatively conforms to several features of the observed behavior. They are, with particular reference to xenon, the shell character of the interaction, the maximum energy transfer, the dependence of the average energy transfer on the intensity of irradiation, the frequency dependence of the energy transfer, and the weak influence of polarization. Furthermore, it is postulated that the sharp variations in Z noted for the heavy materials is due to a reverse Coster-Kronig mechanism in which inner-shell excitations are produced by interaction with multiply excited outer shells. These points naturally imply the existence of a systematic trend in nonlinear properties which extends throughout the Periodic Table. This would then constitute a principle of classification which appears to bear some analogy to that developed earlier for electron potentials, binding energies, and electron scattering phase shifts.[80]

ACKNOWLEDGMENTS

The authors wish to acknowledge the expert technical assistance of M. J. Scaggs, J. R. Wright, and D. M. Gustafson. This work was supported by the U.S. Air Force Office of Scientific Research under Contract No. F49630-83-K-0014, the U.S. Department of Energy under Grant No. DE-AS08-81DP40142, the U.S. Office of Naval Research, the National Science Foundation under Grant No. PHY-81-16626, the U.S. Defense Advanced Research Projects Agency, and the Avionics Laboratory, U.S. Air Force Wright Aeronautical Laboratories, Wright Patterson Air Force Base, Ohio.

[1]T. S. Luk, H. Pummer, K. Boyer, M. Shahidi, H. Egger, and C. K. Rhodes, Phys. Rev. Lett. 51, 110 (1983).

[2]T. S. Luk, H. Pummer, K. Boyer, M. Shahidi, H. Egger, and C. K. Rhodes, in *Excimer Lasers—1983*, edited by C. K. Rhodes, H. Egger, and H. Pummer (American Institute of Physics, New York, 1983), Vol. 100, p. 341.

[3]P. Lambropoulos, in *Advances in Atomic and Molecular Physics*, edited by D. R. Bates and B. Bederson (Academic, New York, 1976), Vol. 12, p. 87.

[4]H. B. Bebb and A. Gold, Phys. Rev. 143, 1 (1966).

[5]Y. Gontier and M. Trahin, J. Phys. B 13, 4384 (1980); Phys. Rev. 172, 83 (1968).
[6]A. L'Huillier, L-A. Lompré, G. Mainfray, and C. Manus, in *Proceedings of the Conference on Laser Techniques in the Extreme Ultraviolet*, edited by S. E. Harris and T. B. Lucatorto (American Institute of Physics, New York, 1984), Vol. 119, p. 79.
[7]H. Egger, T. S. Luk, K. Boyer, D. F. Muller, H. Pummer, T. Srinivasan, and C. K. Rhodes, Appl. Phys. Lett. 41, 1032 (1982).
[8]W. C. Wiley and I. H. McLaren, Rev. Sci. Instrum. 26, 1150 (1955).
[9]H. Egger, T. S. Luk, W. Müller, H. Pummer, and C. K. Rhodes, in *Proceedings of the Conference on Laser Techniques in the Extreme Ultraviolet*, edited by S. E. Harris and T. B. Lucatorto (American Institute of Physics, New York, 1984), Vol. 119, p. 64.
[10]*Table of Isotopes*, 7th ed., edited by C. Michael Lederer and Virginia S. Shirley (Wiley, New York, 1978).
[11]T. S. Luk, U. Johann, H. Jara, and L. Haddad (private communication).
[12]R. D. Cowan, *The Theory of Atomic Structure and Spectra* (University of California Press, Berkeley, 1981).
[13]T. A. Carlson, C. W. Nestor, Jr., N. Wasserman, and J. McDowell, At. Data 2, 63 (1970).
[14]B. L. Schram, A. J. H. Boerboom, W. Kleine, and J. Kistemaker, *Amplification Factors of a Particle Multiplier for Multiply Charged Noble Gas Ions*, in *Proceedings of the 7th International Conference on Phenomena in Ionized Gases (Beograd, 1965)*, edited by B. Perović and D. Tosić (Gradevinska Knjiga House, Beograd, 1966), Vol. 1, p. 170.
[15]J. Blackburn, P. K. Carroll, J. Costello, and G. O'Sullivan, J. Opt. Soc. Am. 73, 1325 (1983).
[16]G. J. Pert, J. Phys. B 8, L173 (1975).
[17]J. Gersten and M. H. Mittleman, Phys. Rev. A 10, 74 (1974).
[18]L. V. Keldysh, Zh. Eksp. Teor. Fiz. 47, 1945 (1964) [Sov. Phys.—JETP 20, 1307 (1965)].
[19]A. L'Huillier, L-A. Lompré, G. Mainfray, and C. Manus, Phys. Rev. Lett. 48, 1814 (1982).
[20]A. L'Huillier, L-A. Lompré, G. Mainfray, and C. Manus, Phys. Rev. A 27, 2503 (1983).
[21]H. S. Brandi, L. Davidovich, and N. Zagury, J. Phys. (Paris) Colloq. 43, C2-397 (1982).
[22]S. Geltman and M. R. Teague, J. Phys. B 7, L22 (1974).
[23]M. J. Van der Wiel and T. N. Chang, J. Phys. B 11, L125 (1978).
[24]M. Ya Amusia, in *Advances in Atomic and Molecular Physics*, edited by D. R. Bates and B. Bederson (Academic, New York, 1981), Vol. 17, p. 1.
[25]M. Ya. Amusia and N. A. Cherepkov, in *Case Studies in Atomic Physics 5*, edited by E. W. McDaniel and M. R. McDowell (North-Holland, Amsterdam, 1975), p. 47.
[26]A. Zangwill and P. Soven, Phys. Rev. A 21, 156 (1980); Phys. Rev. Lett. 45, 204 (1980); W. Ekardt and D. B. Tran Thoai, Phys. Scr. 26, 194 (1982); A. Zangwill, Ph.D. thesis, University of Pennsylvania, 1981.
[27]H. R. Reiss, Phys. Rev. A 1, 803 (1970); Phys. Rev. Lett. 25, 1149 (1970); Phys. Rev. D 4, 3533 (1971); Phys. Rev. A 6, 817 (1972).
[28]H. S. Brandi and L. Davidovich, J. Phys. B 12, L615 (1979).
[29]R. P. Madden, D. L. Ederer, and K. Codling, Phys. Rev. 177, 136 (1969).
[30]I. C. Percival, Proc. R. Soc., London Ser. A 353, 289 (1977).
[31]C. Kittel, *Quantum Theory of Solids* (Wiley, New York, 1983), p. 116.
[32]David Pines, *Elementary Excitations in Solids* (Benjamin, New York, 1984).
[33]Marc J. Feldman and Raymond Y. Chiao, Phys. Rev. A 4, 352 (1971); E. S. Sarachik and E. R. Schappert, Phys. Rev. D 1, 2738 (1970).
[34]James E. Gunn and Jeremiah P. Ostriker, Phys. Rev. Lett. 22, 728 (1969).
[35]N. F. Mott and H. S. W. Massey, *The Theory of Atomic Collisions* (Oxford University Press, London, 1965); H. S. W. Massey and E. H. S. Burhop, *Electronic and Ionic Impact Phenomena* (Oxford University Press, London, 1969), Vol. 1; H. A. Bethe, Ann. Phys. (Leipzig) 5, 325 (1930).
[36]James H. Scofield, Phys. Rev. A 18, 963 (1978).
[37]L. B. Golden, P. H. Sampson, and K. Omidvar, J. Phys. B 11, 3235 (1978).
[38]L. B. Golden and D. H. Sampson, J. Phys. B 13, 2645 (1980).
[39]D. C. Gregory and D. H. Crandall, Phys. Rev. A 27, 2338 (1983); C. Achenbach, A. Müller, E. Salzborn, and R. Becker, J. Phys. B 17, 1405 (1984).
[40]T. Darrah Thomas, Phys. Rev. Lett. 52, 417 (1984).
[41]E. J. McGuire, in *Atomic Inner-Shell Processes*, edited by B. Crasemann (Academic, New York, 1975), Vol. 1, p. 293.
[42]T. Aberg, in *Photoionization and Other Probes of Many-Electron Interactions*, edited by F. J. Wuilleumier (Plenum, New York, 1976), p. 273.
[43]G. Wendin, *Breakdown of the One-Electron Pictures in Photoelectron Spectra*, Vol. 45 of *Structure and Bonding* (Springer, Berlin, 1981); S. Lundquist and G. Wendin, J. Electron. Spectrosc. Relat. Phenom. 5, 513 (1974).
[44]G. Wendin, in *Vacuum Ultraviolet Radiation Physics*, edited by E. E. Koch, R. Haensel, and C. Kunz (Pergamon, Braunschweig, 1974), p. 225.
[45]G. Wendin, in *Photoionization and Other Probes of Many-Electron Interactions*, edited by F. J. Wuilleumier (Plenum, New York, 1976), p. 61; H. P. Kelly and S. L. Carter, Phys. Scr. 21, 448 (1980).
[46]J. A. R. Samson and G. N. Haddad, Phys. Rev. Lett. 33, 875 (1974); J. A. R. Samson, in *Photoionization and Other Probes of Many-Electron Interactions*, edited by F. J. Wuilleumier (Plenum, New York, 1976), p. 419.
[47]J. P. Connerade, J. Phys. B 10, L239 (1977).
[48]Ken-Ning Huang, Michio Aoyagi, Mau Hsiung Chen, Bernd Crasemann, and Hans Mark, At. Data Nucl. Data Tables 18, 243 (1976).
[49]Frank Herman and Sherwood Skillman, *Atomic Structure Calculations* (Prentice-Hall, Engelwood Cliffs, 1963).
[50]B. L. Doyle and S. M. Shafroth, Phys. Rev. A 19, 1433 (1979).
[51]M. O. Krause, F. J. Wuilleumier, and C. W. Nestor, Jr., Phys. Rev. A 6, 871 (1972).
[52]B. F. Rozsnyai, V. L. Jacobs, and J. Davis, Phys. Rev. A 21, 1798 (1980).
[53]P. Venugopala Rao, Mau Hsiung Chen, and Bernd Crasemann, Phys. Rev. A 5, 997 (1972).
[54]S. Southworth, U. Becker, C. M. Truesdale, P. H. Kobrin, D. W. Lindle, S. Owaki, and D. A. Shirley, Phys. Rev. A 28, 261 (1983).
[55]Masahide Ohno, Phys. Rev. B 29, 3127 (1984); A. Fahlman, M. O. Krause, and T. A. Carlson, J. Phys. B 17, L217 (1984).
[56]T. A. Carlson, W. E. Hunt, and M. O. Krause, Phys. Rev. 151, 41 (1966).
[57]T. S. Axelrod, Phys. Rev. A 13, 376 (1976); T. Åberg, in *Proceedings of the International Conference on Inner-Shell Ionization and Future Applications, Oak Ridge, 1972*, edited

by R. W. Fink, S. T. Manson, J. M. Palms, and P. V. Rao, Natl. Tech. Info. Service Spec. Publ. No. CONF-720 (U.S. Dept. of Commerce, Springfield, VA, 1972), p. 404; John W. Cooper, in *Atomic Inner-Shell Processes*, edited by B. Crasemann (Academic, New York, 1975), Vol. I, p. 160.

[58]T. A. Carlson, W. E. Moddeman, and M. O. Krause, Phys. Rev. A 1, 1406 (1970).

[59]L. M. Middleman, R. L. Ford, and R. Hofstadter, Phys. Rev. A 2, 1429 (1970); K. Ishii, M. Kamiya, K. Sera, S. Morita, H. Tawan, M. Cyamada, and T. C. Chu, Phys. Rev. A 15, 906 (1977).

[60]I. Martinson, in *Beam-Foil Spectroscopy*, edited by S. Bashkin (Springer, Berlin, 1976), p. 33.

[61]D. H. Madison and E. Merzbacher, in *Atomic Inner-Shell Processes*, edited by B. Crasemann (Academic, New York, 1975), Vol. I, p. 1; U. Fano and W. Lichten, Phys. Rev. Lett. 14, 627 (1965); M. Barat and W. Lichten, Phys. Rev. A 6, 211 (1972); P. Ziem, R. Bruch, and N. Stoltefoht, J. Phys. B 8, L480 (1975); J. M. Hansteen, in *Advances in Atomic and Molecular Physics*, edited by D. R. Bates and B. Bederson (Academic, New York, 1975), Vol. I, p. 299; P. H. Mokler and F. Folkmann, in *Structure and Collisions of Ions and Atoms*, edited by I. A. Sellin (Springer, Berlin, 1978), p. 201.

[62]Robert J. Walen and Chantel Briancon, in *Atomic Inner-Shell Processes*, edited by B. Crasemann (Academic, New York, 1975), Vol. I, p. 233; M. S. Freedman, in *Photoionization and Other Probes of Many-Electron Interactions*, edited by F. J. Wuilleumier (Plenum, New York, 1976), p. 255.

[63]W. Bambynek, H. Behrens, M. H. Chen, B. Crasemann, M. L. Fitzpatrick, K. W. D. Ledingham, H. Genz, M. Mutterer, and R. L. Intemann, Rev. Mod. Phys. 49, 77 (1977).

[64]C.-O. Almbladh and L. Hedin, in *Handbook on Synchrotron Radiation*, edited by Ernst-Eckhard Koch (North-Holland, Amsterdam, 1983), Vol. 16, p. 607.

[65]T. B. Lucatorto, T. J. McIlrath, J. Sugar, and S. M. Younger, Phys. Rev. Lett. 47, 1124 (1981).

[66]J. P. Connerade, K. Dietz, M. W. D. Mansfield, and G. Weymans, J. Phys. B 17, 1211 (1984); B. Sonntag, T. Nagata, Y. Satow, A. Yagistita, and M. Yanagihara, J. Phys. B 17, L55 (1984).

[67]K. Nuroh, M. J. Shott, and E. Zaremba, Phys. Rev. Lett. 49, 862 (1982).

[68]S.-T. Lee, S. Süzer, E. Matthias, R. A. Rosenberg, and D. A. Shirley, J. Chem. Phys. 66, 2496 (1977); R. D. Cowan, Nucl. Instrum. Methods 110, 173 (1973).

[69]Ernst-Rudolf Radtke, Dissertation, Universität Bonn, December, 1980.

[70]H. R. Moser, B. Delley, W. D. Schneider, and Y. Baer, Phys. Rev. B 29, 2947 (1984).

[71]M. Pantelouris and J. P. Connerade, J. Phys. B 16, L23 (1983).

[72]T. S. Luk and K. Boyer (private communication).

[73]U. Johann, T. S. Luk, H. Egger, H. Pummer, and C. K. Rhodes (unpublished).

[74]K. Boyer, H. Egger, T. S. Luk, H. Pummer, and C. K. Rhodes, J. Opt. Soc. Am. B 1, 3 (1984).

[75]T. Srinivasan, H. Egger, T. S. Luk, H. Pummer, and C. K. Rhodes, in *Laser Spectroscopy VI*, edited by H. P. Weber and W. Lüthy (Springer, Berlin, 1983), p. 385.

[76]H. Egger, T. S. Luk, W. Müller, H. Pummer, and C. K. Rhodes, "Collision-Free Multiple Ionization of Atoms and XUV Stimulated Emission in Krypton at 193 nm," *AIP Conference Proceedings on Laser Techniques in the Extreme Ultraviolet, Boulder, Colorado, 1984* (AIP, New York, in press).

[77]H. Pummer, H. Egger, T. S. Luk, and C. K. Rhodes, SPIE J. 461, 53 (1984).

[78]M. E. Kellman and D. R. Herrick, Phys. Rev. A 22, 1536 (1980).

[79]A. R. P. Rau, J. Phys. B 16, L699 (1983).

[80]A. R. P. Rau and U. Fano, Phys. Rev. 167, 7 (1968).

APPENDIX H

RARE GAS ELECTRON ENERGY SPECTRA PRODUCED BY COLLISION-FREE MULTIQUANTUM PROCESSES *

U. Johann, T. S. Luk, H. Egger,† and C. K. Rhodes
Department of Physics, University of Illinois at Chicago
P. O. Box 4348, Chicago, Illinois 60680

ABSTRACT

The energy spectra of electrons generated by collision-free multiphoton ionization of Xe, Kr, Ar and Ne irradiated at intensities up to $\sim 10^{15}$ W/cm^2 with picosecond 193 nm (6.41 eV) radiation have been studied with an energy resolution of ~50 meV. For the first time, the formation of multiply charged ions by a sequential process of ionization has been directly detected in the electron spectra by the observation of a characteristic pattern of interwoven above threshold ionization (ATI) ladder line series. The appearance and relative intensity of specific electron lines depends strongly on the presence of near-resonances and features of the interaction involving the laser pulse shape, saturation, and the shift of the ionization threshold arising from the influence of the ponderomotive potential. The experimental results are compared qualitatively with data from ion time-of-flight experiments and with differing models of multiphoton ionization.

---

†Present address: Lambda Physik, Hans-Böckler-Strasse 12, D-3400 Göttingen, Federal Republic of Germany.

*Submitted to Physical Review A

I. INTRODUCTION

With the development of spectrally bright infrared and ultraviolet light sources in the last decade, it has become possible to study the detailed mechanism of nonlinear coupling of an intense laser field to isolated atoms unaffected by collisions. Several experiments[1] have been performed to analyze the ion charge state production,[2-5] determine the electron energy spectrum,[6-9] and to measure the optical radiation emitted.[4,10] For processes that occur under these conditions, one of the areas of substantial interest involves the possibility of producing atomic excitations suitable for the generation of stimulated emission in the x-ray range.[1b]

For a "weak" laser field (intensity $< 10^{11}$ W/cm^2), the coupling of radiation to an isolated atom can be described fairly well within the framework of lowest order perturbation theory (LOPT) in which only one electron at a time is assumed to be involved in multiphoton ionization.[1,11] However, for much higher laser intensities (10^{12} - 10^{17} W/cm^2), the situation is poorly understood and other coupling mechanisms involving many electrons may play an appreciable role.

Experimentally, the electron energy spectra produced by radiation with a quantum energy $\hbar\omega$ exhibit certain salient characteristics. A prominent feature of the observed electron spectra is the process known as above threshold ionization (ATI), a phenomenon associated with the absorption of a number of photons N greater than the minimum value N_{min} required, on energetic grounds, to produce ionization.[7,12] When $N > N_{min}$, the measured electron energy spectrum consists of a series of discrete lines each corresponding to the order N with an energy separation of adjacent orders equaling the quantum $\hbar\omega$. Furthermore, it is found that the electron lines are not significantly shifted by the effect of the ponderomotive force.[13] Recently, two-photon free-free transitions have also been analyzed.[14] In addition, the order of

nonlinearity observed for higher order ATI electron lines is approximately the same as for the threshold ionization line, a finding which stands in contradiction to LOPT.[13] This result is, however, consistent with the order of nonlinearity measured in ion yield experiments,[15] although more recent experiments may alter this picture.[16] It is also seen that certain low energy electron lines disappear with increasing laser intensity at characteristic values which depend upon the frequency of irradiation.[13] Finally, high energy electrons (> 100 eV) have been observed[8,17] in low resolution experiments with intense infrared lasers (> 10^{15} W/cm^2).

Studies[2,3,4] of ion production by multiquantum processes have indicated the presence of an anomalously strong coupling for materials in certain regions of the periodic table. It appears that the magnitude of this coupling is sufficiently great that reasonable account cannot be made by a mechanism involving the sequential stripping of individual valence electrons in a step-wise process. Furthermore, the results on ion production exhibited readily observed dependencies on the atomic shell structure, or equivalently, the atomic number, and the frequency of irradiation.

The hypothesis has been advanced that multiply excited states representing highly organized coherent motions of several valence shell electrons may play an important role in the coupling at sufficiently high laser intensity.[18] This mechanism is an alternative to the sequential process described above if the multiply excited state is produced by a direct multiphoton amplitude from the neutral atomic ground state. Such an excited state would be expected to decay by multiple electron emission to energetically available continuum states. In addition, it has been shown theoretically, that multiply excited states of outer-shell electrons can transfer energy into inner-shell excitations.[19,20]

In this paper, we describe the results of experiments in which the energy spectra of electrons generated by collision-free multiphoton ionization of xenon,

krypton, argon, and neon irradiated at 193 nm in the intensity range spanning 10^{13} - 10^{15} W/cm^2 were studied. The field strengths E corresponding to this range are $0.06 \leq E \leq 0.60$, as measured in atomic units (e/a_o^2). This investigation had two goals. One involved obtaining information concerning the mechanism of coupling leading to the high ion charge states observed in earlier experiments[3,4] under similar conditions, while the second sought an understanding of the conditions necessary for the production of inner-shell excitations by processes of intra-atomic energy transfer.

II. EXPERIMENTAL

A. 193 nm Laser System and Beam Properties

For irradiation of the target gas, a 193 nm picosecond ArF* excimer laser system has been used.[21] This system delivers, in both temporal and spatial characteristics, a nearly transform limited output beam whose properties are the following: pulse energy ∿ 40 mJ, pulse length ∿ 5 psec, quantum energy $\hbar\omega$ ∿ 6.4 eV, and repetition rate ∿ 1 Hz. In order to perform the experiments, the 193 nm beam was focussed with a quartz lens (f = 205 mm at 193 nm) into the interaction region of an electron spectrometer. As shown below, the focal volume is several times larger than the diffraction limited value, a fact mainly attributed to imperfections in the optical system such as spherical abberation. It follows that the maximum intensity produced in the interaction region is on the order of 10^{15} W/cm^2. In addition to the short picosecond pulse, amplified spontaneous emission (ASE) at λ ∿ 193 nm is also present and may represent a substantial contribution to the energy in the form of a ∿ 10 nsec background pulse.[21] With no picosecond input into the 193 nm amplifier chain, the ∿ 10 nsec ASE pulse has an energy of ∿ 50-100 mJ. Although this relatively low intensity radiation produces no detectable ionization of Ne and Ar, the intensity is sufficient to singly ionize a considerable fraction of the experimental material in the focal volume for Kr and Xe. However,

examination of the distributions of the pulse energies for both the ASE and picosecond components showed that the ASE focus only partially overlaps the focal volume associated with the picosecond pulse. Consequently, the ASE is expected to have little influence on the interaction dynamics of the picosecond pulse with the atoms in the focal region of the short pulse beam. This was confirmed experimentally by changing the temporal position of the picosecond feature within the much broader ASE pulse, a procedure which, in some cases, altered slightly the relative intensity of the electron lines. Therefore, no qualitative influence on the electron spectra was present. Finally, from analyses of the 193 nm beam,[21] it is believed that the presence in the interaction volume of large spatial and temporal spikes was unlikely.

Electron Spectrometer and Signal Processing

The space charge produced in the experimental volume can appreciably alter the characteristics of the observed electron energy spectra. In order to minimize the influence of the space charge on the electron spectra, it is necessary to produce only a few electrons per laser shot in the focal region. Therefore, the electron spectrometer should have a high collection efficiency in addition to a reasonable energy resolution. The magnetic mirror time-of-flight electron spectrometer designed for this purpose allows a collection solid angle of about 2π steradians at an energy resolution of approximately $\sim$ 50 meV. The principles of operation and physical properties of this type of spectrometer [22,23] have been extensively studied by Kruit and Read.[24]

The interaction volume, in which the electrons are produced, is located in the strong field region ($\sim$ 3000 Gauss) of a Co-Sm-permanent magnet as shown in Fig. (1). The electrons produced are immediately bound to the magnetic field and execute a cyclotron motion as they are accelerated in the magnetic field gradient along the symmetry axis of the spectrometer. The electronic

trajectories, although complicated in detail, occur with conservation of the total kinetic energy of the electrons. The laser polarization is oriented parallel to the magnetic field axis. Those electrons emitted into the forward 2π steradian solid angle enter the low field region (5-1 Gauss) after travelling a distance of about 200 mm with their velocity oriented nearly parallel to the z-axis. The electron energy can now be measured with a time-of-flight technique. In the 800 mm drift tube region, which is shielded against stray magnetic fields by μ-metal layers to a value less than ∿10 mG, a weak magnetic guide field of 0.5 - 5 Gauss is maintained by a solenoid. The time that the electrons spend in the drift tube can be increased by the application of a retarding electric field, which considerably improves the energy resolution for the more energetic electrons. The electrons are detected by a two-stage multi-channel plate detector, (MCP-Chevron type), which is connected to a transient digitizer (Tektronix 7912 AD). The data taking, processing and storage were handled by a PDP-11 computer.

The basic properties[24] of the electron spectrometer are now described. Without retardation, the total flight time T for an electron from the focal volume at position Z_o on the z-axis to the detector located at point Z_D is given by

$$T(E_o,\theta_o) = \sqrt{\frac{m}{2E_o}} \int_{Z_o}^{Z_D} \frac{dz}{\sqrt{1 - \frac{B(z)}{B_o}\sin^2\theta_o}} \quad . \tag{1}$$

In expression (1) E_o is the initial electron kinetic energy, $0 \leq \theta_o \leq \pi/2$ is the angular range of emission with respect to the z-axis, B(z) is the magnetic field as a function of position along the z-axis, and $B_o \equiv B(Z_o)$. The time distribution function dn_e/dt, for n_o monoenergetic simultaneously generated and isotropically emitted electrons, which describes their arrival at the detector, is given by

$$\frac{dn_e}{dt}\,[n_o, T(E_o,\theta_o)] = \sqrt{\frac{E_o}{2m}}\;\frac{n_o B_o}{\cos\theta_o}\left[\int_{Z_o}^{Z_D} \frac{B(z)\,dz}{\left[1 - \frac{B(z)}{B_o}\sin^2\theta_o\right]^{3/2}}\right]^{-1} . \qquad (2)$$

Physically, the spread in electron arrival times occurring at the detector arises from the influence of the magnetic field as the velocities of the electrons become parallel. For anisotropic electron emission with a $\cos^2\theta_o$ distribution,[24] Eq. (2) is multiplied by a factor of $3\cos^2\theta_o$. Fig. (2) illustrates the calculated time-of-flight distribution at the detector for anisotropic emission along with the measured influence of the retarding potential on the electron linewidth.

The target gas uniformly fills the whole vacuum system and typical operating pressures were between 2×10^{-8} Torr to 5×10^{-6} Torr. Experimentally it was found that, depending on the laser intensity and the ionization probability, both the effects of space charge in the focal region and detector saturation could severely limit the highest useful gas density. The space charge tends to broaden the width of the electron lines, as shown in (Fig. 2), and generates a low energy tail on the distribution. Consequently, the total ion production was usually kept below $\sim$ 1000 per laser pulse. At low signal intensity, the MCP was operated in an event counting mode, a procedure which supresses electrical noise and allows integration over several hundred laser shots. Since the background pressure in the vacuum

Since the magnetic field diverges in the drift region, this type of electron spectrometer exhibits a magnification whose value depends upon the ratio of the magnetic field strength in the interaction region to that present at the detector. By varying the magnetic field in the drift tube, a circle with a diameter between ∿ 250 μm and ∿ 500 μm can be imaged onto the detector surface. With this knowledge, an approximate estimate of the interaction volume has been made through a comparison of the electron yield with the number density of the target gas. Working at a sufficiently high intensity so that the ionization of the sample is saturated; and taking into account the overall efficiency of detection (∿ 25%), we find a diameter of approximately 18 μm. This result is in good agreement with the value of ∿ 14 μm estimated independently from the limit imposed by spherical abberation. Furthermore, the spectra are observed to be insensitive to the position of the focussing lens when it is moved along the laser beam axis for a distance of about 1 mm. This indicates that the intensity varies rather slowly in the vicinity of the focal plane. Since exact information on the intensity distribution throughout the interaction volume is not known, an uncertainty of approximately a factor of three remains for the absolute laser intensity used in these experiments.

III. RESULTS AND DISCUSSION

In the following, the general characteristics of the measured electron energy spectra are presented and discussed. Since xenon exhibits a more rich and complex spectrum than those characteristic of the other rare gases, the features specific to this case will be emphasized in the discussion below.

A. Above Threshold Ionization in Rare Gas Electron Spectra

Figure 3 illustrates typical electron time-of-flight spectra recorded at a peak laser intensity of ∿ 5 x 10^{14} - 10^{15} W/cm^2 for neon, argon, and krypton along with a

spectrum for xenon corresponding to an intensity of $\sim 5 \times 10^{13}$ W/cm^2. Also shown are the relevant energy level diagrams[26] with the multiphoton transitions and the electron emission lines indicated. The gas density was adjusted to keep the total electron production below $\sim$ 1000 per pulse.

Several features of the data are apparent. In addition to the prominent lowest order ionization lines corresponding to the absorption of two photons by xenon, three photons by krypton and argon, and four photons by neon, which leave the corresponding ions in the ground $ns^2np^5{}^2P^o_{3/2}$ states, several above threshold ionization lines are present. The intensity of the observed ATI lines, however, drops rapidly with increasing order. Only in the case of xenon is a resolved line present indicating that the first ion (Xe^+) is left in its lowest excited state $ns^2np^5{}^2P^o_{1/2}$.

Several relevant experimental parameters are summarized in Table I. The measured ionization threshold laser intensities are well below the actual peak intensities corresponding to these spectra, a fact which places them well into the saturation regime in which the electron yield grows much slower with increasing laser intensity than that characteristic of the threshold region due to depletion of neutral atoms in the interaction region.[27] This means that a substantial number and, indeed, in certain circumstances, most of the singly charged ions may be formed before the laser peak intensity is obtained in the experimental volume.

The experimental linewidth, if obtained under conditions of high resolution for which space-charge broadening is avoided, allows an estimate of the upper limit for the transition rate to be made. This width, which varies between 200 meV and 400 meV at the highest laser intensities used in these studies, yields values for the transition rate spanning the range between 3×10^{14} sec^{-1} and 6×10^{14} sec^{-1}. Since a full analysis of the observed linewidth has not been performed, the actual transition rate could be substantially lower than

the upper limit. Factors that could contribute to excessive broadening are shot-to-shot fluctuations of the line positions and the influence of dynamic stark shifts of atomic levels caused by varying field intensities in the interaction volume.

Table I also contains a comparison of the measured threshold intensities with values calculated according to the Keldysh-Raiser formula in the multiphoton ionization limit.[28,29] This formulation gives

$$W = B_{-}\omega \cdot N_{min}^{3/2}(e^2\vec{E}_o^2/8m\omega^2 \cdot T(\vec{E}))^{N_{min}} \quad (3)$$

in which W is the transition rate, B is a factor of order unity, N_{min} is the minimum number of photons with quantum energy ($\hbar\omega$) necessary to be absorbed in the ionization process, $T(\vec{E})$ is the generalized field dependent ionization threshold discussed below in Section III,B.1, and $\vec{E}_o$ is the laser electric field amplitude. The transition probability P then becomes

$$P = W \cdot \tau_p \quad (4)$$

in which τ_p denotes the laser pulse length. Reasonable agreement is found with this formula for both Ne and Ar. In contrast, the experimental values are considerably lower than the corresponding Keldysh values for both Kr and Xe. The threshold intensity is defined in these calculations as that necessary to produce a one electron signal per laser pulse at the detector. It should be noted in this connection that the non-perturbative Keldysh formula fails to reproduce the production rate observed for highly charged ions.[4] Clearly, the influence of atomic resonances is responsible for the lower thresholds observed in Kr. In this case, a set of three known[30] two-photon near-resonances exists involving transitions from the $4s^24p^6$ ground state to those with the excited configuration $4s^24p^56p$. The energy parameters describing the detuning from exact resonance are small with values of $\delta E \approx$ -6 meV, -36 meV, and 44 meV, respectively.

One of these transitions, occurring in the overall process

$$4s^2 4p^6 {}^1S_0 + 2\gamma(6.41\ eV) \rightarrow 4s^2 4p^5 ({}^2P^o_{3/2}) 6p + 1\gamma \rightarrow 4s^2 4p^5 {}^2P^o_{3/2} + e^-(5.25\ eV), \quad (5)$$

strongly favors the excitation channel leading to the J = 3/2 core level, the state corresponding to the ground ionic term. In comparison, the more off-resonant channel

$$4s^2 4p^6 {}^1S_0 + 2\gamma(6.41\ eV) \rightarrow 4s^2 4p^5 ({}^2P^o_{1/2}) 6p + 1\gamma \rightarrow 4s^2 4p^5 {}^2P^o_{1/2} + e^-(4.56\ eV), \quad (6)$$

with detuning $\delta E \sim 630$ meV, leads to formation of the ion in the first excited state. Thus, the near-resonance in process (5) explains the absence or the weakness of the 4.56 eV electron line corresponding to reaction (6) in the Kr spectrum. A similar situation holds for Ar, in which a two-photon near-resonance, with upper level configuration $3s^2 3p^5 4p$ and detuning parameter $\delta E \sim 85$ meV, may enhance ion ground state formation in the process

$$3s^2 3p^6 {}^1S_0 + 2\gamma(6.41\ eV) \rightarrow 3s^2 3p^5 ({}^2P^o_{3/2}) 4p + 1\gamma \rightarrow 3s^2 3p^5 {}^2P^o_{3/2} + e^-(3.48\ eV). \quad (7)$$

It should be noted, however, that the energy of detuning can change significantly at high laser fields due to the dynamic stark shift, a fact that can significantly alter resonance effects[31,32] of this kind.

The situation is complicated in xenon by the fact that the two-photon energy (12.82 eV) falls in the energy region containing the autoionizing Rydberg series which converges to the excited $5s^2 5p^5 {}^2P^o_{1/2}$ ion state. On account of the rather close spacing of Rydberg levels, near-resonances occur in this region. For example, the observed[33] even parity state

$5s^2 5p^5 ({}^2P_{1/2}) 5f {}^1[\frac{5}{2}]_2$, which falls at 12.886 eV, has a weak field detuning parameter of only $\delta E = +64$ meV. This level, as well as other even parity states, could have an appreciable influence on the overall transition rate.

In xenon with 193 nm radiation, sufficient energy is available to populate both the ionic $^2P^o_{3/2}$ ground state and the corresponding $^2P^o_{1/2}$ excited state with three and four photon absorption. Interestingly, the observed branching ratio ($R_N \equiv {}^2P^o_{1/2}/{}^2P^o_{3/2}$) for the corresponding electron line intensities I_e gives

$R_3 = I_e(5.79\ eV)/I_e(7.10\ eV) \sim 5$ and

$R_4 = I_e(12.20\ eV)/I_e(13.51\ eV) \sim 4.$

This indicates a strong enhancement of the channel forming the excited $^2P^o_{1/2}$ state, a finding that strongly contrasts with the statistical value of 0.5 and the measured ratio of 0.62 for single photon ionization at a comparable total energy.[34] Branching ratios in other multiphoton experiments have been reported to be $R_5 \sim 1$ for 5 photon absorption[35] at $\hbar\omega = 2.81$ eV and $R_N = 1.35$, 0.43, and 0.3 for 6, 7, and 8 photon absorption at $\hbar\omega = 2.34$ eV, respectively.[12] Apparently, several factors, including the laser intensity, the presence of near-resonances, and the order of the process, influence the value of this ratio.

Since the experimental results provide information on the relative intensities of the electron lines originating from ATI-processes of different order, a comparison to other studies performed under different conditions can be made. As shown in Table I, a more rapid decrease is observed in the ultraviolet at 193 nm as compared to the corresponding results obtained at visible and infrared wavelengths.[12,13] An experimental test ruling out normal inverse bremsstrahlung as the mechanism producing the higher order electron lines in the low density plasma formed in the focal region was made. On the basis of the linear density dependence observed for the intensities of the electron lines, inverse bremsstrahlung heating in the plasma was found to be insignificant at least up to pressures of $\sim 10^{-5}$ Torr, the highest values

used in the experiment. The signature of the bremsstrahlung mechanism would have been a quadratic dependence of the electron intensity on gas density.

Examination of the intensity distributions on the ATI lines also indicates that the highly excited configurations of the neutral atoms occurring above the first ionization threshold, as well as levels of excited ionic configurations, do not appreciably affect the rates of ionization for the observed channels. The boxed regions shown on the energy level diagrams in Fig. (3) indicate the range of energies in which levels of excited ionic configurations occur. Although it is seen in all four cases that these regions overlap the energies associated with certain observed ATI features (e.g. N = 8,9 in Ne and N = 5,6 in Ar), the intensities observed for these lines do not exhibit anomalous variations in comparison with other electron lines falling outside these specific energy regions. Further comments related to this observation are reserved for Section III.B.5 below.

Theoretical values for the relative probabilities of ATI lines have been calculated by Chu and Cooper[36] for hydrogen. Other analyses describing the dynamics of the process have been given by Crance and Aymar[37] and by Gontier and Trahin[38] who assume a well defined spatial and temporal intensity distribution for characterization of the laser beam. Although a quantitative comparison of our data with these calculated hydrogenic probabilities is not strictly valid because of experimental uncertainties and the electronic complexity of the rare gas atoms as compared to hydrogen, the experimental results qualitatively reflect the behavior predicted by the earlier work of Chu and Cooper[36] and Gontier and Trahin.[38]

Briefly, at ultraviolet wavelengths, relatively low order processes (e.g. N = 2 and N = 3) can energetically lead to ionization of the neutral system for most materials. Because of this, the intensity level needed to produce an ionization rate comparable to the inverse of the pulse width, a condition that leads to saturation, is relatively low. Indeed, resonances in the amplitude, such as those noted above for argon, krypton, and xenon

with 193 nm radiation, can further reduce this requisite intensity for rapid ionization. Consequently, during the risetime of the laser pulse, a substantial fraction of the atoms can become ionized into the first ionization channel before the intensity becomes sufficiently great to produce a comparable transition rate for higher order processes. For longer wavelengths, which require a higher order process to accomplish ionization, it is anticipated that the saturation intensity for ionization and the intensity required for comparable ATI transition rates will have values that are closer together. In addition, if the ATI process is pictured physically as an inverse-Bremsstrahlung mechanism involving the intimately associated electron-ion pair, the absorption rate at shorter wavelengths is expected to be suppressed in comparison to longer ones[39] on account of the wavelength dependence of the absorption coefficient which, in standard form, is proportional to the square of the wavelength. Therefore, it is expected, at ultraviolet wavelengths, that the enhancement of the higher-order processes of absorption requires a sharp risetime of the ultraviolet pulse. This condition, which is examined further below in Section III. B.5, enables the intensity experienced by the atom to reach values of a sufficient magnitude in a sufficiently short time so that higher order channels can compete effectively with those of lower order. In the present experiments, the requirements of this condition do not appear to be well fulfilled. Highly charged ions, however, because of the significantly increased energy of ionization, may tend to exhibit more pronounced ATI absorption, since the order N of the lowest ionization channel is greater, a condition that will generally lead to a substantially increased saturation intensity. The same consideration applies in the comparison of the strengths of the higher order features of the ATI spectra of the rare gases which are observed to increase in the expected fashion (Table I and Fig. 3) from Xe to Ne.

Multiply excited atomic states may play an important role in the many-quantum absorption process, particularly if sufficient intensity can be rapidly applied to the atom and if appropriate resonances are present in the amplitude. Indeed, a picture based on a collective atomic response involving several electrons occupying excited orbitals has been considered in certain models.[40,41,42] These analyses display features which are, in principle, compatible with the extant experimental data.[3,4]

A common feature of multiply excited atomic configurations is the specific issue of a discrete state coupled to adjacent continua.[43] The simplest prototype of these multiply excited configurations is doubly excited helium, which has an observed sequence of double excitations[44-46] $2s n\ell$ beginning at approximately 60 eV above the $(1s)^2$ ground state. More complex multiply excited systems, known as planetary atoms,[44,47] have also been considered.

The rare gases have been a prime subject of investigation of two-electron processes. Double ionization measurements are summarized by Holland et al.[48] for photon energies in the 40- to 300-eV region. Whereas double ionization of He, Ne, and Ar in this region is due to pair excitation of electrons in the valence shell, that of Kr and Xe is mainly a result of Auger processes following one-electron ionization of the core. Shake-up experiments in the rare gases have also been performed. Spears et al.[49] have used x-ray sources to eject an inner-shell electron and observe the satellite lines in the photo-electron spectrum, which are due to valence-shell excitation. Finally, two-electron excitation in the photoabsorption of the rare gases was observed by Codling, Madden, and Ederer[44,50-54] in the 8- to 60-nm region. Additional

oretical treatments of two-electron excitations are available[55-64] in the recent literature.

Specific detailed information is available for argon, krypton, and xenon for low lying multiply excited levels in the region below 50 eV. For krypton, the multiply excited manifold begins at ∿ 23.3 eV above the neutral ground state[52,65,66] and is, therefore, reached by a four quantum process at 193 nm (25.64 eV). We note that the excited states in this region have been strongly implicated in the recent study[67,68] of radiative mechanisms exhibited by krypton under excitation at 193 nm. For argon, 3s inner-shell excitation begins at 26.61 eV and doubly excited levels exist[50] above 29.0 eV. Finally, for xenon, autoionizing levels corresponding to single 5p-shell excitation and double 5p-shell excitation have been observed[52] above ∿ 20.95 eV. Interestingly, although levels in krypton with single 4s-shell excitations and double 4p-shell excitations apparently play an important role in the radiative response[67,68] for 193 nm intensities in the range of 10^{12} - 10^{14} W/cm^2, no clear evidence for the influence of these states upon the ATI-ladder lines was observed in the electron spectra at an intensity of ∿ 5 x 10^{14} W/cm^2, as shown in Table I. Similarly, as noted above, for neon, argon, and xenon, the observed ATI pattern did not give evidence of substantial influence arising from the known multiply excited levels. If the intensity of the ATI electron lines is interpreted as a measure of the photon absorption rate for higher order processes, only a fraction on the order of one percent or less of the higher charged ion states produced could be attributed to this type of direct excitation mechanism under the given experimental conditions.

B. Additional Lines in the Xe-Electron Spectrum

A question of principal significance concerns the identification of the dominant mechanism responsible for the production of highly charged ions under

collision-free irradiation.[69] The sequential stripping of single electrons with increasing laser intensity, a stepwise process which leaves the ions in their ground or low excited states, should generate an electron energy spectrum consisting of a group of sharp lines which accompanies the normal ATI-ladder series associated with the neutral ground state. In an alternative process involving the direct multiple autoionization or photoionization of multiply excited states, the liberated electrons can mutually redistribute the excess energy available and generate a continuous component of relatively low energy electrons to the measured spectrum. In addition, atomic inter-shell energy transfer may occur in which energy associated with the excitation of outer-shell electrons can be communicated to inner-shells by an interaction that has been pictured as a form of dynamic configuration interaction.[19,20] The inner-shell excited states produced could subsequently decay radiatively or by the emission of Auger electrons with characteristic energies.

Experimentally, all of these different excitation and decay channels can occur simultaneously in the interaction region, a situation which may seriously complicate the interpretation on the observed electron energy spectra. Some simplification, however, arises from the use of ultraviolet quanta because the characteristic spacing that occurs between ATI lines is relatively large, a factor that more readily permits resolution of fine details in the spectrum.

Evidence for the presence of the sequential process is shown in Fig. (3) for xenon. In this case, at an intensity of $\sim 2 \times 10^{13}$ W/cm^2, a weak line at 4.44 eV is observed which indicates the formation of the Xe^{2+} $(5s^2 5p^4)$ $^3P_2$ ground state which arises from a four photon absorption from the Xe^+ $(5s^2 5p^5)$ $^2P^o_{3/2}$ ionic ground level. Upon an increase in the 193 nm laser intensity, the energy distribution of the electrons observed in the xenon spectrum changes dramatically,

AD-A168 263 EQUIPMENT FOR SUBPICOSECOND EXTREME ULTRAVIOLET FACILITY(U) ILLINOIS UNIV AT CHICAGO CIRCLE DEPT OF PHYSICS C K RHODES ET AL 05 FEB 86 AFOSR-TR-86-0281 2/2

UNCLASSIFIED AFOSR-84-2289 F/G 20/5 NL

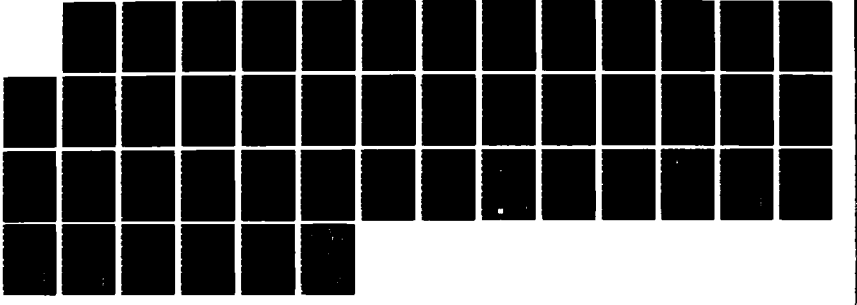

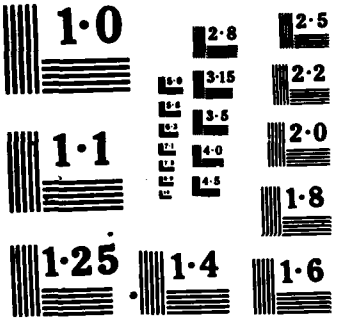

as shown in Fig. (4), a low resolution time-of-flight recording spanning the energy range between ∿ 0.3 eV and ∿ 100 eV. It is seen that the lowest order ionization line weakens and splits nearly symmetrically into two features whose separation grows with increasing intensity. At the greater intensity, the line group around 5 eV, comprised of the two 3-photon ATI-ladder lines and the 4-photon line indicating the sequential Xe^{2+} ground state formation, begins to dominate the spectrum. In addition, a broad quasi-continuous feature at ∿ 3 eV and new line groups between ∿ 8 eV and ∿ 30 eV are apparent. In Fig. (5), the Xe-spectrum is displayed with high resolution at an intensity of ∿ 10^{15} W/cm^2 and converted to a linear energy scale. More than twenty sharp lines are visible in this spectrum. In order to interpret this complex spectrum, several physical effects have to be considered.

1. Shift of Ionization Thresholds

The weakening of low energy photoelectron lines with increasing laser intensity has been reported by Kruit *et al.*[13] in experiments at 1.06 μm. Subsequently, several theoretical papers have appeared giving descriptions and explanations of this effect.[36,70-74] In the discussion below, we adopt the analysis developed by Szöke.[75]

The energy conservation governing the motion of an electron undergoing photoionization by a multiphoton process in an intense electromagnetic field is expressed by the relation

$$\varepsilon_D(N) \equiv \varepsilon_{Aq}(\vec{E}) + N\hbar\omega = \varepsilon_{Aq+1}(\vec{E}) + \frac{1}{4}\frac{\vec{E}_o^2 e^2}{m\omega^2} + \frac{\vec{p}^2}{2m} . \qquad (8)$$

In expression (8) $\varepsilon_D(N)$ is the energy of the "dressed" atom (ion) state and $\varepsilon_{Aq}(\vec{E})$ and $\varepsilon_{Aq+1}(\vec{E})$ are the energies, respectively, of the initial state of the q-times charged ion and the final state of the q+1-charged ion in the electro-

magnetic field $\vec{E}$. Both states are shifted in energy by the dynamic stark effect by amounts given by

$$\Delta\varepsilon_{Aq}(\vec{E}) \equiv \varepsilon_{Aq}(\vec{E}) - \varepsilon_{Aq}(0) \qquad \text{and} \tag{9}$$

$$\Delta\varepsilon_{Aq+1}(\vec{E}) \equiv \varepsilon_{Aq+1}(\vec{E}) - \varepsilon_{Aq+1}(0) \tag{10}$$

from their zero field energy. This effect is usually small (< 100 meV) for the more tightly bound initial states (ground levels) of the rare gases. The last two terms represent the total motional energy of the electron, which consists of the piece described by the ponderomotive potential, which arises from the oscillatory motion of the electron in the alternating field, and the term denoting the translational energy with momentum $\vec{P}$. The oscillating motion of the ion[74] is neglected in this expression, since its very large mass causes that contribution to be extremely small. Once the electron is outside the influence of the ionic coulomb field, it cannot emit or absorb real photons. It has been previously shown[75] that the influence of Compton scattering is entirely negligible under the conditions relevant to these experiments. Therefore, the total energy of the electronic motion is conserved and the component represented by the rapidly oscillating quiver motion is converted into translational kinetic energy by the ponderomotive force[76] as the particle moves to the zero field region ($\vec{E} \rightarrow 0$) on its way to the detector.

The essential point here is that, if the electron is excited to a total energy in the continuum <u>less</u> than that associated with the ponderomotive potential, namely, the quiver energy, under those field conditions it cannot escape from the Coulomb potential and is trapped. This is equivalent to stating that the ionization or continuum threshold, which can be defined as the series limit characterizing the liberation of a Rydberg electron from a "dressed" state, is upshifted by an amount equal to the quiver energy. Therefore, the expression

$$T(\vec{E}) = T_o + \frac{1}{4}\frac{\vec{E}_o^2 e^2}{m\omega^2} + \Delta\varepsilon_{Aq+1}(\vec{E}) - \Delta\varepsilon_{Aq}(\vec{E}), \qquad (11)$$

in which $T_o = \varepsilon_{Aq+1}(0) - \varepsilon_{Aq}(0)$ is the usual low field ionization threshold, can be considered as a generalized ionization threshold. The principal consequence of this condition is the closing of low energy ionization channels above certain characteristic laser intensities. This effect has been discussed earlier by Razier.[29] Furthermore, since the total energy of the electron after the multiphoton absorption event is conserved, its deficit in translational kinetic energy in the high field region is regained upon expulsion from that zone, leaving its kinetic energy altered relative to a low field event only by the small difference arising from the dynamic stark shifts of the initial and final atomic or ionic states. This situation holds for the condition that the escape velocity of the electron is sufficiently fast with respect to the rate of variation of the laser field.[75]

These considerations lead to a characteristic behavior for the electron spectrum of an ATI-ladder of lines. As the peak intensity of irradiation is increased, the lower energy ionization channels close and the spectrum of emitted electrons shifts towards the higher order lines while the line positions remain nearly unaffected. It should be noted, however, that a perceptible shift of the electron spectrum could already occur before the lower energy channels close.[36,38,71,73] Further, on account of the ω^{-2} dependence of the ponderomotive potential, the radiative influence on the shift of the ionization threshold is considerably stronger in the infrared region than in the ultraviolet.

Interestingly, energetic electrons have been observed in experiments conducted at 1.06 μm at a peak intensity of $\sim 10^{16}$ W/cm^2. In these relatively

low resolution studies,[8,17] performed by Baldwin, Boreham, and Luther-Davis, electrons with energies up to several hundred electron volts were detected and the origin of their acceleration was attributed to the ponderomotive force. However, the unshifted line positions observed by Kruit and coworkers[13] seem to be at variance with this result. In this connection it is noted that, due to the upshift of the ionization threshold by the ponderomotive potential, the lowest ionization channel open for 1.06 μm radiation at this intensity corresponds to a transition involving several hundred photons. Of course, low energy electrons are simultaneously observed as a result of ionization early in the rise of the pulse or from generation in peripheral regions of the interaction volume that are exposed to a lower intensity. Similar findings have been recently reported by Lompré and coworkers[16] who observed, in low energy resolution experiments, electrons with energies up to 50 eV. In this case,[16] it was assumed that the virtual excitation of multiply excited states enhanced the probability for ATI processes. However, this analysis did not take into account the radiative shift of the ionization threshold.

The relative weakening of the two-photon (0.7 eV) ionization line and the related strengthening of the three quantum ionization lines observed in the xenon electron spectrum can both be attributed to the closing of the lower (0.7 eV) channel throughout a considerable fraction of the interaction volume. The intensity of 193 nm radiation necessary to shift the ionization threshold an energy equivalent to 0.7 eV is $\sim 2 \times 10^{14}$ W/cm^2, a value in good agreement with our experiment. On the other hand, these results indicate that a substantial fraction of neutral Xe atoms is still present when the laser pulse reaches the intensity of $\sim 2 \times 10^{14}$ W/cm^2, since most of the observed higher order processes appear to occur between that value and the threshold closing of the

three-photon ionization at $\sim 1.5 \times 10^{15}$ W/cm^2. The closing of the latter channel is not observed in these experiments indicating that intensities greater than 1.5×10^{15} W/cm^2 were not produced in the current studies.

2. Dynamic Stark Splitting of the Xe Two-Photon Ionization Line

The splitting of the two-photon ionization line at $\sim$ 0.7 eV in xenon illustrated in Fig. (6) that develops with increasing 193 nm intensity occurs in the intensity range between $\sim 10^{10}$ W/cm^2 and $\sim 10^{12}$ W/cm^2. Since these intensities are rather low, the splitting is readily observed with the relatively low power ASE pulse $\sim$ 10 nsec duration without the presence of the considerably more intense picosecond radiation. The experimental signature of the splitting appears to rule out a spurious instrumental origin for this effect. The splitting is seen to be independent of both pressure and the position of the interaction region along the magnetic field axis. The influence of space charge generated by scattered 193 nm radiation from surfaces has been examined by independently illuminating the surfaces near the interaction zone with a separate beam. As a result of the charge density produced in this way, the line is shifted to higher electron energy with a perceptibly altered shape, but importantly, with the splitting preserved.

As noted above, the two-photon absorption in xenon is distinguished by the fact that the equivalent two-photon energy is located in the autoionizing Rydberg series converging to the $5s^2 5p^5 {}^2P^o_{1/2}$ series limit, a property leading to the presence of near resonances.[77] It is well known that if a sufficiently strong coupling is established between two states by an intense resonant field, a splitting can develop which arises from the dynamic stark effect of the "dressed" atomic states.[78] For the circumstance in which the upper state is an autoionizing level, the influence of the Autler-Townes effect on the electron energy spectrum has been studied extensively by K. Rzażewski and

Eberly[79] for a transition involving a single photon. Moreover, this dynamic stark splitting, in the context of multiphoton transitions and electron energy spectra, has been discussed by Lambropuolos and Zoller[1a] and Bialynicka-Birula.[73] Both the near resonant discrete state and the continuum are coupled to each other by the coulomb interaction as described in the model developed by Fano.[80] The energy distribution of the photoelectrons released from the autoionizing state acts as a probe to detect the splitting. The actual shape of the resulting photoelectron line depends sensitively on the parameters governing the behavior of the system. The relevant parameters are the radiative coupling strength linking the two resonant levels, the autoionization linewidth, the laser bandwidth, the pulselength, the dephasing rate, the intensity dependent detuning of the laser from the discrete resonances, and the Fano asymmetry parameter. We tentatively interpret the observed splitting of the 0.7 eV line in xenon as arising from the dynamic stark effect. By fitting the measured line profile to the parameters mentioned above, the observed electron line shape, including the intensity dependence, could be reproduced for parameters representing reasonable physical values. A more detailed analysis is currently underway and will be published elsewhere.

3. Evidence Concerning High Charge State Production

Table II lists the relative ion charge state abundances for Xe, Kr, and Ar which have been obtained previously in an ion time-of-flight experiment,[3,4] under conditions which are similar to those of the present electron energy measurements. These data are presented along with the expected relative electron yield for each charge state for two distinct limiting cases. They are (a) the purely sequential and (b) direct processes, respectively. According to this comparison, in the direct process, approximately 70% for xenon, 30% for krypton, and 15% for argon of all electrons that are produced arise from the formation of higher charged

ions. It is expected that these electrons would contribute a relatively low energy continuum to the electron spectra. No unambiguous evidence for the existence of such a contribution to the continuum has been found, but its presence could be obscured by the surface background electrons produced by scattered radiation and the low energy wings of the prominent ATI-ladder lines shown in Fig. (3). The gas density has been kept low in order to avoid detector saturation caused by the higher energy lines. The possibility that these electrons are trapped in the space charge of the residual ion cloud was tested and ruled out by the application of a static electric field across the interaction region.

If the model of sequential electron production is adopted, several channels for ionization have to be simultaneously considered on account of the number of possible excited states that could be produced in conjunction with the distribution of the observed ionic species. Table III.a lists some of the processes which are believed to be significant. They are, of course, related to the observed lines illustrated in Fig. (5). As shown in the figure, the lines which are manifest in the measured xenon electron energy spectrum for intensities above $\sim 2 \times 10^{14}$ W/cm^2 closely match a pattern of overlapping ATI-ladder series with each series associated with the population of a respective ionic state. The branching ratios for the different excited states of the residual ions are not known and, as discussed in Sec. III. A above, may depend strongly on intensity dependent resonances. We note the accidental coincidence of several line energies, a fact which makes it difficult to isolate certain individual ladder contributions, especially those for processes leading to Xe^{3+} and higher charge states. The lowest energy lines are seen to be grouped in the range between $\sim$ 2 eV and $\sim$ 6 eV. More energetic groups are apparent with

corresponding spacings of lines given approximately by the photon energy of 6.41 eV. Estimates of the relative intensities for the most prominent lines are listed in Table IV. Except for the first group of lines in the 2-4 eV range shown in Fig. (5), the relative line intensity within each of the higher energy groups is repeated, although the absolute intensity of these features drops rapidly with increasing energy. At a density of $\sim 2 \times 10^{-5}$ Torr, weak line groups up to an energy of $\sim$ 60 eV could be observed in this experiment.

These data indicate that in the sequential production of the higher charge states of the xenon ions, ATI occurs with a greater probability than in the multiphoton ionization of the neutral xenon atom. This observation may be attributable to the higher saturation intensity expected to be characteristic of the ionized species resulting from the larger energy of ionization and the correspondingly greater order N of the threshold process. The comparison of the relatively weak group of lines in the 2-4 eV region of Fig. (5) with those lines of the next higher order indicates that the lowest order channels close, at least for the maximum intensity region of the interaction volume. The closing of these channels corresponds to a range of intensities spanning from $\sim 5.6 \times 10^{14}$ W/cm^2 ($\sim$ 2 eV) to $\sim 1.4 \times 10^{15}$ W/cm^2 ($\sim$ 5 eV). This closing of the lowest order channels of ionization could explain the fact that the lowest energy feature (f5) in the next higher order group is the most intense. A close examination of the line energies reveals that the individual ATI-ladder series are shifted in energy relative to each other by an amount on the order of $\sim$ 50 meV. Although these apparent shifts have to be interpreted with caution, since they may be subject to the influence of space charge induced by scattered radiation, they may represent the relative dynamic stark shifts of the initial and final ionic states according to Eq. 11.

The total integrated intensity of the neutral ionization lines is approximately equal to that of the ionization lines arising from the ions. As presented in Table II, the sequential process can account for the total ion production observed in xenon to within the experimental uncertainty. The question of the existence of an additional continuum contribution underlying the densely packed features between 0.5 and 6 eV, although possible, cannot be answered with the energy resolution available in this experiment. L'Huillier and coworkers[81] concluded from their experimental ion data that direct excitation of the neutral atom is the dominant process at intensities below the saturation level. Above that intensity, due to the depletion of neutral atoms in the interaction volume, the sequential ionization of ions becomes increasingly important. This view is not in conflict with the results of the present work, since the spectra were taken well in the saturation regime. The direct excitation process could become significant at ultraviolet wavelengths for the production of charge states higher than the triply charged ion, because the situation for these species, as noted in Section III. A above, is similar to that governing the interaction of atoms with infrared fields.

More information concerning the competition between the sequential and direct processes should be obtainable from a study of the electron spectra of the other rare gases. The behavior of xenon contrasts with that exhibited by argon and krypton. As Table II shows, the electron contributions arising from the formation of higher charged ions is considerably less for argon and krypton at intensities below $\sim 10^{15}$ W/cm^2 than they are for xenon. In addition, for krypton the experimental situation is aggravated by the fact that the low energy electron continuum between $\sim$ 0 eV and $\sim$ 2 eV generated by scattered radiation may obscure all weak line features in this range. Furthermore, the krypton pressure has to be kept below $\sim 2 \times 10^{-7}$ Torr in order to avoid

detector saturation caused by the dominant 5.24 eV-line shown in Fig. (3), an effect which will suppress any lower energy features.

The sequential ionization of the $Kr^+ {}^2P^o_{3/2}$ ground state to the ground and low lying excited Kr^{2+}-ion states produces electron lines grouped around 0.9 eV - 1 eV for 4-photon absorption (Table IIIb) and around 6.8 - 7.5 eV for 5-photon absorption. The lowest order channels close at intensities in the range of 1.5×10^{14} - 3×10^{14} W/cm^2. A careful study of many electron spectra recorded under different experimental conditions revealed that the feature observed in the krypton spectrum shown in Fig. (3) between 6.5 eV and 8.5 eV can be associated with these 5-photon processes.

In Ar the sequential Ar^{2+} formation leads to electron lines around 4.3 eV (Table III.c). The inset illustrated in the argon spectrum of Fig. (3), which was recorded at a higher energy resolution, clearly shows the expected feature, but slightly upshifted at around 5 eV. In addition, on the low energy side of the structured peak occurring at $\sim$ 10 eV, another line is seen which corresponds to 6-photon ionization of $Ar^+ {}^2P^o_{3/2}$ with the final Ar^{2+} ion in the excited $^1D_2$ level (Table III.c). The combined intensity of these lines, relative to the neutral Ar ladder sequence, approximately reflects the measured relative abundances of the Ar^+ and Ar^{2+} ions listed in Table II.

If the direct process is important for argon and krypton and if a substantial fraction of the electrons produced comprise a relatively low energy continuum, then the experimental difficulties noted above interfere with their detection. Also, we recall, from the discussion in Section III.A, that the probability for direct multiphoton absorption above the second ionization threshold must be quite low under the given experimental conditions.

4. Multiphoton Inner-Shell Excitation

In addition to the photoionization of outer-shell electrons, highly charged ions can be a final result arising from the initial formation of an inner-shell vacancy followed by electron rearrangement with the emission of radiation and Auger electrons in a cascade process.[82-86] The Auger spectra of the rare gases have been measured using both single-photon and electron impact ionization.[87-94] In multiphoton experiments inner-shell excitation is possible, in principle, either by direct high-order multiphoton coupling to the inner electron or by energy transfer from multiply excited outer-shell configurations. For the latter, it has been possible to formulate a model describing a possible mode of intra-shell coupling by drawing an analogy with fast ion-atom and atom-atom collisions.[19,20] The known properties of free atoms suggest that this kind of coupling could be quite strong, particularly in certain regions of the periodic table.[4] In Xe, for example, the 5p, 5s, and 4d shells exhibit substantial intra-shell coupling and behave in a collective fashion like a single super shell.[85,95-97] Direct inner-shell photoexcitation by the ultraviolet radiation is expected to be unlikely because of the screening[98] provided by the outer-shells, an effect which is significant because the single photon energy is below the outer-shell excitation energy.[99] However, at very high laser intensities, the strong inter-shell coupling is expected to cause a nonlinear response of the outer-shell electrons to the laser field and, consequently, the generation of higher harmonics of the field, which can then penetrate to inner-shells and cause their ionization.[20,100]

Independent of the mechanism of excitation, the Auger decay of an inner-shell vacancy should result in an electron energy spectrum with a characteristic pattern of lines. The spectrum consists of the principal decay line, leaving the doubly charged ion in the ground state, and an array of satellite lines caused by electron correlation[95,96] (shake-up) which leads to ion formation in an excited state.

In xenon, the energies of the $4d^9 5s^2 5p^6 {}^2D_{5/2,3/2}$ 4d-hole states are known[92,101] to be at 67.55 eV and 69.52 eV, respectively. The corresponding energies for the krypton 3d-hole states $3d^9 4s^2 4p^6 {}^2D_{5/2,3/2}$ are measured[101] to be at 93.82 eV and 95.04 eV, respectively. The strongest decay lines in the N_{45}-OO Auger spectrum of xenon are grouped around 35 eV with observed[92,94] low energy satellites extending down to ∿ 8 eV. In the M_{45}-NN Auger spectrum of krypton, the corresponding lines[93] are grouped around 55 eV with satellites of significant strength down to 25 eV. However, a close examination of our electron spectrum for xenon for intensities below 10^{15} W/cm^2, although revealing several prominent lines in the 8 - 22 eV region with spacings matching[102,103] the known[92] $4d_{5/2}$ - $4d_{3/2}$ fine-structure splitting of 2 eV, does not give evidence for the expected features in the ∿ 35 eV range. At the same time, as described in Section III.A and shown in Table III,a and Fig. (5), the main features of the observed electron spectra for xenon at intensities below ∿ 10^{15} W/cm^2 can be understood as arising from ATI-ladder sequences involving the formation of Xe^+, Xe^{2+}, and Xe^{3+} with allowance made for the production of certain identified excited ionic states. Experimentally, the accidental coincidence, for 193 nm radiation, of certain ATI lines with the energies characteristic of the low energy satellites of the xenon to 4d-Auger decay prevents isolation of any Auger features even if present in the data. Nevertheless, the possibility exists, that under appropriate circumstances, an inner-shell vacancy produced in a nonlinear process would undergo an Auger decay with a rate on the order of 10^{14} sec^{-1} and electron energies characteristic of the charge state involved.[104] Since an atom responding in this way would be strongly perturbed by the intense ambient electromagnetic field, considerable energy shifts,[105] variations in the level widths, and changes of the branching ratios for Auger transitions are expected. In this connection it is interesting

to recall that, in preliminary experiments[4] conducted at 193 nm intensities in the 10^{16} - 10^{17} W/cm^2 range, evidence was found for the production of energetic radiation (10 eV $\leq \hbar\omega \leq$ 80 eV) emitted by xenon with irradiation under collision-free conditions. Radiation of this energy could be produced by inner-shell transitions[86] or the emission of flouresence following the multiphoton excitation of a near resonance in the outer-shell of a xenon ion. However, since no evidence for such a process has been found in the electron spectra, the probability for this process at intensities below $\sim 10^{15}$ W/cm^2 must be fairly low unless the process of autoionization is suppressed or energetically forbidden.

5. Competition between Direct and Sequential Processes

The present results on electron spectra indicate that the process of sequential ionization, modified by the presence of ATI, dominates the production of the electrons observed. However, it has also been indicated[19,20] that a direct mechanism of interaction, capable of producing both multiple ionization and inner-shell excitation,[103] could occur if certain motions of the atomic outer-shell electrons can be driven by the incident electromagnetic field. In the competition of these two mechanisms, we now examine the nature of the conditions necessary for the enhancement of the direct process.

In order to maximize the probability for energy transfer between multiply excited configurations of outer-shell electrons and those occupying inner-shell orbits, the decay rate of the outer-shell excitation by electron emission must be sufficiently low[106] to permit the overall act of multiquantum absorption, involving both the excitation of outer electrons by the radiation field and the inter-shell energy transfer, to occur. Specifically, we want the escape of electrons from the vicinity of the atomic potential to be retarded. A

possible means to achieve this is through the presence of the ponderomotive potential (of Eq. 8)

$$U(I,\omega,t) = \frac{e^2 E_o^2(t)}{4m\omega^2} , \tag{12}$$

provided that its strength can be developed with sufficient rapidity to effectively discourage electron emission into the available channels. In expression (12) the explicit dependencies on laser intensity I through the field strength E_o, frequency ω, and time t have been indicated. One possible statement of the condition necessary is that the ponderomotive potential $U(I,\omega,t)$ increases an amount equal to the quantum energy ($\hbar\omega$) in the time scale τ_e characterizing electron emission during the course of irradiation. In this situation, the atomic electrons experience a sequence of closing channels at succesively higher energies as radiation is absorbed by the atom. This statement can be written as

$$\frac{\partial U(I,\omega,t)}{\partial t} = \frac{\hbar\omega}{\tau_e} . \tag{13}$$

Since the ponderomotive potential [cf. Eq. (8)] can be written as

$$U(I,\omega,t) = \left(\frac{2\pi e^2}{mc\omega^2}\right) I(t) , \tag{14}$$

the result

$$\frac{dI(t)}{dt} = \frac{mc\hbar\omega^3}{2\pi e^2 \tau_e} \tag{15}$$

follows. If, for simplicity, we consider a triangular pulse with a maximum intensity I_o which rises linearly in time over a period τ, equation (15) for the theoretically required condition can be put in the form

$$\frac{I_o}{\tau} = \beta \equiv \frac{mc\hbar\omega^3}{2\pi e^2 \tau_e} , \tag{16}$$

or equivalently,

$$\tau = \tau_e \left(\frac{2\pi e^2 I_o}{mc\omega^3}\right) = (2\pi\alpha)\tau_e \left(\frac{I_o}{I_\omega}\right) \qquad (17)$$

with

$$I_\omega \equiv m\omega^3 \qquad (18)$$

and α denoting the fine structure constant. In expression (17), for the time scale τ necessary, two parameters occur. One characterizes the maximum intensity I_o, a factor under experimental control, while the other is the electron emission time τ_e, viewed in this simple picture as an intrinsic atomic parameter. It may be, of course, that τ_e is influenced by the instantaneous intensity and the order N of the process, but these complications are not considered here.

An approximate value for the time scale τ_e can be related to the data on the electron spectra shown in Table III, Fig. (3), and Fig. (5). We observe that, although ionic excited states are evident, no levels with excited configurations are present. Specifically, no state representing a configuration involving an excited (n,ℓ) orbital is detected and, as discussed in Section III.A, no influence of such excited states was seen on the intensity distributions of the observed electron spectra. This experimental fact suggests that the process of electron removal is adiabatic with respect to the electronic orbital motion. Equivalently, shake-up arising from the electron emission is negligible. Since all the ionic species of xenon listed in Table III.a have states with excited configurations lying approximately[26] $10^5 cm^{-1}$ above their respective ionic ground states, the time τ_e should be long compared to $\sim 3.3 \times 10^{-16}$ sec in order to respect this condition for adiabaticity. Therefore, for the estimates furnished below in Table V, we will use the value $\tau_e = 10^{-15}$ sec.

Table V contains a compilation of the parameters for several extant studies of collision-free nonlinear processes and gives the characteristic ranges over which these experiments have been performed. The conditions of these studies can then be compared to the criterion stated in Eq. (13) by the introduction of a factor γ defined as

$$\gamma \equiv I_{ex}/\tau_p \ , \tag{19}$$

the experimental counterpart of the theoretically required condition stated in Eq. (16). The column (β/γ) then gives a direct measure of the departure of the experimental conditions from that expressed in Eq. (13). Specifically, values of $\beta/\gamma > 1$ indicate that the necessary conditions are not satisfied. The large values of β/γ shown in Table V demonstrate that all the experiments conducted thus far fail to satisfy the conditions of Eq. (13) by a significant margin, most by factors of a thousand or more. Therefore, within the framework of this type of physical picture, the sequential process would be expected to play the major, if not dominant role, in these experiments. Finally, a comparison of the peak ponderomotive potential $U(I_{ex}, \omega)$ appearing in Table V for the experiment of Baldwin and Boreham,[17] who observed a maximum electron energy of 400 - 500 eV, shows that the observed electron energy corresponds approximately to a value one order of magnitude lower than the peak ponderomotive potential. This correspondence gives an indication of the physical significance of the criterion estimated with Eq. (13).

We now inquire into the possibility of entering the regime for which $\beta/\gamma \leq 1$, the range of intensities and pulse widths which is in conformance with the general criterion of Eq. (13). On the basis of earlier estimates[4,19,20] it has been suggested that the direct process is favored if the atom is exposed to a radiative electric field E significantly greater than an atomic unit ($E_a = e/a_o^2$). An intensity $I_o \simeq 10^{18}$ W/cm^2, a value corresponding to a few atomic units of electric field and believed to be technically feasible with modern light sources,[1b] would satisfy this condition. Therefore, we will use this intensity scale in order to estimate the maximum pulse width permissible for 248 nm radiation. At the wavelength of 248 nm, $I_\omega = 3.9 \times 10^{13}$ W/cm^2,

or equivalently, $\beta = 8.5 \times 10^{29}$ W/cm^2-sec. Consequently, $\beta/\gamma = 1$ implies that $\tau_p \approx 1.2 \times 10^{-12}$ sec. Therefore, a KrF* (248 nm) source capable of ~ 1 ps operation and focusable to $\sim 10^{18}$ W/cm^2 would enable experiments to be conducted under the appropriate physical conditions. Fortunately, the technical feasibility of such an instrument is manifest,[1b] so that studies in this interesting physical regime will be conducted in the near future. According to this analysis, with irradiation at 248 nm at a peak pulse intensity of $\sim 10^{18}$ W/cm^2, the electrons would be trapped in a ponderomotive potential with a depth of several kilo-electron volts.

Finally, the simple picture presented above can be viewed in a manner similar to that used in the description of atomic collisions which involve a curve crossing.[108] If the transitions between adjacent "dressed" levels[109] corresponding with the ATI channels are regarded as a level crossing phenomenon, then, in analogy with the collisional problem, the canonical energy parameter becomes $\hbar\omega$ and the time scale associated with the transition corresponds to τ_e. Hence, the standard condition for adiabaticity, and, consequently, a low transition rate, is given by

$$\omega\tau_e >> 1, \tag{20}$$

a condition that is fulfilled at ultraviolet wavelengths with $\tau_e \sim 10^{-15}$ sec.

IV. Summary

The energy spectra of electrons generated by collision-free multiphoton ionization of Xe, Kr, Ar, and Ne exposed to picosecond 193 nm radiation have been studied up to an intensity of $\sim 10^{15}$ W/cm^2. In addition to the appearance of the lowest order ionization lines, all spectra exhibit above threshold ionization (ATI) transitions, although with considerably lower intensity. The probabilities of ionization and the branching into specific final ion states

appear sensitive to the presence of near-resonances with excited atomic states. The rapid decrease in the electron line intensity with increasing nonlinear order N of the process, in comparison to corresponding spectra obtained at visible and infrared wavelengths, is qualitatively in agreement with calculations of the transition probability which take into account certain features of the interaction including the temporal laser pulse shape and saturation. No shift of the measured electron spectral features could be unambiguously attributed to the dynamic stark effect or the influence of the ponderomotive force. Furthermore, the influence of excited ionic configurations, multiply excited valence shell levels, or inner-shell excited states on the observed intensity patterns of ATI-lines appears to be negligible.

In the formation of higher charged ions, the data indicate that the sequential liberation of electrons is the dominant process governing the interaction over the range of physical parameters studied. This characteristic of the process is most evident in the electron spectra exhibited by xenon. In this case, the appearance of overlapping ATI-ladder series shows that the sequential mechanism is the main process leading to the formation of Xe^{2+} and Xe^{3+}.

The closing of specific low energy channels due to the influence of the ponderomotive potential has also been observed and the intensities at which these channels are suppressed conform qualitatively to that predicted theoretically. It seems possible, that in properly conducted experiments, that this effect could be used to measure the maximum intensity occurring in the focal volume.

An examination of the competition between mechanisms of direct multiple ionization and sequential ionization leads to the conclusion that, given the range of physical conditions studied, all experiments conducted so far are

expected to strongly favor ionization by the sequential process. Conversely, enhancement of the direct process may occur in a physical regime for which the emission of electrons in low energy channels is sufficiently retarded by the influence of the ponderomotive potential. The conditions necessary to examine this situation can be experimentally realized by modern ultraviolet sources operating in the sub-picosecond region.

The two-photon line for Xe, the lowest order ionization process for that material at 193 nm, is located energetically adjacent to the autoionizing Rydberg series which converges to the $5s^2 5p^5 {}^2P^o_{1/2}$ excited ion state. This feature is observed to split into a well resolved doublet at laser intensities between 10^{10} - 10^{12} W/cm^2. This observation has been tentatively interpreted as arising from the Autler-Townes effect.

5. Acknowledgements

The authors wish to acknowledge fruitful discussions with A. P. Schwarzenbach, I. A. McIntyre, A. McPherson, K. Boyer, and A. Szöke as well as the technical assistance of M. Scaggs, R. Slagle, and J. Wright. This work was supported by the Office of Naval Research, the Air Force Office of Scientific Research under contract number F49620-83-K-0014, the Innovative Science and Technology Office of the Strategic Defense Initiative Organization, the Department of Energy under grant number DE-AC02-83ER13137, the Lawrence Livermore National Laboratory under contract number 5765705, the National Science Foundation under grant number PHY 84-14201, the Air Force Office of Scientific Research, Department of Defense University Research Instrumentation Program under grant number USAF 840289, the Defense Advanced Research Projects Agency, and the Los Alamos National Laboratory under contract number 9-X54-C6096-1.

REFERENCES

1. For reviews see:

   (a) Multiphoton Ionization of Atoms, edited by S. L. Chin and P. Lambropoulos, Academic Press, New York, 1984); (b) C. K. Rhodes, Science 229, 1345 (1985).

2. A. L'Huillier, L. A. Lompré, G. Mainfray, and C. Manus, Phys. Rev. Lett. 48, 1814 (1982); ibid., Phys. Rev. A27, 2503 (1983).

3. T. S. Luk, H. Pummer, K. Boyer, M. Shahidi, H. Egger, and C. K. Rhodes, Phys. Rev. Lett. 51, 110 (1983).

4. T. S. Luk, U. Johann, H. Egger, H. Pummer, and C. K. Rhodes, Phys. Rev. A32, 214 (1985).

5. S. L. Chin, F. Yergeau, and P. Lavigne, J. Phys. B18, L213 (1985).

6. M. Hollis, Opt. Commun. 25, 395 (1978).

7. P. Agostini, F. Fabre, G. Mainfray, G. Petite, N. K. Rahman, Phys. Rev. Lett. 42, 1127 (1979).

8. B. W. Boreham and B. Luther-Davis, J. Appl. Phys. 50, 2533 (1979).

9. P. Kruit, J. Kimman and M. J. van der Wiel, J. Phys. B14, L597 (1981).

10. K. Boyer, H. Egger, T. S. Luk, H. Pummer, and C. K. Rhodes, J. Opt. Soc. Amer. B1, 3 (1984).

11. G. Petite, F. Fabre, P. Agostini, M. Crance and M. Aymar, Phys. Rev. A29, 2677 (1984).

12. F. Fabre, G. Petite, P. Agostini, and M. Clement, J. Phys. B15, 1353 (1982).

13. P. Kruit, J. Kimman, H. G. Muller, and M. J. van der Wiel, Phys. Rev. A28, 248 (1983).

14. M. Gavrila, A. Maquet, and V. Véniard, Phys. Rev. A32, 2537 (1985).

15. A. L'Huiller, L. A. Lompré, G. Mainfray, and C. Manus, J. Phys. B16 1363 (1983).

16. L. A. Lompré, A. L'Huillier, G. Mainfray and J. Y. Fan, J. Phys. B17, L817 (1984).

References, continued

17. K. G. H. Baldwin and B. W. Boreham, J. Appl. Phys. 52, 2627 (1981).

18. C. K. Rhodes, Fundamentals of Laser Interactions, Lecture Notes in Physics No. 229, edited by F. Ehlotzky (Springer-Verlag, Berlin, 1985) p. 111.

19. K. Boyer and C. K. Rhodes, Phys. Rev. Lett. 54, 1490 (1985).

20. A. Szöke and C. K. Rhodes, "A Semiclassical Model of Inner-Shell Excitation By Outer-Shell Electrons," submitted to Phys. Rev. Lett.

21. H. Egger, T. S. Luk, K. Boyer, D. R. Muller, H. Pummer, T. Srinivasan, and C. K. Rhodes, Appl. Phys. Lett. 41, 1032 (1982).

22. P. Hsu and J. L. Hirshfield, Rev. Sci. Instrum. 47, 236 (1976).

23. C. Beamson, H. Q. Porter, and D. W. Turner, J. Phys. E13, 64 (1980).

24. J. Kruit and F. H. Read, J. Phys. E16, 373 (1983).

25. B. W. Boreham and H. Hora, Phys. Rev. Lett. 42, 776 (1977).

26. C. E. Moore, Atomic Energy Levels, Volume I-III, NSRDS-NBS (U. S. Government Printing Office, Washington, D. C., 1971).

27. S. L. Chin and N. R. Isenor, Can. J. Phys. 48, 1446 (1970).

28. L. V. Keldysh, Sov. Phys.-JETP 20, 4 (1965).

29. Yu. P. Raizer, Sov. Phys.-Usp. 8, 650 (1966).

30. W. M. Bischel, J. Bokor, D. J. Kligler, and C. K. Rhodes, IEEE J. Quant. Electron, QE-15, 380 (1979); J. Bokor, J. Zavelovich, and C. K. Rhodes, Phys. Rev. A21, 1453 (1980).

31. L. A. Lompré, G. Mainfray, C. Manus, and J. Trebault, J. Phys. 39, 610 (1978); T. Srinivasan, H. Egger, T. S. Luk, H. Pummer, and C. K. Rhodes, IEEE J. Quantum Electron. QE-19, 1874, (1983).

32. N. B. Delone and V. P. Krainov, Atoms in Strong Light Fields (Springer-Verlag, Berlin, 1985).

33. R. F. Stebbings, F. B. Dunning, and R. D. Rundel in Atomic Physics 4, G. zu Putlitz, E. W. Weber, and A. Winnacher, editors (Plenum Press, New York, 1975) p. 713.

References, continued

34. F. J. Wuilleumier, M. Y. Adam, P. Ihez, N. Sandner, V. Schmitz and W. Mehlhorn, Phys. Rev. A16, 646 (1977).

35. R. N. Compton, J. C. Miller, A. E. Carter, and P. Kruit, Chem. Phys. Lett. 71, 87 (1980).

36. Shih-I Chu and J. Cooper, Phys. Rev. A32, 2769 (1985).

37. M. Crance and M. Aymar, J. Phys. B13, L421 (1980).

38. Y. Grontier and M. Trahnin, J. Phys. B13, 4383 (1980).

39. T. P. Hughes, Plasmas and Laser Light (John Wiley and Sons, New York, 1975).

40. M. Crance, J. Phys. B17, L355 (1984).

41. M. Crance, J. Phys. B17 L155 (1984).

42. H. Egger, U. Johann, T. S. Luk, and C. K. Rhodes, "Multiphoton Ionization in Ultrahigh Optical Fields: A Statistical Description," submitted to *J. Opt. Soc. Am. B.*

43. Etats Atomiques et Moleculaires Couples a un Continuum Atoms et Molecules Hautement Excites, Colloques Internationaux de C.N.R.S. no. 273, Paris, 1977.

44. R. P. Madden and K. Codling, Astrophys. J. 141, 364 (1965).

45. U. Fano in Atomic Physics, ed. by B. Bederson, V. W. Cohen, and F. M. J. Pichanik (Plenum, New York, 1969) p. 209.

46. The following volumes also contain considerable information on multiple excited atomic states: Beam-Foil Spectroscopy, edited by S. Bashkin (Springer-Verlag, Berlin, 1976); Beam-Foil Spectroscopy, Volumes 1 and 2, ed. by I. A. Sellin and D. J. Pegg (Plenum Press, New York, 1976).

47. I. C. Percival, Proc. Roy. Soc. (London) A353, 289 (1977).

References, continued

48. D. M. P. Holland, K. Codling, J. B. West, and G. V. Marr, J. Phys. B12, 2465 (1979).

49. D. P. Spears, H. J. Fishbeck, and T. A. Carlson, Phys. Rev. A9, 1603 (1974).

50. R. P. Madden, D. L. Ederer, and K. Codling, Phys. Rev. 177, 136 (1969).

51. K. Codling and R. P. Madden, J. Res. Natl. Bur. Std. 76A, 1 (1972).

52. K. Codling and R. P. Madden, Phys. Rev. 4, 2261 (1971).

53. K. Codling, R. P. Madden, and D. L. Ederer, Phys. Rev. 155, 26 (1967).

54. K. Codling and R. P. Madden, Appl. Opt. 4, 1431 (1965).

55. D. R. Herrick and M. E. Kellman, Phys. Rev. A21, 418 (1980).

56. U. Fano, Rep. Prog. Phys. 46, 97 (1983).

57. D. R. Herrick in Advances in Chemical Physics, Vol. LII, edited by I. Prigogine and S. A. Rice (John Wiley, New York, 1983) p.1.

58. C. H. Greene, A. R. P. Rau. and U. Fano, Phys. Rev. A26, 2441 (1982).

59. G. S. Ezra and R. S. Berry, Phys. Rev. A28, 1989 (1983).

60. G. S. Ezra and R. S. Berry, Phys. Rev. A28, 1974 (1983).

61. C. H. Greene and A. R. P. Rau, Phys. Rev. Lett. 48, 533 (1982).

62. F. Iachello and A. R. P. Rau, Phys. Rev. Lett. 47, 501 (1981).

63. D. R. Herrick, M. E. Kellman, and R. D. Poliak, Phys. Rev. A22, 1517 (1980).

64. J. Macek, J. Phys. B (Proc. Phys. Soc.) 1, 831 (1968).

65. R. W. Carman, private communication.

66. J. A. Baxter, P. Mitchell, and J. Comer, J. Phys. B15, 1105 (1982).

67. T. Srinivasan, W. Müller, M. Shahidi, T. S. Luk, H. Egger, H. Pummer, and C. K. Rhodes, "Properties of Stimulated Emission below 100 nm in Krypton," submitted to J. Opt. Soc. Am. B, in press.

68. T. Srinivasan, H. Egger, T. S. Luk, H. Pummer, and C. K. Rhodes in Laser Spectroscopy VI, edited by H. P. Weber and W. Lüthy (Springer-Verlag, Berlin, 1983) p. 385; K. Boyer, H. Egger, T. S. Luk, H. Pummer, and C. K. Rhodes, J. Opt. Soc. Am. B1, 3 (1984).

References, continued

69. C. K. Rhodes in Multiphoton Processes, P. Lambropoulos and S. J. Smith editors (Springer-Verlag, Berlin, 1984) p. 31; L. A. Lompré and G. Mainfray in Multiphoton Processes, P. Lambropoulos and S. J. Smith editors (Springer-Verlag, Berlin, 1984) p. 23; D. Feldman, H.-J. Krautwald, and K. H. Welge in Multiphoton Ionization of Atoms, edited by S. L. Chin and P. Lambropoulos (Academic Press, New York, 1984) p. 223; W. B. Delone, V. V. Suran, and B. A. Zon in Multiphoton Ionization of Atoms, edited by S. L. Chin and P. Lambropoulos (Academic Press, New York, 1984) p. 235.

70. H. G. Muller, A. Tip, and M. J. van der Wiel, J. Phys. B16, L679 (1983).

71. H. G. Muller and A. Tip, Phys. Rev. A30, 3039 (1984).

72. M. Edwards, L. Pan, and L. Armstrong, Jr., J. Phys. B17, L515 (1984).

73. Z. Bialynicka-Birula, J. Phys. B17, 2097 (1984).

74. M. H. Mittleman, Phys. Rev. A29, 2245 (1984).

75. A. Szöke, J. Phys. B18, L427 (1985).

76. T. S. B. Kibble, Phys. Rev. A150, 1060 (1966).

77. E. J. McGuire, Phys. Rev. A24, 835 (1981).

78. S. H. Autler and C. H. Townes, Phys. Rev. 100, 703 (1955).

79. K. Rzążewski and J. H. Eberly, Phys. Rev. A27, 2026 (1983).

80. U. Fano, Phys. Rev. 124, 1866 (1961).

81. A. L'Huillier, L. A. Lompré, G. Mainfray, and C, Manus, J. Physique 44, 1247 (1983).

82. T. A. Carlson, W. E. Hunt, and M. O. Krause, Phys. Rev. 151, 41 (1966).

83. M. O. Krause and T. A. Carlson, Phys. Rev. 158, 18 (1967).

84. J. Berkowitz, Photoabsorption, Photoionization and Photoelectron Spectroscopy (Academic Press, New York, 1979).

85. M. J. van der Wiel and T. N. Chang, J. Phys. B11, L125 (1978).

References, continued

86. H. Hertz, Z. Physik 274, 289 (1975).

87. W. Mehlhorn, W. Schmitz, and D. Stalherm, Z. Physik 252, 399 (1972).

88. L. O. Werme, T. Bergmark, and K. Siegbahn, Physica Scripta 8, 149 (1973).

89. L. O. Werme, T. Bergmark, and K. Siegbahn, Physica Scripta 6, 141 (1972).

90. S. Ohtani, H. Nishimura, H. Swruki, and K. Wakiya, Phys. Rev. Lett. 36, 863 (1976).

91. W. Eberhardt, G. Kalkoffen, and C. Kunz, Phys Rev. Lett. 41, 156 (1978).

92. S. Southworth, U. Becker. C. M. Truesdale. P. H. Kobrin, D. W. Lindle, S. Owaki, and D. A. Shirley, Phys. Rev. A28, 261 (1983).

93. H. Akrela, S. Akrela, and H. Pulkkinin, Phys. Rev. A30, 2456 (1984).

94. H. Akrela, S. Akrela, and H. Pulkkinin, Phys. Rev. A30, 865 (1984).

95. M. Ya. Amusia in Advances in Atomic and Molecular Physics, Vol. 17, edited by D. R. Bates and B. Bederson (Academic Press, New York, 1981) p. 1.

96. G. Wendin, Breakdown of the One-Electron Picture in Photoelectron Spectra, Structure and Bonding Vol. 45 (Springer-Verlag, Berlin, 1981).

97. G. Wendin, "Theoretical Aspects of Many-Electron Effects in Atomic Systems," Comments in Atomic Physics, in press.

98. A. Zangwill and P. Soven, Phys. Rev. Lett. 45, 204 (1980); A. Zangwill and P. Soven, Phys. Rev. A21, 1561 (1980).

99. A. L'Huillier, L. Jönsson, and G. Wendin, "Many Electron Effects in Multiphoton Ionization," to be published.

100. A. Zangwill, J. Chem. Phys. 78, 5926 (1983).

101. K. Codling and R. P. Madden, Phys. Rev. Lett. 12, 106 (1964).

102. U. Johann, T. S. Luk, H. Egger, H. Pummer, and C. K. Rhodes, "Evidence for Atomic Inner-Shell Excitation in Xenon from Electron Spectra Produced by Collision-Free Multiphoton Processes at 193 nm," Conference on Lasers and Electro-Optics '85, Baltimore, Maryland, p. 152.

References, continued

103. U. Johann, T. S. Luk, and C. K. Rhodes, "Multiphoton Inner-Shell Atomic Excitation and Multiple Ionization," XIVth International Conference on the Physics of Electronic and Atomic Collision, edited by D. C. Lorents, W. E. Meyerhof, and J. R. Peterson, (North-Holland, Amsterdam, in press).

104. D. C. Griffin, C. Bottcher, M. S. Pindzola, S. M. Younger, D. C. Gregory, and D. H. Crandall, Phys. Rev. A29, 1720 (1984).

105. F. P. Larkins, J. Phys. B6, 2450 (1973).

106. P. Lambropoulos, "Mechanisms for Multiple Ionization of Atoms by Strong Pulsed Lasers," Phys. Rev. Lett., submitted.

107. L. A. Lompré and G. Mainfray in Fundamentals of Laser Interactions, Lecture Notes in Physics No. 229, edited by F. Ehlotzky (Springer-Verlag, Berlin, 1985) p. 125.

108. H. S. W. Massey, Electronic and Ionic Impact Phenomena, Vol. 3 (Oxford University Press, London, 1921) p. 1915; C. Zener, Proc. Roy. Soc. A137, 606 (1932).

109. C. Cohen-Tannoudji and S. Haroche in Polarisation, Matiére et Rayonnement (Presses Universitaires de France, Paris, 1969) p. 191.

TABLE I. Typical experimental parameters for photoelectron ATI-ladder lines observed in the ionization of neutral rare gas atoms. The energy shift is caused by space charge induced by scattered radiation. The calculated threshold laser intensity is defined for a probability of $\Gamma = 5 \times 10^{-3}$ (detection limit) and based on the Keldysh Model.[28,29]

ELEMENT	LASER INTENSITY [W/cm^2]	GAS PRESSURE [Torr]	THRESHOLD LASER INTENSITY [W/cm^2] EXPERIMENTAL	CALCULATED	N PHOTONS ABSORBED	CALCULATED ELECTRON ENERGY [eV]	EXPERIMENTAL ELECTRON ENERGY [eV]	HALF WIDTH [meV]	RELATIVE INTENSITY [%]
Neon	$\sim 5 \times 10^{14}$	1×10^{-5}	$\sim 3 \times 10^{13}$	1.3×10^{14}	4	4.09	4.58(5)	$\sim$ 380	100
					5	10.50	10.95(10)		9
					6	16.91	—		1.5
					7	23.32	—		0.5
					8	29.73	—		0.2
					9	36.14	—		0.1
					10	42.55	—		0.05
					11	48.96	—		0.02
					12	55.37	—		0.01
Argon	$\sim 5 \times 10^{14}$	2×10^{-7}	$\sim 1 \times 10^{13}$	2.4×10^{13}	3	3.48	4.03(15)	$\sim$ 250	100
					4	9.89	10.43(10)		12
					5	16.30	16.85(8)		2
					6	22.71	22.80(5)		0.8
					7	29.12	—		0.2
Krypton	$\sim 5 \times 10^{14}$	1×10^{-7}	$\sim 1 \times 10^{9}$	2.2×10^{13}	3	5.24	5.85(10)	$\sim$ 250	100
					4	11.65	12.02(15)		2.5
					5	18.06	18.70(5)		< 0.1
					6	24.47			<< 0.1
Xenon	$\sim 2 \times 10^{13}$	4×10^{-7}	$\sim 1 \times 10^{10}$	1.3×10^{12}	2	0.69	0.72	$\sim$ 230	100
					3	5.79	5.92		4
					3	7.10	7.24		0.8
					4	12.20			< 0.04
					4	13.51			< 0.04

TABLE II. Relative ion charge state abundance for Xe, Kr, and Ar obtained in an ion time-of-flight experiment[3,4] under conditions comparable to the present electron data. Based on this distribution, the expected relative electron production rate in purely sequential or direct processes, respectively, are given.

ELEMENT	RELATIVE ABUNDANCE [%]	ION CHARGE STATE 1+	2+	3+	4+	5+	6+
Xenon	ions	49	31	17	2.6	1.1	0.27
	electrons sequential	56	29	12	2.2	0.8	0.15
	electrons direct	27	35	28	5.8	3	1
Krypton	ions	82	14	3.3	0.3		
	electrons sequential	82.3	14.5	2.7	0.25		
	electrons direct	68	23	8.2	1		
Argon	ions	91	9				
	electrons sequential	92	8				
	electrons direct	84	16				

III.a. Important multiphoton channels of ionization in the production of xenon charge states by the sequential mechanism. The electron energy (in eV) is the calculated excess energy above the residual ion state energy and refers to the number of photons absorbed in the ATI-process. The last column shows the experimental energy shift (in meV) of different ATI-ladders normalized to the lowest order ladder process (a) and obtained after identification with observed lines in the xenon spectrum shown in Fig. (5).

CODE	PROCESS	ELECTRON ENERGY (eV)	ENERGY SHIFT (meV)
a	$Xe\ 5s^2 5p^6\ ^1S_0 + 2\gamma,3\gamma,4\gamma,5\gamma \rightarrow Xe^{1+}\ 5s^2 5p^5\ ^2P^0_{3/2} + e^-$	0.69, 7.10, 13.51, 19.92	0
b	$3\gamma,4\gamma,5\gamma \rightarrow\ ^2P^0_{1/2} + e^-$	5.79, 12.20, 18.61	40
c	$Xe^{1+}\ 5s^2 5p^5\ ^2P^0_{3/2} + 4\gamma,5\gamma,6\gamma,7\gamma \rightarrow Xe^{2+}\ 5s^2 5p^4\ ^3P_2 + e^-$	4.44, 10.85, 17.26, 23.67	263
d	$4\gamma,5\gamma,6\gamma,7\gamma \rightarrow\ ^3P_1 + e^-$	3.23, 9.64, 16.02, 22.46	56
e	$4\gamma,5\gamma,6\gamma,7\gamma \rightarrow\ ^3P_0 + e^-$	3.43, 9.84, 16.25, 22.66	71
f	$4\gamma,5\gamma,6\gamma,7\gamma \rightarrow\ ^1D_2 + e^-$	2.32, 8.73, 15.14, 21.55	0
g	$Xe^{1+} 5s^2 5p^5\ ^2P^0_{1/2} + 4\gamma,5\gamma,6\gamma,7\gamma \rightarrow Xe^{2+}\ 5s^2 5p^4\ ^3P_2 + e^-$	5.75, 12.16, 18.57, 24.98	
h	$4\gamma,5\gamma,6\gamma,7\gamma \rightarrow\ ^3P_1 + e^-$	4.54, 10.95, 17.36, 23.77	
i	$4\gamma,5\gamma,6\gamma,7\gamma \rightarrow\ ^3P_0 + e^-$	4.74, 11.15, 17.56, 23.97	
j	$4\gamma,5\gamma,6\gamma,7\gamma \rightarrow\ ^1D_2 + e^-$	3.63, 10.04, 16.45, 22.86	
k	$Xe^{2+}\ 5s^2 5p^4\ ^3P_2 + 6\gamma,7\gamma,8\gamma \rightarrow Xe^{3+}\ 5s^2 5p^3\ ^4S^0_{3/2} + e^-$	6.27, 12.78, 19.19	
l	$6\gamma,7\gamma,8\gamma \rightarrow\ ^2D^0_{3/2} + e^-$	4.73, 11.14, 17.55	
m	$6\gamma,7\gamma,8\gamma \rightarrow\ ^2D^0_{5/2} + e^-$	4.20, 10.61, 17.02	
n	$6\gamma,7\gamma,8\gamma \rightarrow\ ^2P^0_{1/2} + e^-$	2.89, 9.30, 15.71	
o	$6\gamma,7\gamma,8\gamma \rightarrow\ ^2P^0_{3/2} + e^-$	1.18, 7.59, 14.00	(496)
p	$Xe^{2+}\ 5s^2 5p^4\ ^1D_2 + 5\gamma,6\gamma,7\gamma \rightarrow Xe^{3+}\ 5s^2 5p^3\ ^4S^0_{3/2} + e^-$	2.05, 8.46, 14.87	(-374)

TABLE III.b. Important multiphoton channels of ionization in the production of krypton charge states by the sequential mechanism. Listed quantities are represented similarly to those in TABLE III.a.

CODE	PROCESS	ELECTRON ENERGY (eV)
a	$Kr\ 4s^2 4p^6\ ^1S_0 + 3\gamma,4\gamma,5\gamma,6\gamma \rightarrow Kr^{1+}\ 4s^2 4p^5\ ^2P^0_{3/2} + e^-$	5.24, 11.65, 18.06, 24.47
b	$Kr^{1+}\ 4s^2 4p^5\ ^2P^0_{3/2} + 4\gamma,5\gamma \rightarrow Kr^{2+}\ 4s^2 4p^4\ ^3P_2 + e^-$	1.08, 7.49
c	$4\gamma,5\gamma \rightarrow\ ^3P_1 + e^-$	0.52, 6.93
d	$4\gamma,5\gamma \rightarrow\ ^3P_0 + e^-$	0.43, 6.84
e	$5\gamma \rightarrow Kr^{2+}\ 4s^2 4p^4\ ^1D_2 + e^-$	5.67
f	$5\gamma \rightarrow\ ^1S_0 + e^-$	3.38
g	$Kr^{2+}\ 4s^2 4p^4\ ^3P_2 + 6\gamma,7\gamma \rightarrow Kr^{3+}\ 4s^2 4p^3\ ^4S^0_{3/2} + e^-$	1.57, 7.98
h	$^3P_1 + 6\gamma,7\gamma \rightarrow + e^-$	1.01, 7.42
i	$^3P_0 + 6\gamma,7\gamma \rightarrow + e^-$	0.92, 7.33
j	$^1D_2 + 6\gamma,7\gamma \rightarrow + e^-$	6.16, 12.57
k	$^1S_0 + 6\gamma,7\gamma \rightarrow + e^-$	3.88, 10.29

TABLE III.c. Important multiphoton channels of ionization in the production of argon charge states by the sequential mechanism. Listed quantities are represented similarly to those in TABLE III.b.

CODE	PROCESS	ELECTRON ENERGY (eV)
a	$Ar\ 3s^2 3p^6\ ^1S_0 + 3\gamma,4\gamma,5\gamma,6\gamma,7\gamma \rightarrow Ar^{1+}\ 3s^2 3p^5\ ^2P^0_{3/2} + e^-$	3.48, 9.89, 16.30, 22.71,29,12
b	$Ar^{1+}\ 3s^2 3p^5\ ^2P^0_{3/2} + 5\gamma,6\gamma,7\gamma \rightarrow Ar^{2+}\ 3s^2 3p^4\ ^3P_2 + e^-$	4.44, 10.85, 17.26
c	$5\gamma,6\gamma,7\gamma \rightarrow\ ^3P_1 + e^-$	4.30, 10.71, 17.12
d	$5\gamma,6\gamma,7\gamma \rightarrow\ ^3P_0 + e^-$	4.25, 10.66, 17.07
e	$5\gamma,6\gamma,7\gamma \rightarrow\ ^1D_2 + e^-$	2.70, 9.11, 15.52
f	$5\gamma,6\gamma,7\gamma \rightarrow\ ^1S_0 + e^-$	0.31, 6.72, 13.13

TABLE IV. Relative line intensities in the xenon electron energy spectrum at a peak 193 nm intensity of 10^{15} W/cm^2. The line designations indicated correspond to the codes for the ionization channels (IC) given in TABLE III.a. The number associated with the code letter equals the number of photons absorbed in that channel and is in accord with the markings in Fig. (5). The intensities are normalized to line (b3, g4). The approximate relative ATI intensities for 5, 6, 7, and 8 photon absorption are given in the right column. With the exception of the (a) and (b,g) series, these values are nearly independent of the ionization channel. The approximate relative channel intensities c, (d,e), f are shown in the bottom row for the 5th, 6th, and 7th order. These magnitudes are seen to be nearly independent of the order.

I.C.	INTENSITY	I.C.	INTENSITY	I.C.	INTENSITY	I.C.	INTENSITY	I.C.	INTENSITY	RELATIVE ATI INTENSITY
a2	(60)	b3,g4	100	c4	65	d,e4	(50)	f4	(35)	
a3	15-20	b4,g5	3	c5	13	d,e5	11	f5	48	100
a4	0.6	b5,g6	0.5	c6	2.7	d,e6	2.4	f6	9	20
a5	< 0.01			c7	0.3	d,e7	0.2	f7	1	2
								f8	0.2	0.4
Approximate relative channel intensities for 5,6,7 photon absorption				29		25		100		-

TABLE V. Compilation of the parameters of several experimental studies of collision-free nonlinear processes. The wavelength of irradiation is denoted by λ, I_{ex} is the peak experimental intensity, τ_p is the experimental pulse width, I_ω is defined by Eq.(18), $\gamma \equiv I_{ex}/\tau_p$, and $\beta \equiv mc\lambda\omega^3/2\pi e^2\tau_e$ with $\tau_e = 10^{-15}$ sec. Reference numbers are also listed.

λ(μm)	I_{ex} (W/cm^2)	τ_p (fs)	I_ω (W/cm^2)	γ ($\frac{W}{cm^2\text{-sec}}$)	β ($\frac{W}{cm^2\text{-sec.}}$)	β/γ	$U(I_{ex},\omega)$ (eV)	Ref. No.
0.193	$\sim 10^{15}$	$\sim 5\times10^{3}$	8.3×10^{13}	$\sim2\times10^{26}$	1.8×10^{30}	9.1×10^{3}	~ 3.84	This work
0.355	$\sim 10^{13}$	$\sim 10^{4}$	1.3×10^{13}	$\sim10^{24}$	2.8×10^{29}	2.8×10^{5}	~ 0.12	13
0.53	$\sim 10^{13}$	$\sim 10^{4}$	4.0×10^{12}	$\sim10^{24}$	8.7×10^{28}	8.7×10^{4}	~ 0.26	13
0.53	$\sim 10^{12}$	$\sim 5\times10^{3}$ - 2×10^{5}	4×10^{12}	$\sim5\times10^{21}$ - 2×10^{23}	8.7×10^{28}	4.3×10^{5} - 1.7×10^{7}	~ 0.03	81,107
1.06	$\sim 4\times10^{16}$	$\sim2.5\times10^{4}$	5×10^{11}	$\sim1.6\times10^{27}$	1.1×10^{28}	6.9	~ 4190	8,17
1.06	$\sim 10^{13}$	$\sim 10^{4}$	5×10^{11}	$\sim10^{24}$	1.1×10^{28}	1.1×10^{4}	~ 1.05	13
1.06	$\sim10^{11}$-10^{13}	$\sim 5\times10^{4}$	5×10^{11}	$\sim2\times10^{21}$ - 2×10^{23}	1.1×10^{28}	$\sim5.5\times10^{4}$ - 5.5×10^{6}	$\sim 0.01 - 1.0$	16
1.06	$\sim 10^{13}$	$\sim 5\times10^{3}$ - 2×10^{5}	5×10^{11}	$\sim5\times10^{22}$ - 2×10^{24}	1.1×10^{28}	$\sim5.5\times10^{3}$ - 2.2×10^{5}	~ 1.05	81,107
10.6	$\sim 10^{14}$	$\sim1.1\times10^{6}$	5×10^{8}	9.1×10^{22}	1.1×10^{25}	1.2×10^{2}	~ 1040	5

FIGURE CAPTIONS

Fig. 1: Schematic diagram of the electron time-of-flight spectrometer. Also shown are the z-dependence of the magnetic field on the z-axis and the magnetic field configuration with a helical path of an electron moving from the high field interaction region to the low field region at the detector.

Fig. 2: a) Calculated form of the time-of-flight electron distribution for monoenergetic electrons. An anisotropic $\cos^2\theta_o$-distribution for the emission angle θ_o relative to the z-axis is assumed. For 10 ev electrons, 90% arrive at the detector with a time difference of $\Delta T/T$ - 1.8% corresponding to ΔE = 380 neV. Retarded to 1 eV in the drift tube, the figures are $\Delta T/T$ = 0.8% and $\Delta E \tilde{\sim}$ 17 mev.

b) Measured linewidth of the three photon absorption line (5.24 ev) in Kr at an intensity of $\sim 5 \times 10^{11}$ W/cm^2, leaving the ion in the $^2P^o_{3/2}$ ground state. The dependence on the retarding voltage and gas pressure is shown. The change in energy resolution and the influence of space charge effects are evident.

Fig. 3: Typical electron time-of-flight (TOF) spectra for Xe, Kr, Ar, and Ne irradiated with a 193 nm laser pulse of $\sim$ 5 psec duration. The line identification is given in the schematic energy level diagrams showing relevant energy levels, multiphoton transition (single arrows) and electron emission lines (double arrows). Excited neutral and ionic configurations are indicated by the boxes below the ionization limits. Background lines are labeled are BG. The "prompt" line generated by scattered 193 nm radiation impinging directly on the channel plate is follwed by a group of photoelectrons produced on the accelerating grid placed in front of the detector. The experimental

Figures, continued

parameters associated with these spectra are listed in Table I. The inset in the Ar TOF spectrum was taken with a retarding voltage of -2V. The intensity of the line at ∿ 3.3 eV is underestimated in this recording.

Fig. 4: Laser intensity dependence of the Xe TOF electron spectrum recorded at low energy resolution (no retardation). The electron energy range spanned is between ∿ 0.3 eV and ∿ 100 eV.

Fig. 5: High resolution Xe-electron energy spectrum recorded at a 193 nm laser intensity of ∿ 10^{15} W/cm^2 and a gas pressure of ∿ 4 x 10^{-7} Torr. The energy scale has been calibrated at low laser energy, where the lines are unshifted (see text). The identification of the lines with their respective above threshold ladder series is shown on top of the spectrum. The letter labeling refers to the specific sequential processes listed in Table III.a to which the main component of the observed line is attributed. The associated number indicates the number of the photons absorbed.

Fig. 6: Splitting of the two photon 0.7 eV electron emission line observed in xenon as a function of increasing 193 nm intensity at a gas pressure of ∿ 10^{-6} Torr. Only the 10 nsec ASE component of the 193 nm laser pulse was used for excitation.

Fig. 1

MAGNETIC MIRROR PHOTOELECTRON SPECTROMETER

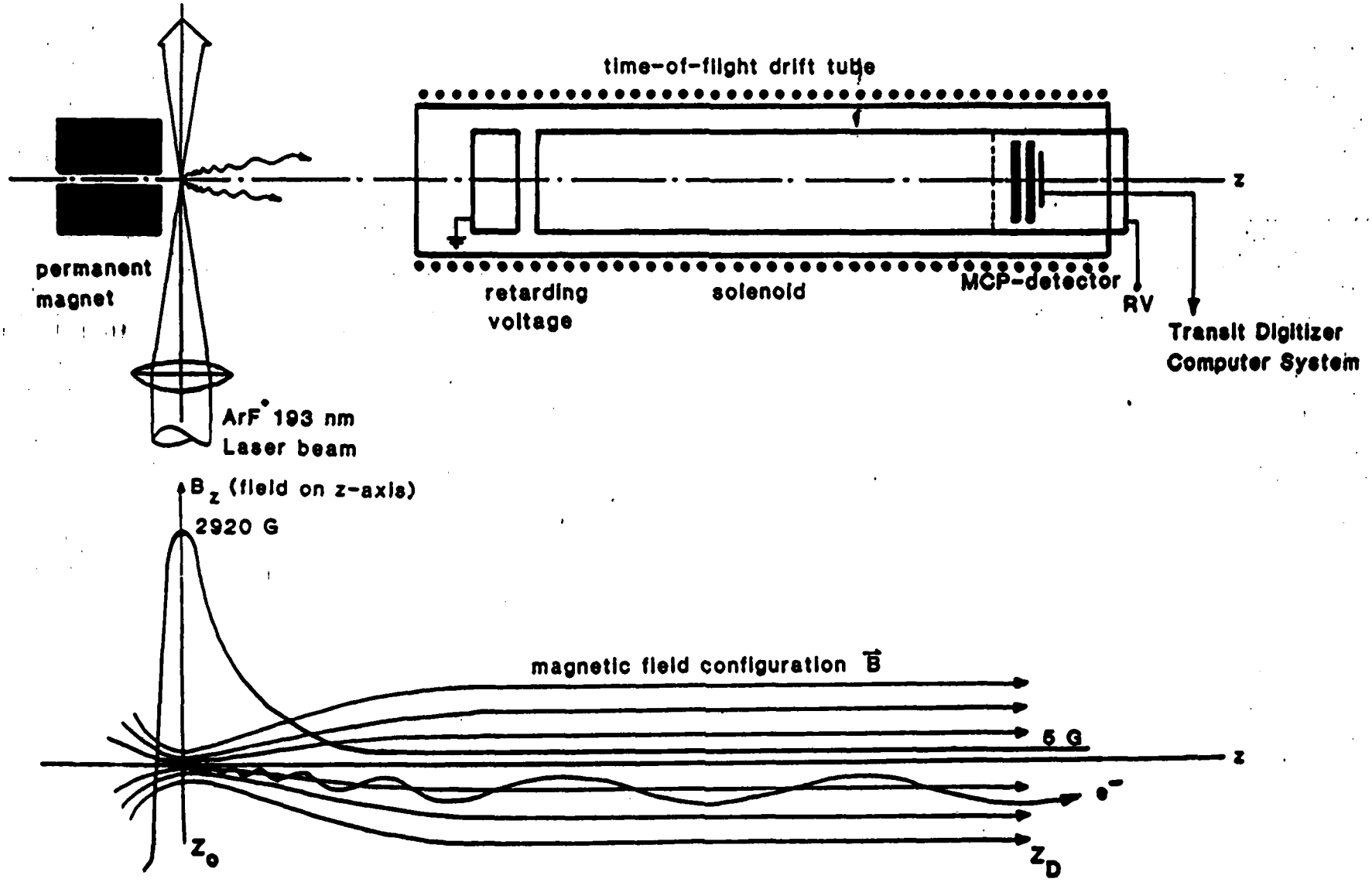

Fig. 2

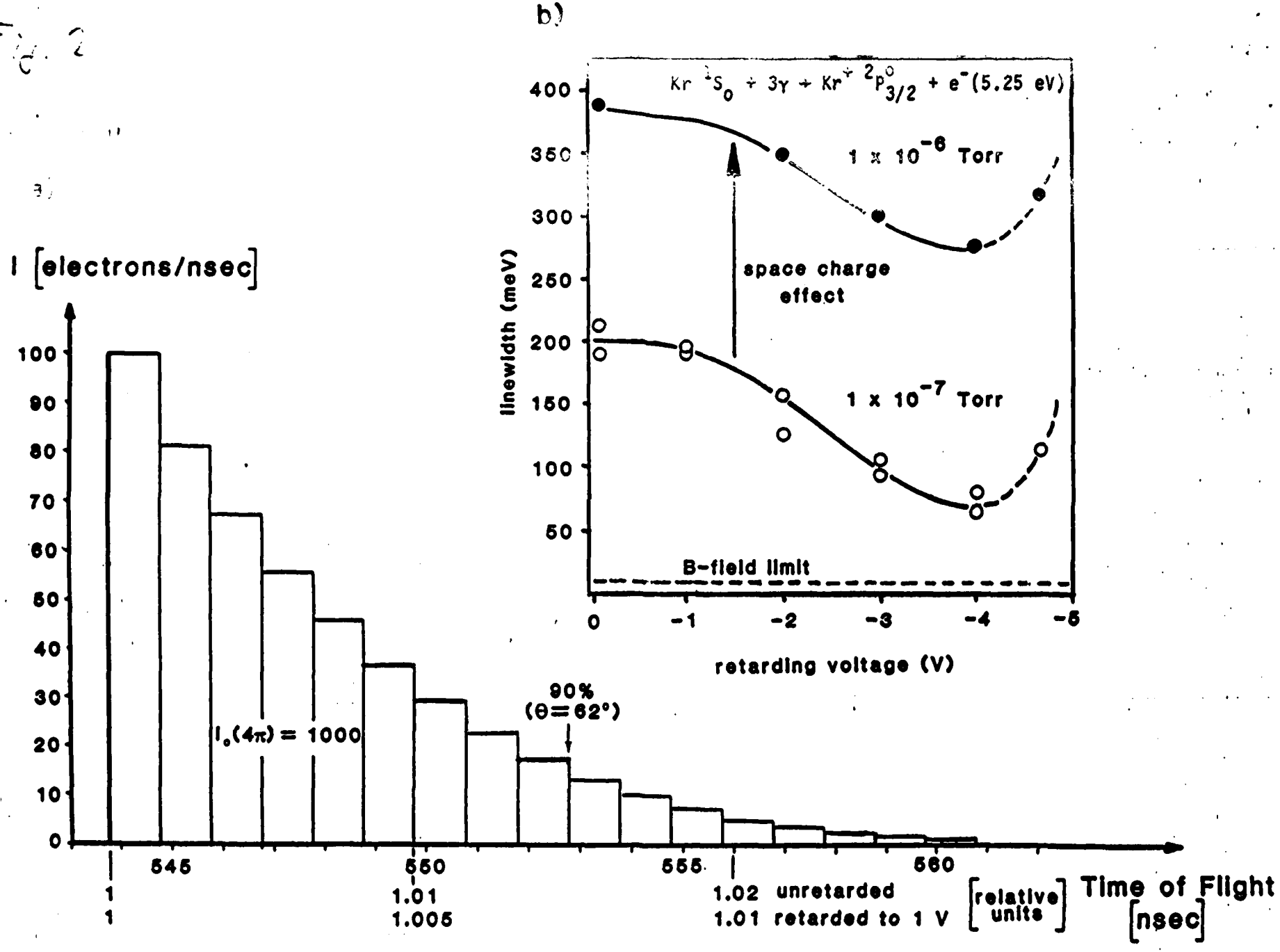
b)
Kr $^1S_0$ + 3γ → Kr$^+$ $^2P^o_{3/2}$ + e$^-$(5.25 eV)
1 x 10^{-6} Torr
space charge effect
1 x 10^{-7} Torr
B-field limit
linewidth (meV)
400
350
300
250
200
150
100
50
0
-1
-2
-3
-4
-5
retarding voltage (V)
I [electrons/nsec]
100
90
80
70
60
50
40
30
20
10
0
$I_o(4\pi) = 1000$
90%
(θ=62°)
545
550
555
560
1
1
1.01
1.005
1.02 unretarded
1.01 retarded to 1 V
[relative units]
Time of Flight
[nsec]

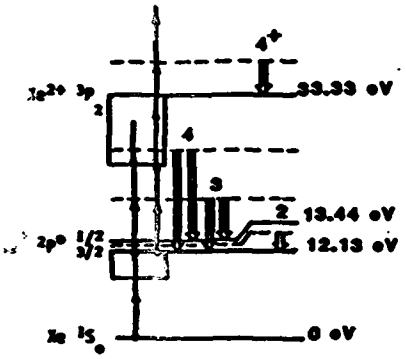

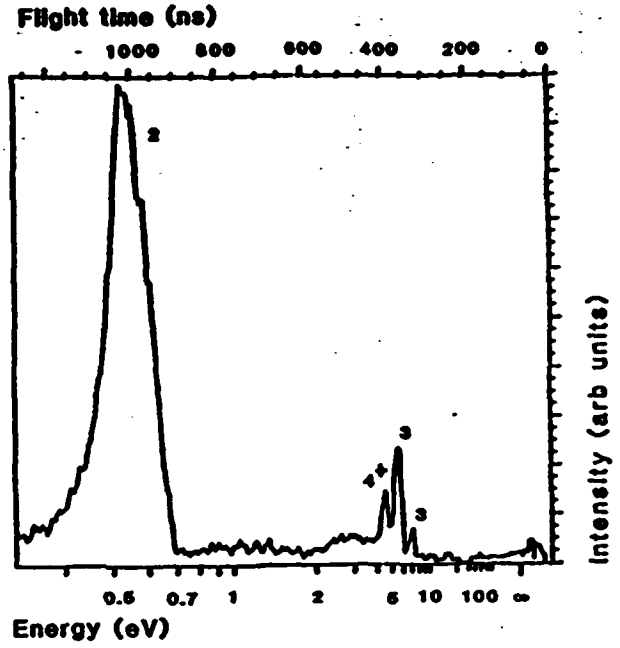

XENON

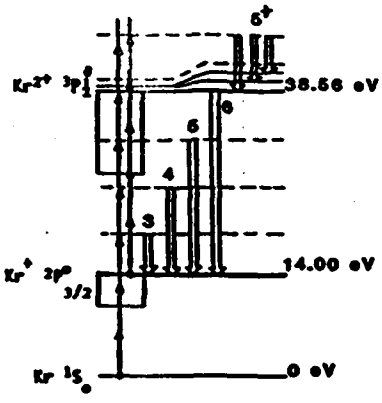

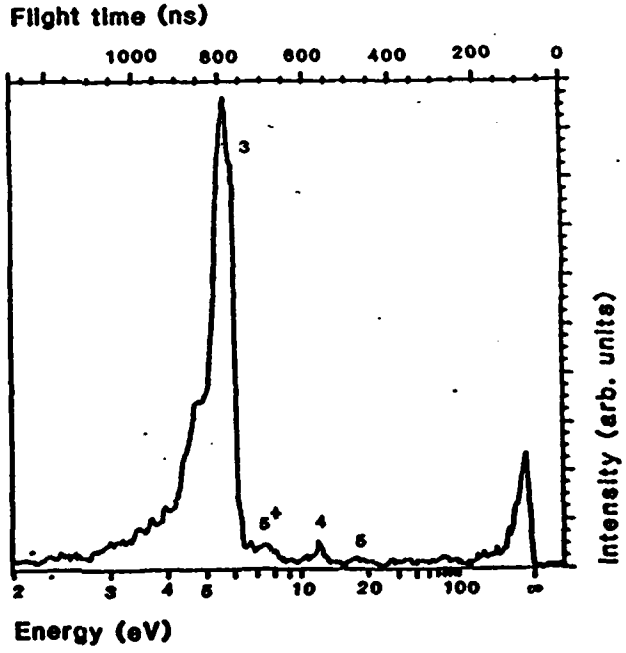

KRYPTON

Fig 3a,

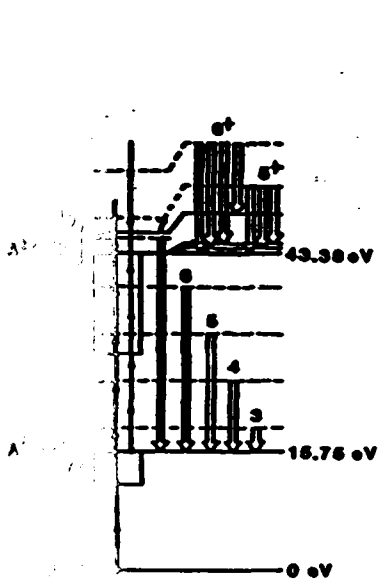

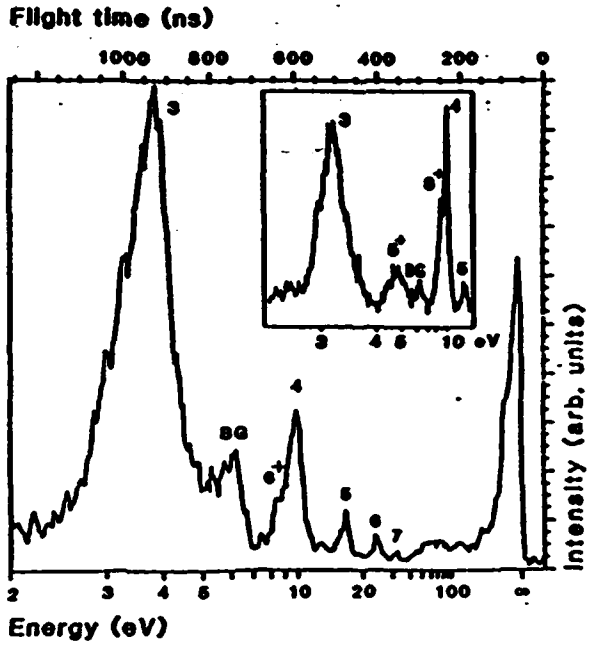

ARGON

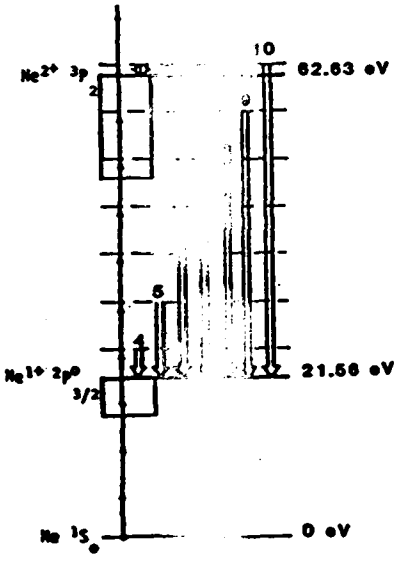

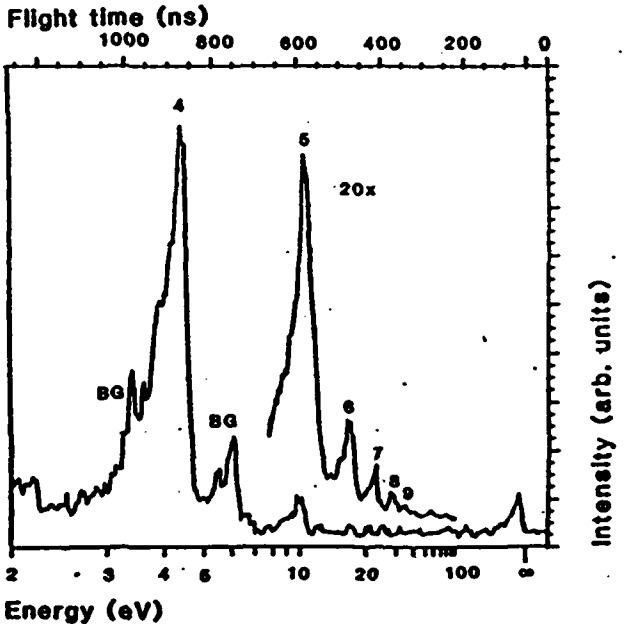

NEON

Fig 3

Fig 3a

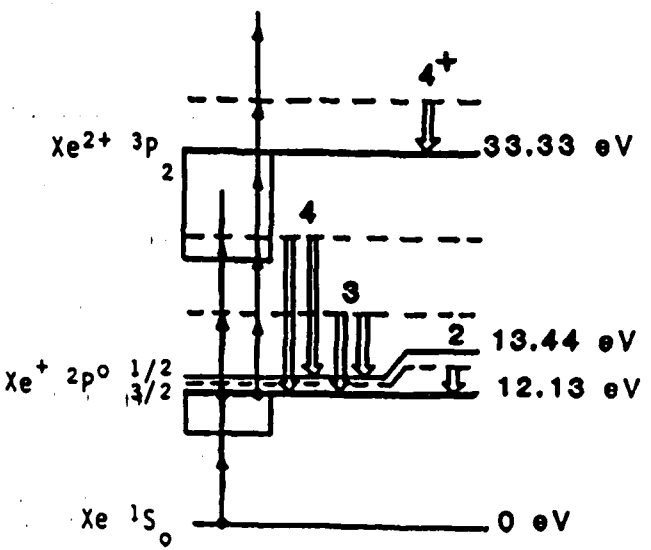
4+
Xe2+ 3P2
33.33 eV
4
3
2
13.44 eV
Xe+ 2P° 1/2
3/2
12.13 eV
Xe 1S0
0 eV

XENON

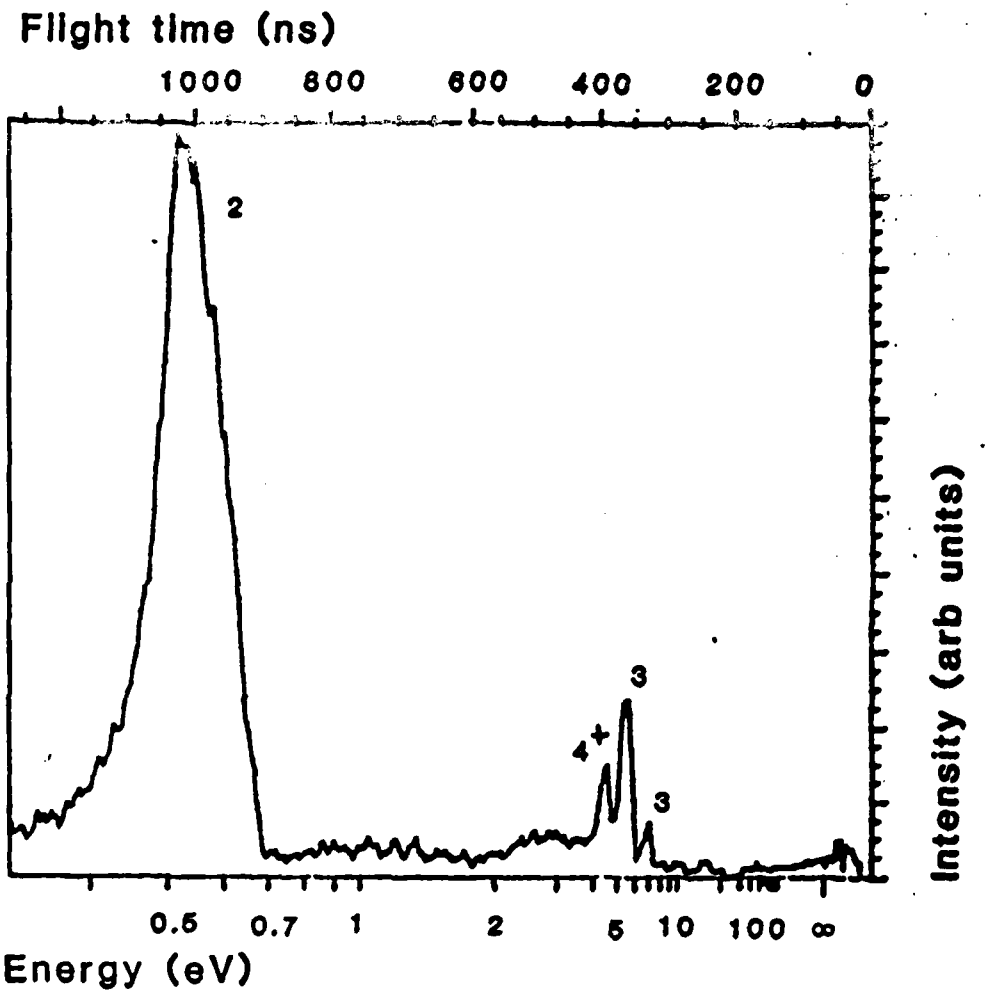
Flight time (ns)
1000
800
600
400
200
0
2
3
4+
3
0.5
0.7
1
2
5
10
100
∞
Energy (eV)
Intensity (arb units)

Fig 36

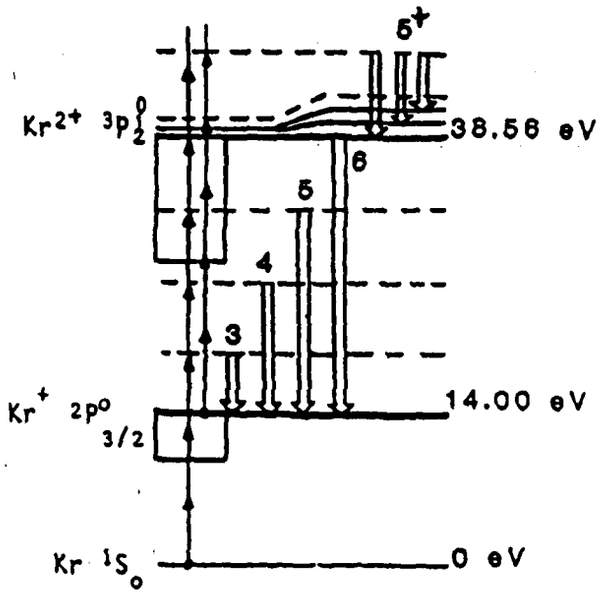

KRYPTON

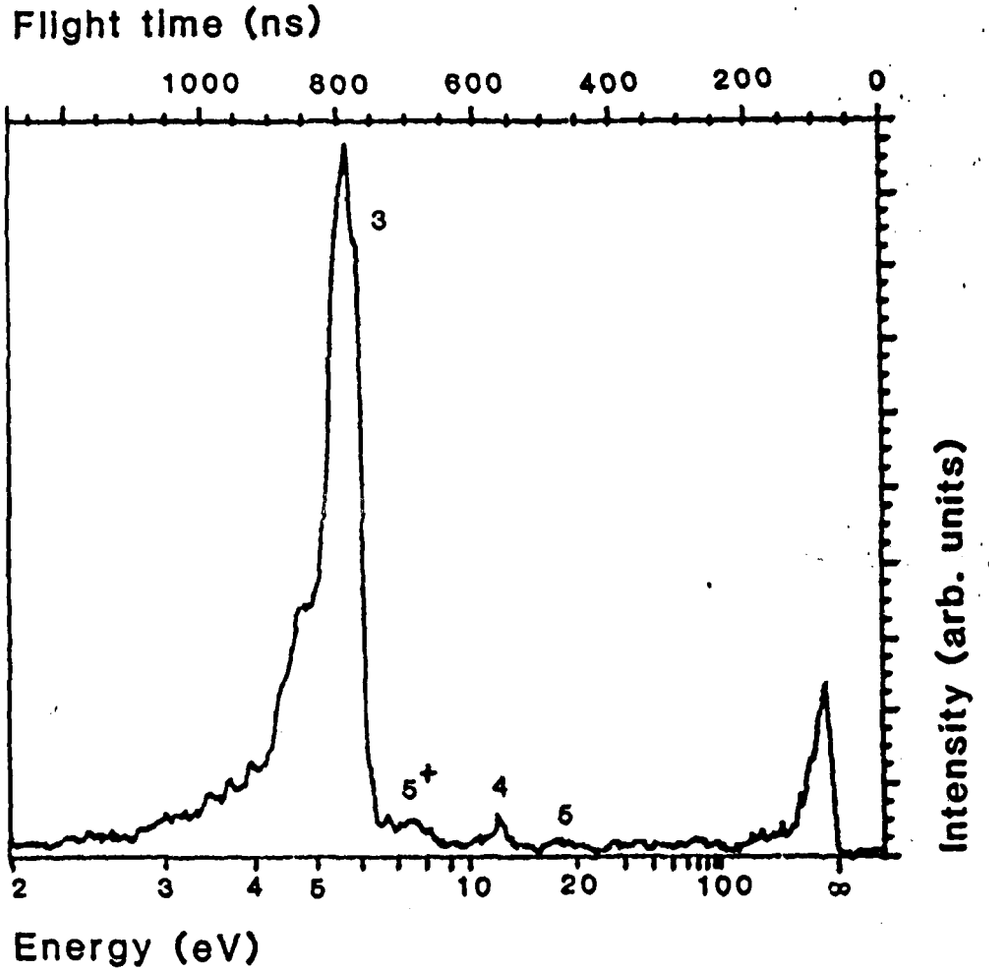

Fig 3c

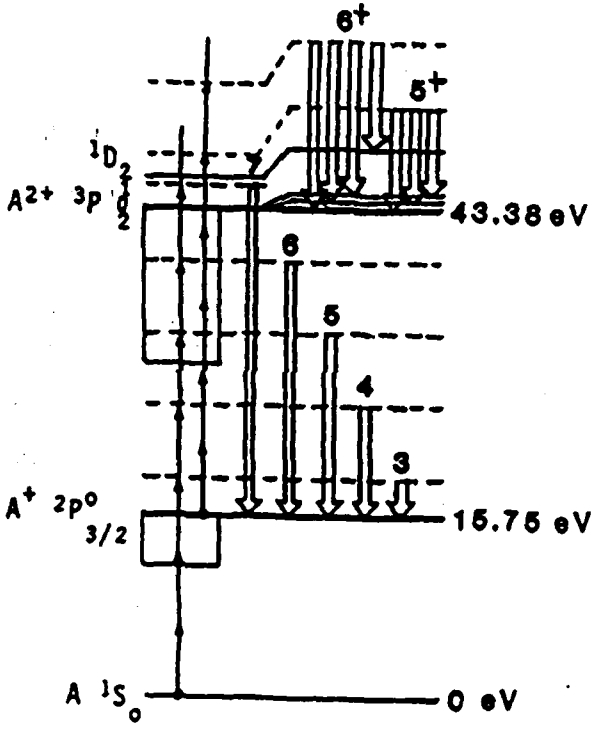
6+
5+
$^1D_2$
A^{2+} $3p\ ^4_2$
43.38 eV
6
5
4
3
A^+ $2p^o_{3/2}$
15.75 eV
A ^1S_o
0 eV

ARGON

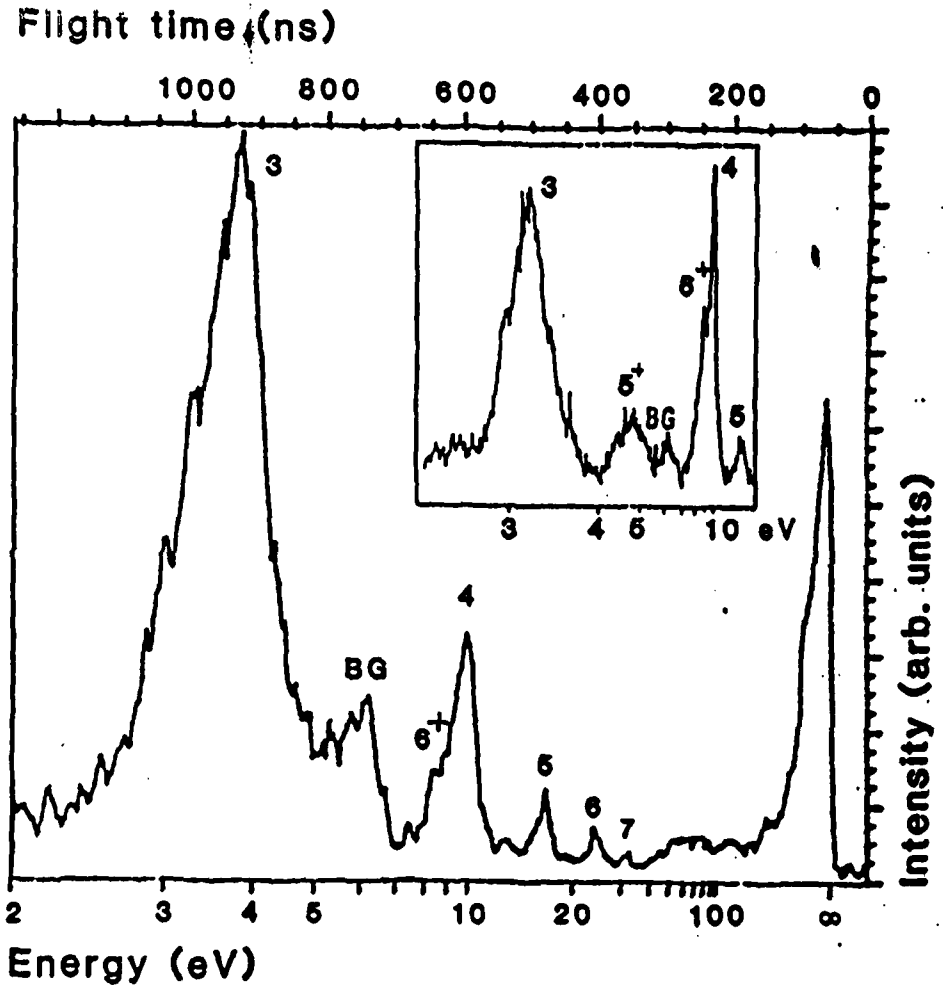
Flight time (ns)
1000
800
600
400
200
0
3
4
6+
5+
BG
5
3
4 5
10 eV
BG
6+
7
8
2
3
4
5
10
20
100
Energy (eV)
Intensity (arb. units)

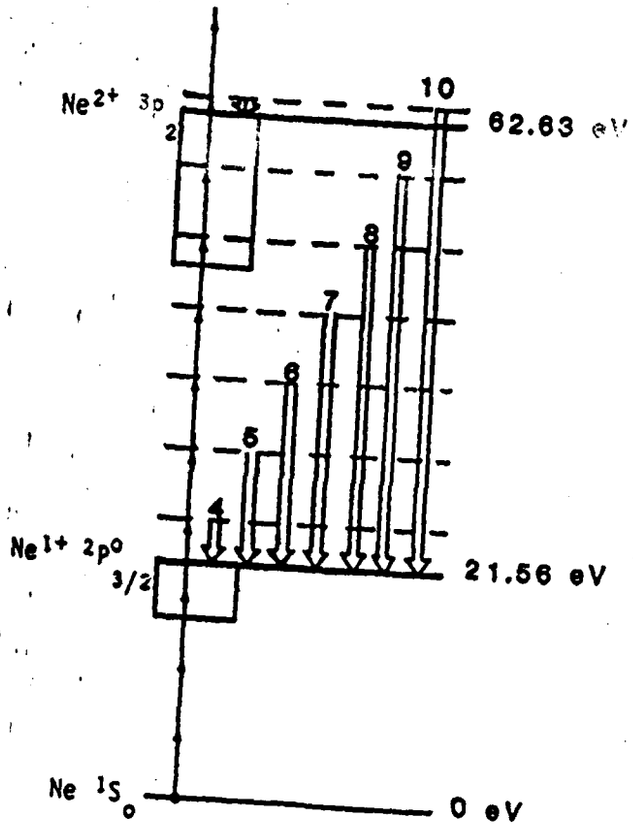
Ne2+ 3p
10
62.63 eV
9
8
7
6
5
4
Ne1+ 2p0 3/2
21.56 eV
Ne 1S0
0 eV

NEON

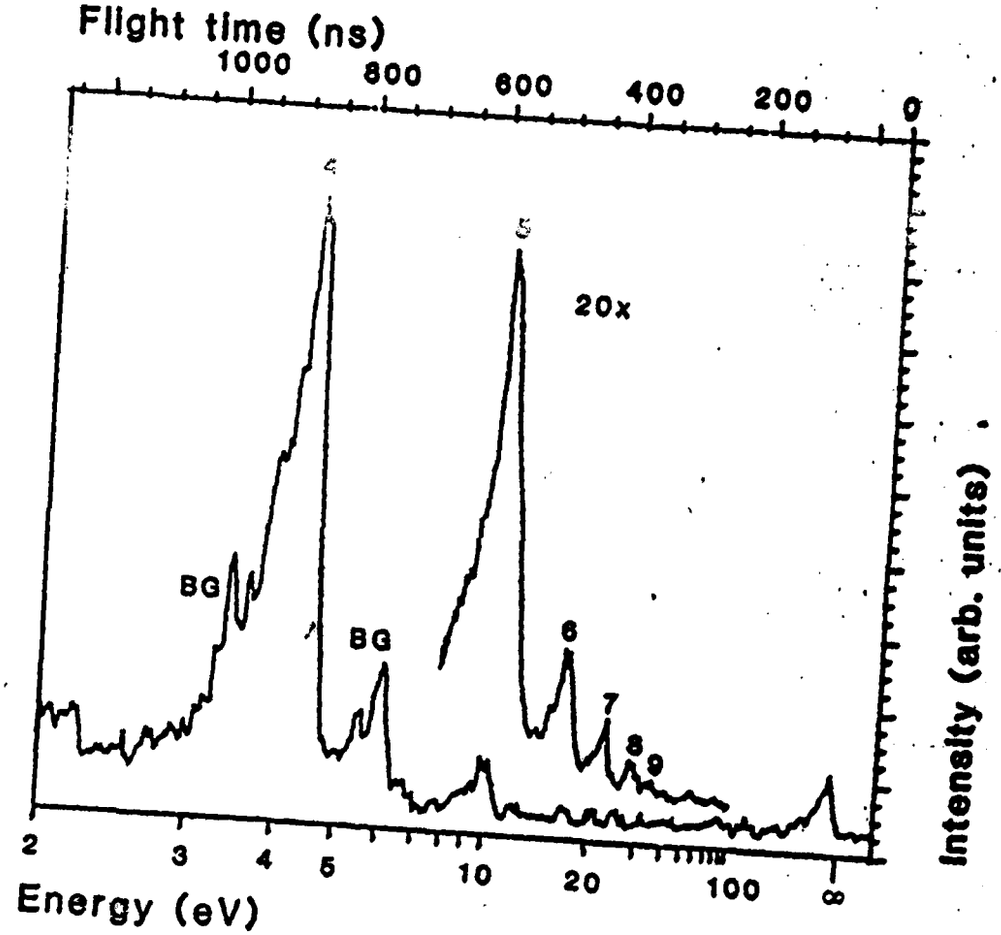
Flight time (ns)
1000
800
600
400
200
0
4
5
20x
BG
BG
6
7
8
9
2
3
4
5
10
20
100
8
Energy (eV)
Intensity (arb. units)

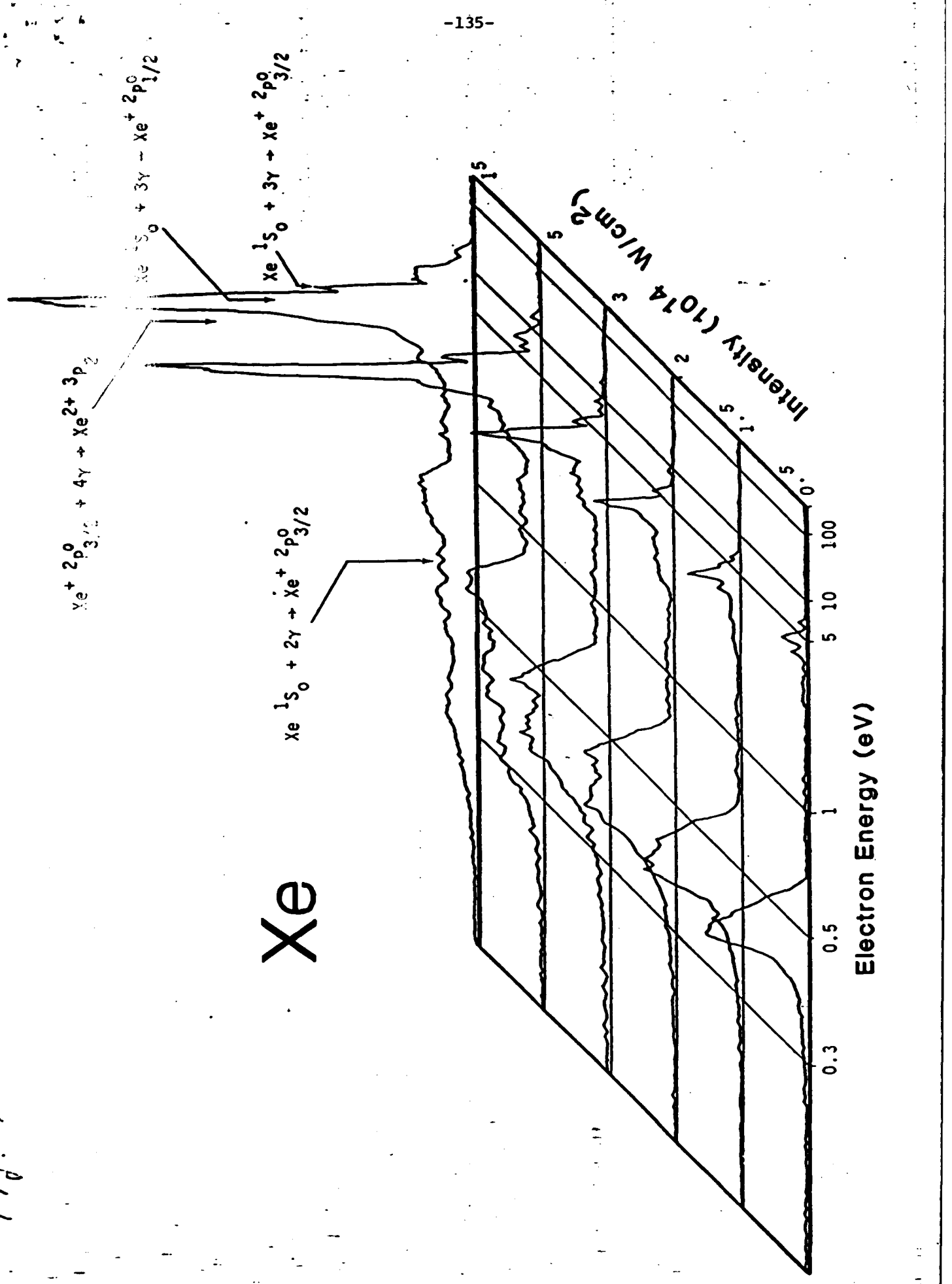
Xe
Xe ^1S_o + 3γ → Xe$^+$ $^2P^o_{3/2}$
Xe ^1S_o + 3γ → Xe$^+$ $^2P^o_{1/2}$
Xe$^+$ $^2P^o_{3/2}$ + 4γ → Xe^{2+} $^3P_2$
Xe ^1S_o + 2γ → Xe$^+$ $^2P^o_{3/2}$
Intensity (10^{14} W/cm^2)
15
5
3
2
1.5
1
0.5
Electron Energy (eV)
0.3
0.5
1
5
10
100

Fig. 4

Fig. 5

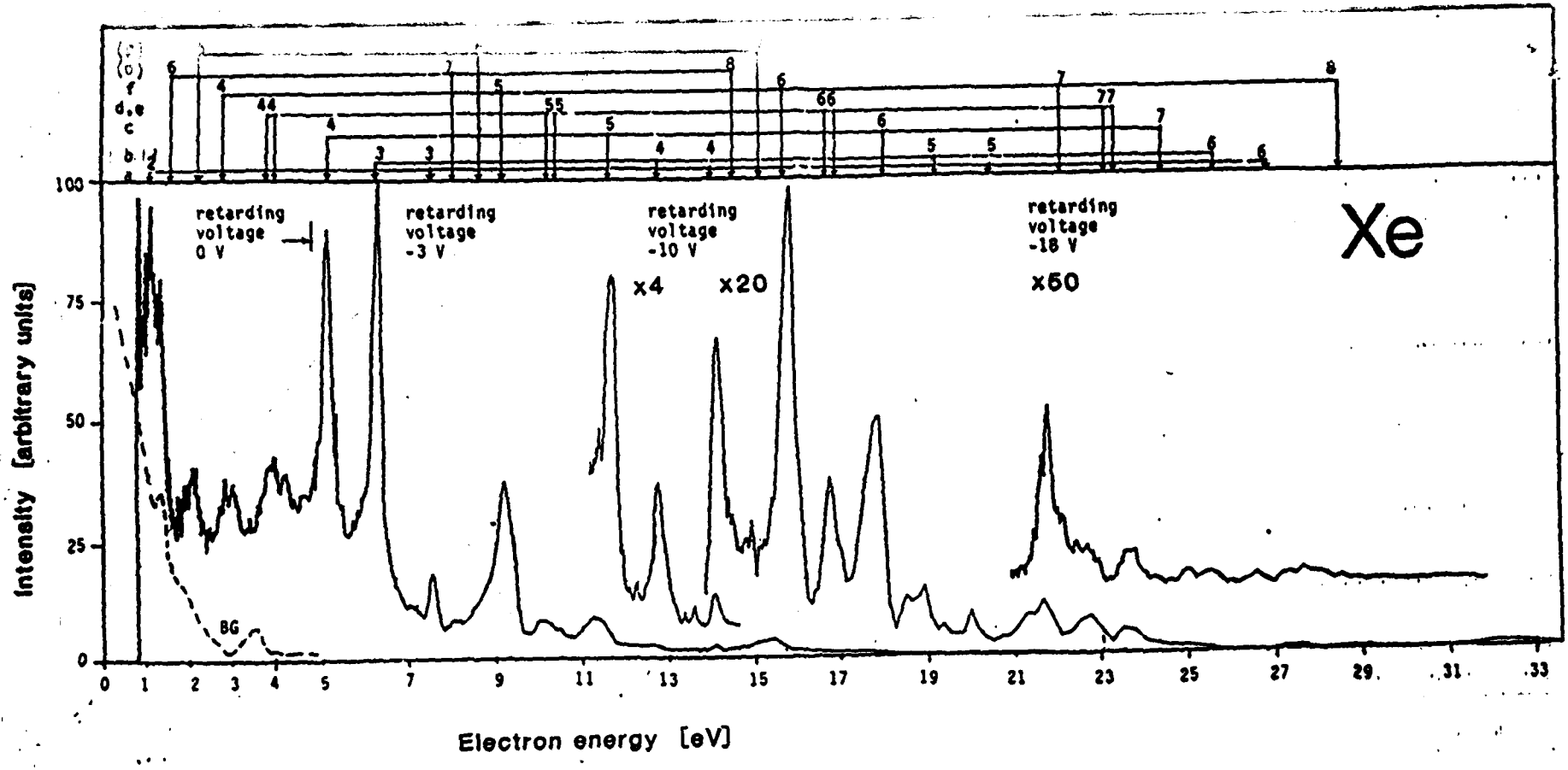
retarding voltage 0 V
retarding voltage -3 V
retarding voltage -10 V
retarding voltage -18 V
x4
x20
x50
Xe
BG
Intensity [arbitrary units]
Electron energy [eV]

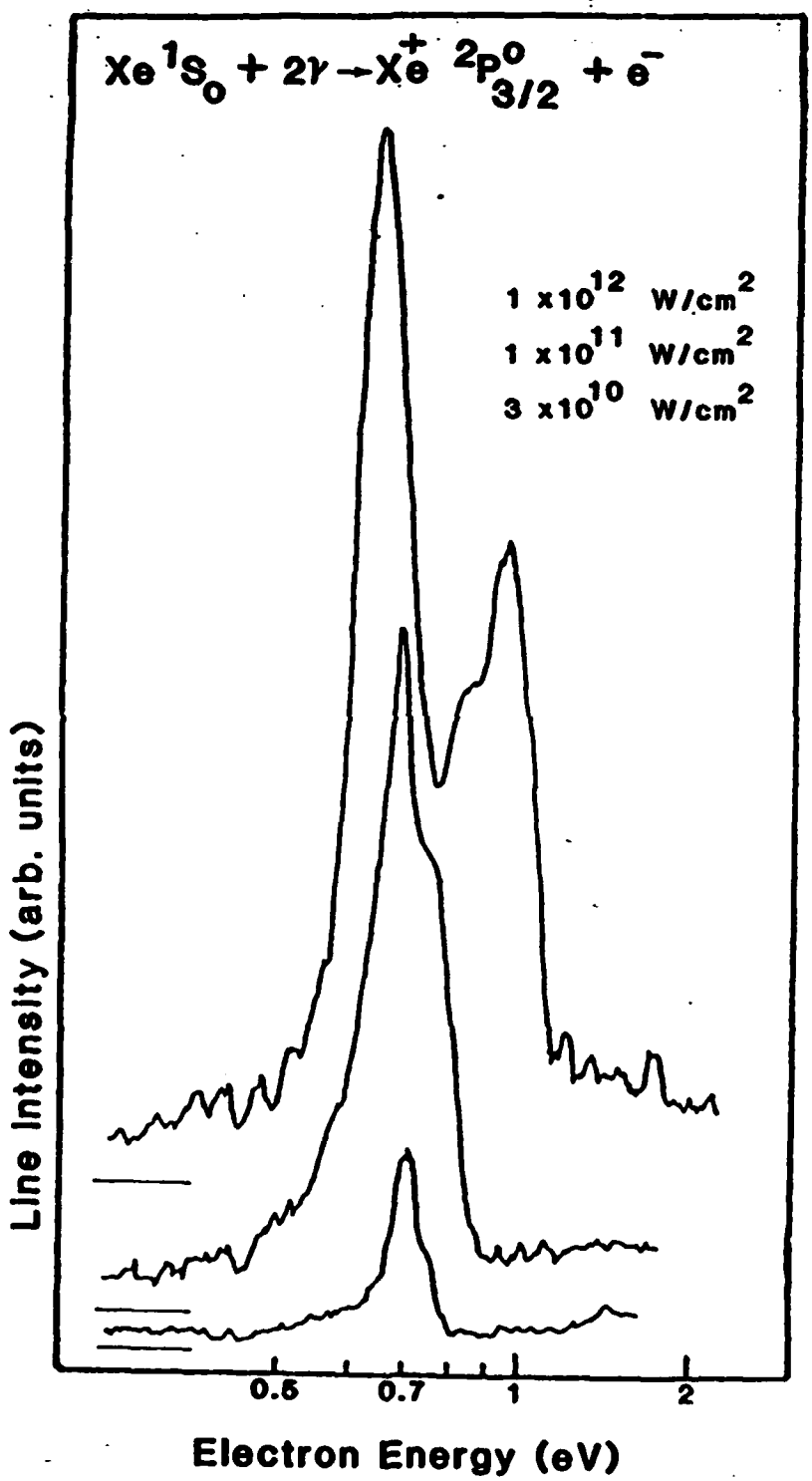
$Xe\ ^1S_o + 2\gamma \rightarrow Xe^+\ ^2P^o_{3/2} + e^-$
1×10^{12} W/cm^2
1×10^{11} W/cm^2
3×10^{10} W/cm^2
Line Intensity (arb. units)
0.6
0.7
1
2
Electron Energy (eV)

END

DTIC

7-86